NUREG/CR-5470
UCID-21820

Component Fragility Research Program

Phase II Development of Seismic Fragilities from High-Level Qualification Data

Prepared by N. C. Tsai, G. L. Mochizuki, NCTEI
G. S. Holman, LLNL

NCT Engineering, Inc.

Lawrence Livermore National Laboratory

Prepared for
U.S. Nuclear Regulatory Commission

DISCLAIMER

AVAILABILITY NOTICE

Availability of Reference Materials Cited in NRC Publications

Most documents cited in NRC publications will be available from one of the following sources:

1. The NRC Public Document Room, 2120 L Street, NW, Lower Level, Washington, DC 20555

2. The Superintendent of Documents, U.S. Government Printing Office, P.O. Box 37082, Washington, DC 20013-7082

3. The National Technical Information Service, Springfield, VA 22161

Although the listing that follows represents the majority of documents cited in NRC publications, it is not intended to be exhaustive.

Referenced documents available for inspection and copying for a fee from the NRC Public Document Room include NRC correspondence and internal NRC memoranda; NRC Office of Inspection and Enforcement bulletins, circulars, information notices, inspection and investigation notices; Licensee Event Reports; vendor reports and correspondence; Commission papers; and applicant and licensee documents and correspondence.

The following documents in the NUREG series are available for purchase from the GPO Sales Program: formal NRC staff and contractor reports, NRC-sponsored conference proceedings, and NRC booklets and brochures. Also available are Regulatory Guides, NRC regulations in the *Code of Federal Regulations*, and *Nuclear Regulatory Commission Issuances*.

Documents available from the National Technical Information Service include NUREG series reports and technical reports prepared by other federal agencies and reports prepared by the Atomic Energy Commission, forerunner agency to the Nuclear Regulatory Commission.

Documents available from public and special technical libraries include all open literature items, such as books, journal and periodical articles, and transactions. *Federal Register* notices, federal and state legislation, and congressional reports can usually be obtained from these libraries.

Documents such as theses, dissertations, foreign reports and translations, and non-NRC conference proceedings are available for purchase from the organization sponsoring the publication cited.

Single copies of NRC draft reports are available free, to the extent of supply, upon written request to the Office of Information Resources Management, Distribution Section, U.S. Nuclear Regulatory Commission, Washington, DC 20555.

Copies of industry codes and standards used in a substantive manner in the NRC regulatory process are maintained at the NRC Library, 7920 Norfolk Avenue, Bethesda, Maryland, and are available there for reference use by the public. Codes and standards are usually copyrighted and may be purchased from the originating organization or, if they are American National Standards, from the American National Standards Institute, 1430 Broadway, New York, NY 10018.

NUREG/CR--5470

TI90 002985

Component Fragility Research Program

Phase II Development of Seismic Fragilities from High-Level Qualification Data

Manuscript Completed: June 1989
Date Published: November 1989

Prepared by
N. C. Tsai, G. L. Mochizuki, NCT Engineering, Inc.
G. S. Holman, Lawrence Livermore National Laboratory

NCT Engineering, Inc.
3650 Mount Diablo Blvd.
Lafayette, CA 94549

Under Contract to:
Lawrence Livermore National Laboratory
7000 East Avenue
Livermore, CA 94550

Prepared for
Division of Engineering
Office of Nuclear Regulatory Research
U.S. Nuclear Regulatory Commission
Washington, DC 20555
NRC FIN A0400

Previous Reports in Series

NUREG/CR-4899, "Component Fragility Research Program — Phase I Component Prioritization," Lawrence Livermore National Laboratory, June 1987.

NUREG/CR-4900, Vol. 1, "Component Fragility Research Program — Phase I Demonstration Tests (Summary Report)," Lawrence Livermore National Laboratory, August 1987.

NUREG/CR-4900, Vol. 2, "Component Fragility Research Program — Phase I Demonstration Tests (Appendices)," Lawrence Livermore National Laboratory, August 1987.

ABSTRACT

To demonstrate how "high-level" qualification test data can be used to estimate the ultimate seismic capacity of nuclear power plant equipment, we assessed in detail various electrical components tested by the Pacific Gas & Electric Company for its Diablo Canyon plant. As part of our Phase I Component Fragility Research Program, we evaluated seismic fragility for five Diablo Canyon components: medium-voltage (4kV) switchgear; safeguard relay board; emergency light battery pack; potential transformer; and station battery and racks. This report discusses our Phase II fragility evaluation of a single Westinghouse Type W motor control center column, a fan cooler motor controller, and three local starters at the Diablo Canyon nuclear power plant. These components were seismically qualified by means of biaxial random motion tests on a shaker table, and the test response spectra formed the basis for the estimate of the seismic capacity of the components. The seismic capacity of each component is referenced to the zero period acceleration (ZPA) and, in our Phase II study only, to the average spectral acceleration (ASA) of the motion at its base. For the motor control center, the seismic capacity was compared to the capacity of a Westinghouse Five-Star MCC subjected to actual fragility tests by LLNL during the Phase I Component Fragility Research Program, and to generic capacities developed by the Brookhaven National Laboratory for motor control centers. Except for the medium-voltage switchgear, all of the components considered in both our Phase I and Phase II evaluations were qualified in their standard commercial configurations or with only relatively minor modifications such as top bracing of cabinets. The results of our study suggest for the components considered (1) a high degree of commonality exists with similar equipment in plants located in regions of relatively low seismicity, and (2) that the equipment in low-seismic-zone plants should have ultimate seismic capacities well above either current qualification requirements or new requirements that might come about as a result of NRC resolving the Charleston earthquake issue.

CONTENTS

FIGURES

TABLES

ACKNOWLEDGMENTS

This work was funded by the U.S. Nuclear Regulatory Commission, Office of Nuclear Regulatory Research, through its Mechanical and Structural Engineering Branch. Dr. John O'Brien was the technical monitor for this project.

The authors wish to express their sincere appreciation to the Pacific Gas & Electric Company for generously furnishing the seismic qualification test data necessary for our evaluation. We particularly wish to thank Sig Auer of the PG&E Electrical Engineering Department for his invaluable assistance and Julius Herbst, also of the PG&E Electrical Engineering Department, who before taking leave from the company provided us with the benefit of his long years of practical experience in the field of electrical equipment qualification.

1. INTRODUCTION

1.1 Background

Over the past decade methods have been developed to assess probabilistically how large earthquakes would affect nuclear power plants, particularly the associated risk to public health and safety. These probabilistic risk assessment (PRA) techniques combine "event trees", which describe the postulated accident scenarios (or "initiating events") capable of causing core melt, with "fault trees" describing the likelihood of equipment failures leading to a reduction in or loss of the ability of certain plant systems to perform their designated safety functions given that an initiating event occurs. A key element in the fault tree analysis is the "fragility" -- or likelihood of failure -- of various components under postulated accident conditions.

Application of probabilistic analysis techniques, both in NRC-sponsored research such as the Seismic Safety Margins Research Program and in commercial PRA studies, has indicated that potential accidents initiated by large earthquakes are one of the major contributors to public risk. However, component fragilities used in these analyses are for the most part based on limited data -- primarily design information and results of component "qualification" tests -- and engineering judgement. The seismic design of components, in turn, is based on code limits and NRC requirements that do not reflect the actual capacity of a component to resist failure; therefore, the real "seismic margin" between design conditions and conditions actually causing failure may be quite large. These elements combine to produce fragilities that are not only highly uncertain but, in the view of many experts, are also overly pessimistic descriptions of the likelihood of failure for many components. The observed performance of mechanical and electrical equipment in non-nuclear industrial facilities that have experienced strong-motion earthquakes tends to support this view. However, this same experience has also indicated that although a component may itself perform well in an earthquake, poor or inadequate support conditions may increase the likelihood of its "failure" in a safety sense. This also holds true in certain cases for aging or environmental effects, which may require attention if an "adequate" description of fragility is to be achieved.

In order to improve the present component fragility data base and establish component seismic design margins, the NRC commissioned a Component Fragilities Research Program (CFRP). The CFRP was conducted in two phases. Phase I comprised parallel efforts to (1) develop and demonstrate procedures for performing component tests to obtain new fragilities data, (2) identify through systematic grouping components influencing plant safety and therefore candidate for independent NRC testing, and (3) compile existing fragilities data obtained from various sources. During Phase I, the Lawrence Livermore National Laboratory (LLNL) performed component testing and prioritization [1,2], while the existing fragilities data base was compiled and evaluated by the Brookhaven National Laboratory (BNL).

The CFRP supports the need for realistic inputs for probabilistic risk assessments and margin studies. This research seeks to test the hypothesis that electrical and mechanical components have greater seismic capacity than is presently assumed in seismic risk assessments, and, as a consequence, that the significance of the earthquake threat might be diminished in licensing decision-making. In particular, the CFRP still result in the following:

- more realistic inputs for PRA applications. Improved descriptions of component fragility, based on actual failure data, will reduce the uncertainty inherent in subjective fragilities drawn from design information and results of equipment qualification testing.

- better understanding of component failure modes, of how various individual factors affect failure, and of the real "margin" between design or qualification requirements and conditions that might actually cause failure.

- guidance for development of seismic review procedures for existing plants, for interpretation of existing qualification or fragility data, and for specification of test procedures of equipment for which in-depth testing to "failure" is warranted.

These results will combine to improve our ability to more realistically assess seismic risk while at the same time contributing to elimination of unnecessary licensing delays to respond to seismic issues.

1.2 The Charleston Issue

One near-term issue facing the NRC in particular and the nuclear industry as a whole is that of potential revisions in the seismic design bases for older plants. Most older plants located in the eastern United States were either not subjected to the in-depth seismic design typical of more modern plants, or were designed for relatively low levels of safe shutdown earthquake (SSE). This practice reflected the long-held view that the eastern United States (i.e. east of the Rocky Mountains) was historically an area of generally low seismicity with only a few isolated records of large earthquakes. However, recent studies have suggested that the seismology of the region is such that the effects of large earthquakes -- such as those near Charleston, South Carolina in 1889 and New Madrid, Missouri in 1811-12 -- could affect much wider geographic areas than originally believed. The results of these studies therefore present NRC with the problem of resolving what constitute "more appropriate" design basis earthquakes for plants in this region.

Resolution of the "Charleston issue" brings with it the prospect of SSE levels significantly higher than the original design bases for plants in the affected region. Reevaluation of certain plants for these higher SSE levels could result in certain design allowables being exceeded, potentially jeopardizing the continued operation of these

plants. However, exceedance of design allowables does not necessarily compromise plant safety, if it can be shown that sufficient "reserve" capacity is available to absorb increases in postulated seismic loads. At least three potential options exist for this purpose:

(1) demonstrate equipment "ruggedness." Mechanical and electrical equipment related to plant safety is typically "qualified" to demonstrate its ability to function as intended during a site-specific SSE. The "seismic margin" between design level and actual failure is not typically measured as a part of qualification testing; most experts contend, however, that many equipment items have sufficiently high seismic capacity -- "inherent ruggedness" -- that they would function adequately even during or after input motions well in excess of qualification requirements.

Demonstrating that this ruggedness exists, either through actual failure tests or by alternate means, therefore represents one potential response to a revision in SSE levels. Many organizations are actively pursuing this option. The Electric Power Research Institute (EPRI), for example, is currently applying existing qualification data to develop "generic equipment ruggedness spectra" (or "GERS") for certain items of plant equipment. Together with EPRI, the Seismic Qualification Utility Group (SQUG) is compiling information on the performance of heavy industrial facilities (which contain many equipment items typically found in nuclear power plants) during actual strong-motion earthquakes.

(2) perform "less conservative" response analyses. Equipment in many older plants may have high seismic margins owing to relatively conservative response analyses being used in plant design (e.g., to predict equipment input motions). Many factors can affect the degree of conservatism, including (1) the specific analytic methods used to predict component response (e.g., two- vs three-dimensional finite-element analysis, time-history vs response spectrum analysis, coupled vs uncoupled analysis), either singly or in combination, (2) input data such as damping values, and (3) application of safety factors to calculated results to "insure" conservatism. Just what constitutes a "conservative" analysis is subject to interpretation, but in general the less sophisticated an analysis is, the more conservative it tends to be.

If a design is done by analysis, the apparent margin is influenced by the particular analytic method used. A "conservative" method of analysis may result in an artificially low margin. Taking advantage of more refined, i.e. "less conservative", analysis techniques to evaluate an older plant thus represents a possible means of more realistically predicting (i.e. reducing) responses

to increased seismic loads in order to meet revised regulatory criteria.

(3) apply revised NRC requirements. Recent or pending changes in NRC regulations affecting postulated design loads allow or would allow relaxations such as decoupling SSE and certain loss-of-coolant accident (LOCA) loads, elimination of dynamic effects (pipe whip, jet impingement, hydrodynamic loads) associated with certain pipe breaks, and use of alternative descriptions of damping. Plants originally designed for loads or load combinations affected by the regulatory actions might benefit in that these loads or load combinations would no longer need to be considered in a reevaluation for increased seismic loads, or would be reduced through use of alternative (i.e. more realistic) input criteria for calculating loads.

The investigation discussed in this report concerns itself with the first of these options, namely equipment ruggedness. It is important to keep in mind, however, that future responses to more stringent seismic design criteria may be able to take credit for all three to one extent or another. Consequently, any assessment of seismic capacity must take the other two factors into account in order to assure it is conducted on a reasonable basis.

1.3 Scope of the Present Evaluation

As part of our Phase I component prioritization effort, we assessed in detail five components tested by the Pacific Gas & Electric Company (PG&E) for its Diablo Canyon nuclear power plant: medium-voltage (4kV) switchgear; safeguard relay board; emergency light battery pack; potential transformer; and station battery and racks. The results of our Phase I evaluation indicated that these components, even in their standard commercial configurations or with relatively minor structural modifications, would rate as "high capacity" according the guidelines established during our Phase I component prioritization effort [2], i.e. the median seismic capacity of each exceeds 2.0g based on local ZPA at the component base. The objective of our Phase II evaluation was to extend the assessment to three additional Diablo Canyon components: a single Westinghouse Type W motor control center column, a reactor containment fan cooler motor controller, and three local starters. We selected these particular components not only for their safety significance, but also because they represent different applications and mounting configurations of nominally similar electrical devices, i.e. contact-operated motor starters.

Located in southern California, the Diablo Canyon plant was originally designed for a 0.4g PGA safe shutdown earthquake. The design basis SSE was later increased to 0.75g PGA following discovery of a previously undetected offshore fault zone (the "Hosgri" fault) passing within a few miles of the plant site. An extensive evaluation performed by PG&E and its consultants demonstrated that, with some modifications, equipment required to shut down and maintain the plant in a safe condition

would be available following the postulated Hosgri earthquake [3]. As in our Phase I evaluation, the fragility evaluation described in this report is based on the "high level" qualification data generated as part of the PG&E study.

The PG&E data is of interest for "low level" sites east of the Rocky Mountains because the Hosgri input motions almost certainly bound any "reasonable" increase in SSE levels resulting from resolution of the Charleston issue. Although less definitive than actual failure ("fragility level") data for assessing ultimate seismic capacity, the high-level qualification can be useful in the following ways:

- if equipment commonality can be shown between high- and low-level plant sites -- for example, through use of standard commercial components -- the fragilities derived from "high-level" data might be directly applicable to equipment qualified for lower earthquake levels. The degree of commonality would, of course, depend in large part on the extent to which the tested equipment had been modified to meet the more stringent seismic qualification requirement. Evaluation of high-level data is most useful for confirming "high" seismic capacity, less so when a more definitive fragility description is desired (e.g. for low-capacity components).

- if the tested equipment had been modified to meet qualification requirements, the test experience might suggest similar modifications that could be made to increase the seismic capacity of like components. These results could also provide guidance for development of seismic review ("walkdown") procedures for in-situ inspection of plant equipment.

- if commonality cannot be established, the "high-level" testing experience would suggest conditions for rigorous testing of the component in question.

It is important to note that we do not view evaluation of qualification data as a substitute for testing if truly definitive fragility descriptions are desired. Typically, qualification tests do not include systematic (i.e. parametric) investigations of factors that potentially affect seismic performance -- mounting conditions, for example. Any "sensitivity studies" during such tests usually arise out of necessity as equipment is modified to meet qualification requirements. As a result, often only minimal detailed information is available for estimating the uncertainty parameters needed to develop a complete fragility description.

However, in cases where "threshold" fragilities might be adequate for making regulatory decisions -- those involving "high capacity" components, for example -- use of high-level qualification data may provide reasonable estimates of seismic capacity.

1.4 Definition of Component Fragility

"Fragility" is a term commonly used to describe the conditions under which a component (or, in general, a structure, a piping system, or piece of equipment) would be expected to fail. In this report we are concerned with seismic fragility, in other words, what levels of seismically-induced input motion would be required to cause component failure; it is important to keep in mind, however, that fragility can in principle be defined for any input condition affecting component performance. Failure can be characterized as either functional (e.g., erratic behavior, failure to perform intended function) or physical, or as the exceedance of some predetermined performance criteria (such as a limit given in a design code).

One interpretation of component fragility -- which we will refer to as the "fragility level" -- evolves from qualification testing. In seismic qualification testing, a component is subjected to input motion characterized by a specified waveform describing input level (seismic acceleration) as a function of frequency. The component is "qualified" if it continues to perform its intended function when its response to this input motion -- the "test response spectrum," or TRS -- meets or exceeds pre-determined acceptance limits (the "required response spectrum," or RRS). In qualification testing, the TRS is usually measured at the component support points.

Although it may establish the adequacy of a component for a particular seismic environment, a successful qualification test does not directly provide data on what input motion levels actually result in component failure. This can be (and often is) done by retaining the original input spectrum and then increasing the input level until "failure" (however it is defined) occurs. The TRS at failure represents the "fragility level" of the component; the difference between the fragility level and the qualification level thus represents the seismic margin or "ruggedness" of the component.

Fragility is described differently when used for PRA purposes or for other types of probabilistic analysis. In this case, the fragility of a component represents the probability of its failure -- or more rigorously speaking, the probability of attaining a defined "limit state" -- conditioned upon the occurrence of some level of forcing or response function. It may be expressed in terms of a local response parameter (for example, input motion at the component mounting location) or can be tied to a more global forcing function such as free field peak ground acceleration (PGA). Note however that when fragility is anchored to a forcing function, the further removed the component is from that forcing function, the more factors there are (such as structural response and soil-structure interaction) that must be considered in the fragility description.

The probability of failure is typically described by a family of "fragility curves" plotted at various levels of statistical confidence (see Fig. 1.1). The central, or "median" function represents the

fragility analyst's best estimate of the "true" fragility of the component taking into account all significant factors which, in the analyst's judgement, might contribute to failure. The central point (50% probability of failure) on this curve represents the "median capacity" of the component. The fragility function is a distribution characterized by a log-normal function with this median value and a logarithmic standard deviation β_r which describes the "random" variation in the parameters affecting fragility. In a description of seismic fragility, for example, this parameter might represent the differences in real earthquake ground motion compared to the input motion that a component is subjected to in qualification or fragilities testing.

The 5% function and 95% function in Fig. 1.1 represent the "modeling uncertainty" in the median fragility function. These bounds, which may also be referred to as 5th- and 95th-percentile confidence limits, are based on the assumption that there is uncertainty in the median capacity; this uncertainty is characterized by a logarithmic standard deviation β_u. Simply stated, a 95% confidence limit implies that there is a 95% subjective probability ("confidence") that actual capacity is less than the median value indicated for the 95% fragility function. Modeling uncertainty, often described as "lack of knowledge" about the component in question, reflects the adequacy (or inadequacy) of information -- component damping values, for example -- used by the fragility analyst to form his judgements about component capacity. Thus, modeling uncertainty in fragility descriptions has a subjective rather than a "random" basis as is true in the statistical sense.

For any given component, empirically developing a statistically meaningful seismic fragility would require that a large population of identical components (e.g., several hundred or several thousand) be subjected to successively higher levels of acceleration and the distribution of failures (however "failure" is defined) be recorded as a function of acceleration level. Practical constraints on time and resources clearly make this infeasible for a single component under well-defined load conditions, let alone for the effectively infinite combinations and permutations of component type, manufacturer, mounting, and loading conditions that could be identified for actual nuclear power plants. Therefore, an alternative approach is necessary to experimentally gain an insight into fragility.

Our approach to fragilities testing takes advantage of the fact that for practical PRA applications, a limited or "lower bound" fragility description may be adequate. In a probabilistic analysis, failure occurs only when the probability distributions of response and fragility overlap; therefore, only the lower tail end of the fragility curve may be of interest from a PRA standpoint. For components having a high seismic capacity (high "ruggedness"), the overlap of the response and fragility distributions could conceivably be so small under all credible loading conditions as to imply that the probability of failure is negligibly low.

One method of developing a "lower bound" fragility is to estimate the so-called "HCLPF" (High Confidence, Low Probability of Failure) capacity for the component. The HCLPF capacity considers both the random and modeling uncertainty in the median capacity, and is defined as that value of the forcing or response function (such as seismic acceleration) for which we have "95% confidence" that the probability of "failure" is less than 5 percent. If the median capacity of a component is defined by a peak acceleration with value A, the corresponding HCLPF capacity (i.e. HCLPF acceleration) is obtained from the following numerical relationship:

$$A_{HCLPF} = \breve{A} \exp [-1.65 (\beta_r + \beta_u)] \qquad (1\text{-}1)$$

where β_r and β_u represent the random and modeling uncertainties, respectively. The median capacity $\breve{A}$ can be determined by component tests, either to actual failure or to some threshold or "cut-off" limit. The cut-off might be applied, for example, in testing certain components whose actual median capacities were significantly above any response levels of regulatory interest.

The HCLPF capacity provides a practical means of addressing variations that inevitably arise between actual plant conditions and test conditions, variations that might otherwise be difficult to parametrically quantify by testing alone. For example, the random uncertainty β_r allows for variations in real earthquake motion compared to test input motion, variations in building floor response, or (e.g., for cabinet-mounted electrical devices) random variations in cabinet response. The modeling uncertainty β_u can account for variations in real damping values, or in component mounting conditions, or in the response of functionally similar components of different size or supplied by different manufacturers. These uncertainties can be quantified by systematically structuring test conditions in the form of "sensitivity studies" to investigating the effect of various parameters on the measured median capacity of the device tested. This was the basic approach taken in our Phase I demonstration tests.

The HCLPF approach has the added advantage that, in the absence of complete fragility data, a "lower bound" fragility can still be defined for a seismically qualified component by assuming its qualification level also represents its HCLPF capacity. Engineering judgement can then be applied to estimate the uncertainty parameters and thus make inferences about the median capacity.

Note that because the HCLPF capacity by definition presumes a five percent probability of failure, while "qualification" implies no failure, it tends to be a conservative measure of seismic performance when so derived. It may in fact be overly conservative if qualification levels are low, as would be the case for many plants in the eastern United States. However, HCLPF capacities based on "high level" qualification data -- from plants in the western United States, for

example -- can provide useful lower bound fragilities for plants having relatively low design basis earthquakes. The CFRP Phase I Prioritization Report [2] first described how we used this approach to infer the actual capacity of selected electrical equipment at the Diablo Canyon nuclear power plant in southern California. This same approach was also applied in our Phase II evaluation of additional Diablo Canyon electrical components.

In itself, the HCLPF capacity is a useful parameter on which to base regulatory decisions concerning seismic performance. However, extreme care must be exercised in selecting "reasonable" values of β_r and β_u when using a HCLPF capacity derived from qualification data to infer the actual capacity or "fragility level" of a component. The reasons for this are two-fold:

- as shown in Fig. 1.2, the slope of the fragility curve becomes more shallow as random uncertainty (β_r) increases. Therefore, the resultant median capacity on the 5% curve (and, for constant β_u, the inferred fragility level) also increases with increasing random uncertainty.

  As shown in Fig. 1.3, however, if the fragility level of the component is known (e.g., from actual failure tests), then the HCLPF capacity derived from the median capacity decreases with increasing random uncertainty.

- similarly, as modeling uncertainty (β_u) increases, the offset between the 5% fragility function and the 50% function also increases, implying an increase in the inferred fragility level. If, on the other hand, the fragility level is known, an increase in modeling uncertainty drives the HCLPF capacity towards lower (i.e. more conservative) values.

These figures illustrate how a "bottom-up" assessment of seismic capacity (i.e. inferred from HCLPF capacity) can imply that fragility level increases with uncertainty, which is clearly non-conservative. The fragility analyst must therefore exercise extreme care when selecting the uncertainty parameters used to infer the ultimate capacity, or "fragility level", of a component. Unfortunately, the information necessary to select these parameters may not be available from existing data, or may be difficult to assess consistently if attempts are made to consolidate data from several diverse sources. The less definitive the data on HCLPF-derived fragility descriptions are based, the higher their degree of inherent uncertainty.

For certain high-capacity components, this uncertainty may be tolerable if only a "lower bound" fragility -- a HCLPF capacity alone, for example, or a 5% fragility function -- is adequate for regulatory decision-making or for PRA applications. This may apply, for example, to high-capacity components at plant sites with relatively low SSE requirements (e.g., in the eastern U.S.), provided that (1) the "high capacity" rating of these components can be substantiated, and (2) commonality in

configuration and mounting conditions can be established between the in-plant components in question and those for which "high level" data is available.

In general, however, high inherent uncertainty suggests that a "top-down" assessment -- estimating HCLPF capacities from measured fragility levels -- is still preferable for assessing seismic performance. This is particularly true when a detailed fragility function, rather than a "threshold" fragility description, is necessary for low-capacity equipment. Parametric "sensitivity" tests, even on a limited scale, are best-suited for this purpose when structured to systematically investigate how individual factors affect seismic performance. The resultant understanding aids not only in developing fragility descriptions directly from the failure data, but also in interpreting and applying data compiled from other sources.

1.5 Technical Basis for the Present Evaluation

As in our earlier Phase I evaluation of the Diablo Canyon equipment tested during the Hosgri requalification program, seismic fragility curves were derived from our subjective judgement based on the dynamic test data available to us. Subjective judgement is necessarily associated with a large uncertainty because there is no information on the response of equipment subjected to levels of test motion above that required for qualification purposes. The fragility results developed for the equipment considered in this report reflect the following basic assumptions:

(1) For the purpose of establishing the fragility, the local seismic motion of the equipment is adequately characterized by the zero period acceleration at its base. This assumption is made for horizontal as well as vertical motion, and allows us to simply express seismic fragility as the probability of failure for any given level of ZPA at the equipment base.

(2) The minimum seismic capability, now expressed by the base motion ZPA experienced during qualification testing, is that associated with a 5% probability of failure at a 95% confidence limit. This assumption follows the definition of HCLPF fragility discussed earlier.

(3) The probability distribution of the fragility is log-normal with modeling uncertainty $\beta_u = 0.18$ and random uncertainty $\beta_r = 0.09$. The assumption of a log-normal distribution reflects common practice in fragility analysis, although it is recognized that other types of distributions may be equally valid.

The values of model uncertainty and random uncertainty assumed in the evaluation represent a key factor because, in the end, these determine how the HCLPF capacity (which is based on actual qualification data) is

extrapolated to infer a median seismic capacity. The values of β_u and β_r given above were selected based on the following observations:

(1) The use of the local ZPA at the component base as the parameter for the fragility description incurs much smaller variability than does the use of either the peak ground acceleration (PGA), which is commonly used in probabilistic risk assessment, or the local spectral response acceleration at the component base. Use of PGA as the fragility parameter, such as that in Ref. 4, must account for the variability in the ground motion and structure dynamic amplification at the component location in addition to the variability in the local ZPA. When using the local spectral response acceleration as the fragility parameter, such as was done by the Seismic Margins Research Program (SSMRP) for electrical components whose fragilities were derived from the SAFEGUARD test data from the U.S. Corps of Engineers [4], one must account for variability in the spectral damping and the shape of the spectrum versus the natural frequencies of the component, which always exceeds the variability in the local base ZPA.

(2) The evaluation described in this report is limited to specific equipment items which have either been seismically strengthened or, through qualification testing, have been shown to be highly resistant to seismically-induced failure in their standard commercial configurations. References 4 and 5, however, both attempt to predict generic fragilities for broad classes of electrical components; such generic fragilities by nature have larger variability than those based on specific data for specific components.

(3) The ratio of β_u to β_r in Refs. 4 and 5 typically ranges from 1.5 to 2.0. We selected the upper end of this range (i.e. 2.0) based on our review of the qualification test data.

In Refs. 4 and 5 the value of β_u typically ranges from 0.35 to 0.50. Based on the above observations, we judge the modeling uncertainty $\beta_u = 0.18$ to be consistent with that assumed in Refs. 4 and 5, which use a different parameter for the fragility description. In addition, we are inferring median seismic capacities through extrapolation of maximum test qualification acceleration data. The extrapolation was done with conservatism in mind because the seismically qualified equipment already exhibits a high seismic capability (as necessitated by plant design), for which purpose a smaller variability will be consistent.

Except where noted otherwise, the same values of β_u and β_r were used for all of the components considered in this evaluation.

In our Phase II evaluation only, we also used another fragility descriptor, the average spectral acceleration (or "ASA"), developed by the Brookhaven National Laboratory as part of its study of generic seismic fragilities for nuclear power plant electrical components [6]. The

ASA, defined as the average spectral acceleration of the applicable 2% damping response spectrum for the frequency range from 4 to 16 Hz, is an attempt to use a single parameter to account for the fact that, at least for relatively "flexible" components, spectral acceleration is a more appropriate parameter on which to base a fragility description. Consistent with the assumptions we applied to the estimate of the HCLPF ZPA, the HCLPF ASA was established from the TRS representing the minimum seismic capability. Because the TRS in the qualification tests was associated with a 3% damping, the ASA derived from this TRS was increased by 1.2 (as suggested by BNL) to account for the adjustment between 3% and 2% damping spectra. The median ASA capacity $\hat{S}$ was then derived from the HCLPF ASA capacity by assuming the same variabilities as those for the ZPA capacity, usually $\beta_r = 0.09$ and $\beta_u = 0.18$.

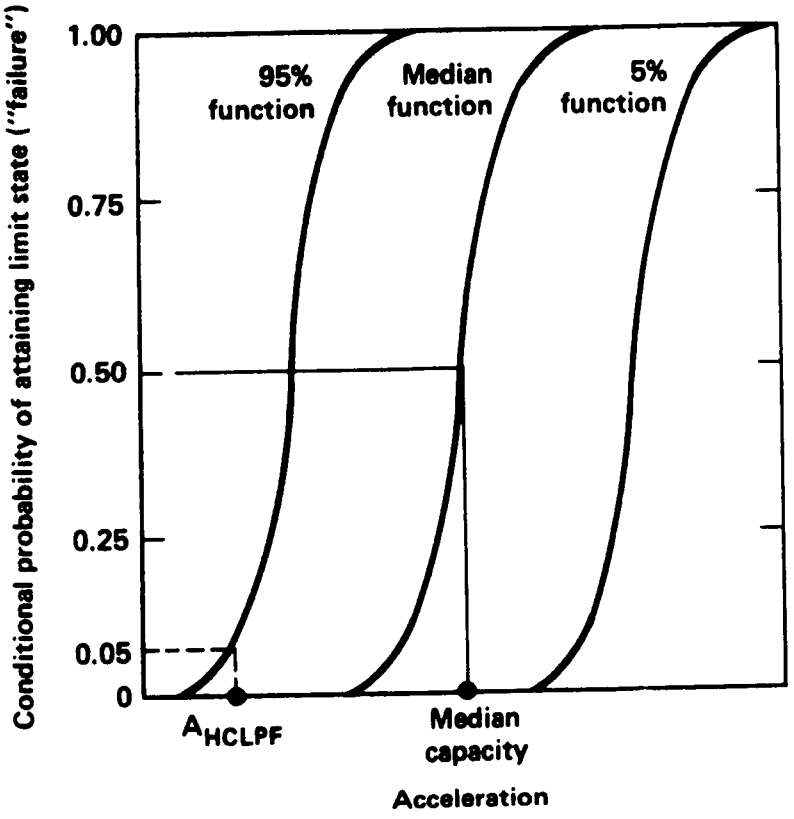

Fig. 1.1 Typical curve set representing component fragility.

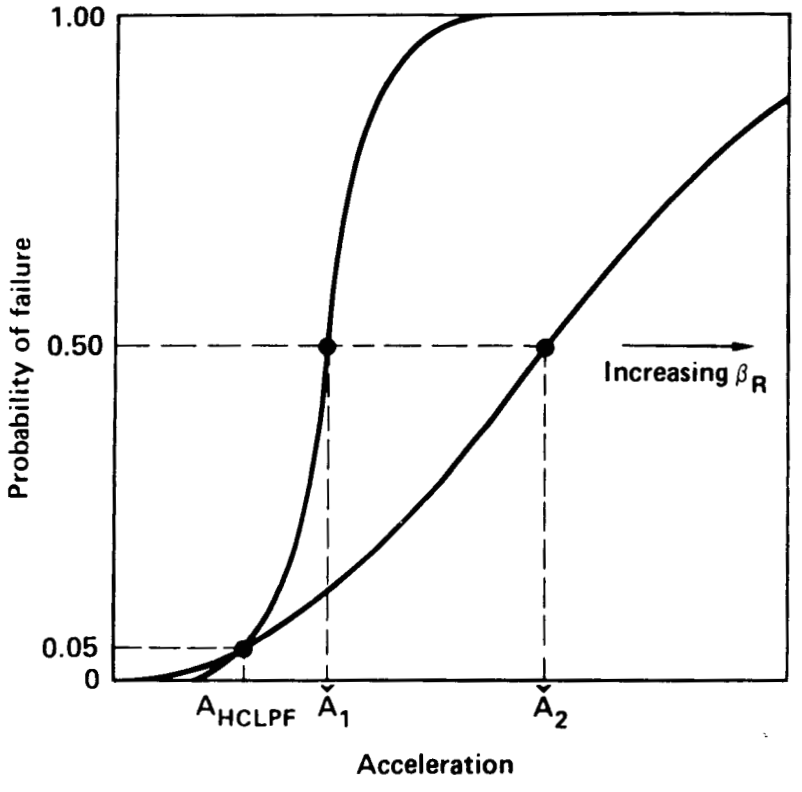

Fig. 1.2 Typical 95% fragility function showing how increasing random uncertainty affects median capacity derived from a HCLPF value. For constant β_u, the inferred fragility level of the component (i.e. median capacity of the 50% function) would be similarly affected.

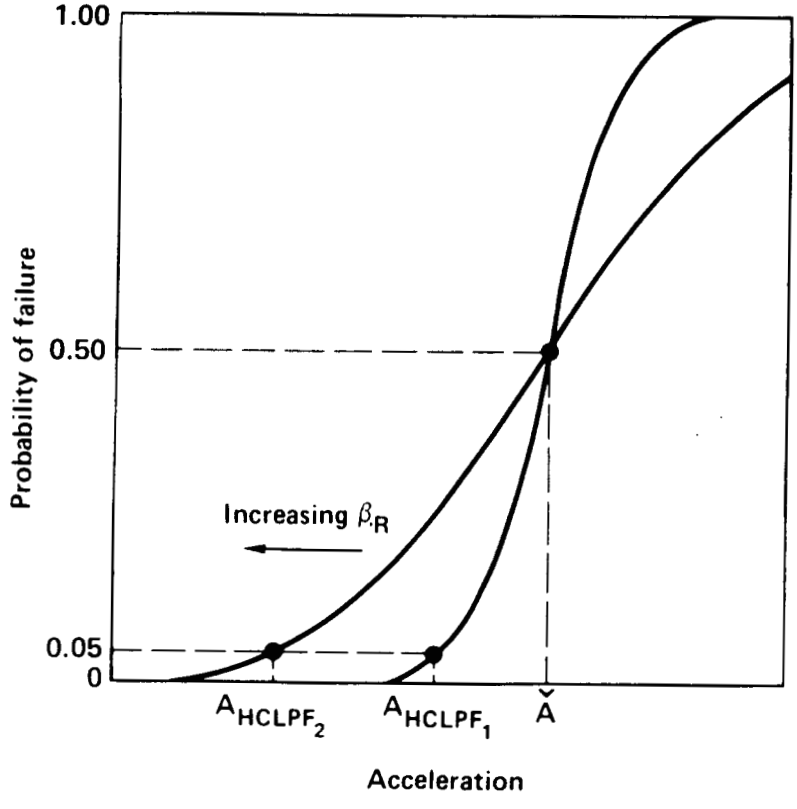

Fig. 1.3 Typical 95% fragility function showing how increasing random uncertainty affects HCLPF value derived from a constant median capacity. For constant β_u, the effect would be the same for HCLPF values derived from a constant component fragility level.

2. MOTOR CONTROL CENTER

2.1 Description of Equipment

The 480VAC motor control center is a Westinghouse Type W housing the following typical devices: starters, breakers, relays, transformers, and indicating lights. A typical plant installation ("line up") comprises several (usually two to eight) vertical columns bolted together side-by-side. Each column comprises modular draw-out units (also called "buckets" or "unit wrappers") housing combination motor controllers or feeder breakers. Electrical bussing is provided horizontally between columns and vertically between draw-out units.

Each combination motor controller consists of a molded-case magnetic-only circuit breaker, contactor and overcurrent relay. Feeder breakers are simply molded-case thermal-magnetic circuit breakers. Each column is typically about 20"x20" in plan by about 90 inches tall, and weighs about 500 pounds (Ref. 7).

The structural framework for each column is typically made of formed steel channels. The sub-frames for the front and rear of each structure are welded. These sub-frames are then bolted to the longitudinal members to form the complete frame which is rigid and self-supporting. Side, back and roof sheets are mounted with screw fasteners for quick and easy removal when desired. All doors are typically 14-gauge steel with a 1/2-inch flange to provide a secure enclosure for all openings. Doors mounted on removable pin hinges are typically provided on all unit compartments, vertical wireways, top horizontal wireways, and bottom horizontal wireways. The unit pan forms the top barrier of each unit space. In conjunction with the draw-out unit this provides isolation between adjacent units and wireways. The guide rails are an integral part of this pan and provide precise alignment of the unit stabs on the vertical bus.

2.2 Safety Function

The MCC must provide power on demand for engineered safety features equipment. The major loads are electric motor operated and ventilation fans. In order to accomplish this function feeder breakers must remain closed, contactors must close on demand and remain closed, and overload relays must not spuriously operate to interrupt power inadvertently. In the event of an earthquake the MCC must be capable of performing the prescribed safety functions during and after the earthquake.

2.3 Seismic Failure Modes

According to the dynamic test qualification data, structural failure is not the prevailing mode of failure of the MCC during seismic events so long as the MCC is properly anchored at the base with bolts and, in particular, braced at the top in the front-to-back (F-B) direction. Note that because the cabinets in a typical line-up are bolted to each other in the side-to-side (S-S) direction, an MCC is by nature stiffer

and more stable in the S-S direction of the line-up; consequently, top bracing in this direction does not materially enhance the structural capability of the MCC. We therefore rank the vulnerability of the MCC to seismic events in the following descending order:

(1) Functional failure due to chattering of relay contacts, especially for those which are normally closed (NC) and in the de-energized state.

(2) Functional failure due to chattering of relay contacts resulting from excessive F-B movements of the draw-out units in the commercial standard Type W motor control center. This potential failure mode was identified during the dynamic qualification tests of the Diablo Canyon MCC, and the probability of its occurrence was minimized by installing additional F-B seismic holddowns (also referred to as "seismic clips") at both sides of every draw-out unit. Details of the seismic clips will be described later when discussing the modification of the MCC for the purpose of seismic qualification.

(3) Structural failure of the base anchor due to F-B motion of the cabinet. Failure of the base anchor due to S-S motion is much less likely because of the typical line-up installation of the multiple cabinets in the MCC in actual applications. In the case of Diablo Canyon, the likelihood of such structural failure of the base anchors is greatly minimized by top-bracing the end columns of each MCC line-up in the F-B direction.

2.4 Modifications to Improve Seismic Performance

As previously mentioned during the discussion of the seismic failure modes, one major structural modification to the MCC is to install a seismic bracket to both sides of each draw-out unit. The modification prevents the excessive F-B movements of the draw-out units that at first caused chattering of the NC relay contacts even during the OBE-level dynamic tests. As shown in Fig. 2.1, the modification consists of a bracket installed at the front corner of the draw-out unit and tied to the rear corner steel channel of the column frame by an angle fastening rod (Ref. 7). This modification was applied to every MCC draw-out unit in the Diablo Canyon plant.

To further enhance seismic performance, the columns at both ends of each MCC line-up in the plant have been top-braced in the F-B direction. A steel channel running in the S-S direction has been welded to the tops of all columns within a line-up so that all columns between the two end ones also benefit from the top bracing installed at the end cabinets. Such bracing of the MCC at the top greatly increases its structural rigidity for seismic vibrations in the F-B direction.

2.5 Seismic Qualification

The seismic qualification of the MCC was accomplished by subjecting one typical column to a series of biaxial random motion dynamic tests on a shake table. Random motions simulated the required response spectrum specified at the base of the MCC, from the OBE to the SSE levels. Figure 2.2 shows the test setup for the single vertical column under consideration. The base of the structural frame was bolted to a 1-inch steel plate which was in turn welded to the top of the test table. The top of the column was bolted to the top of a rigid steel bracing frame at both sides of the cabinet. This bracing support at the top of the column simulated not only the F-B bracing at the top of the MCC line-up in the plant, but also the S-S structural support from the neighboring cabinets that would be present in a typical line-up of the MCC in the plant. A pair of horizontal and vertical accelerometers was mounted on the shake table to monitor the input test motions. Another pair of accelerometers was mounted on the front face of one of the draw-out units located at a height of about one-third the total column height from the base as shown in Fig. 2.2. The purpose of these two accelerometers was to monitor the response of the draw-out unit, which we denote as the "bucket response".

Figures 2.3(a), 2.4 and 2.5 are photographs of the actual setup for the F-B and vertical (X-Y) tests, the S-S and vertical (Z-Y) tests, and the mounting of the bucket response accelerometers on the front face of the Size 5 controller. During the initial tests of the MCC, a fan cooler starter controller was mounted on the same test table and tested concurrently with the MCC for the sake of convenience in qualifying the fan cooler starter controller (see Figs. 2.3(a) and 2.4). It was later removed when the MCC was retested after addition of the seismic clips to the draw-out units. The overall test program proceeded as described in the following sub-sections.

2.5.1 Initial Tests

During the initial dynamic tests, one each of NEMA* Sizes 2, 3, 4 and 5 starters and two 100-amp feeder breakers were mounted in the column. No structural modification was applied to the column, in other words, the MCC column was initially tested in its standard commercial configuration. The column was subjected to a series of biaxial random motion tests simulating the OBE and SSE levels of required base motions. The accelerometers monitoring the MCC bucket responses were mounted on the Size 5 starter. Test runs in the F-B and vertical (X-Y) axes were first made, in the following order:

(1) Three OBE runs with the devices de-energized, and then two more OBE runs with the devices energized.

---

*National Electrical Manufacturers Association

(2) Four SSE runs with the devices energized. In the first two SSE runs, however, the test table motion was only about the OBE level and did not reach the full SSE level.

(3) One SSE run with the devices de-energized.

(4) One additional OBE run with the devices de-energized.

(5) One additional SSE run with the devices de-energized.

The S-S and vertical (Z-Y) direction runs were then conducted, in the following order:

(1) Three OBE runs with the devices de-energized, and then two OBE runs with the devices energized.

(2) Two SSE runs with the devices energized, and one SSE run with the devices de-energized.

The average ZPA of the test table was about 1.2g and 0.8g for the horizontal and vertical directions, respectively, for the OBE runs. The corresponding ZPA of the test table was about 1.7g and 1.1g for the SSE runs. Figure 2.6 shows the 3% damping TRS (Test Response Spectrum) and the 3% damping bucket response spectrum at the Size 5 starter in the F-B (X-) direction during the sixth X-Y axis run at the SSE level. Figure 2.7 shows the corresponding spectrum comparison for the 3% damping vertical spectra during the same X-Y direction SSE run. Similarly, Figs. 2.8 to 2.9 show the spectrum comparison for the third SSE level run in the S-S and vertical (Z-Y) directions. Figures 2.6 to 2.9 show that the first mode horizontal frequency of the bucket containing the Size 5 starter was about 12 Hz and 9 Hz, respectively, for vibration in the F-B (X-) and S-S (Z-) axes, and the first vertical mode frequency was substantially higher than 30 Hz. The fundamental mode frequencies so identified from the SSE level test response spectra were consistent with those identified from the low level resonance search tests in which the test table ZPA was 0.2g. This observation suggests that the dynamic response characteristics of the MCC buckets are essentially linear for test table ZPAs ranging from the low 0.2g to the SSE level.

No relay chatter was observed for all the S-S and vertical (Z-Y) axes tests, at both the OBE and SSE levels. During tests in the F-B and vertical (X-Y) axes, however, excessive F-B movements of the draw-out units were observed.

One NC contact in the Size 4 controller chattered during the fifth SSE test with the devices de-energized. Another NC contact in the Size 2 controller chattered during the third and fourth SSE runs while the devices were energized, and again during the sixth SSE run when the devices were de-energized. In addition, a NC contactor on the Size 5 controller chattered whenever the devices were de-energized, during both the OBE and SSE level tests. Because all starters have horizon-

tally operating armatures it was believed that the relay chattering during the X-Y tests was caused by the excessive F-B movements of the draw-out units and that the seismic performance of the relays could be somehow improved with the installation of seismic clips to both sides of each draw-out unit. In addition, it was determined that a defective spring in the Size 5 starter was the cause for the excessive chattering of the de-energized relay contacts during both the OBE and SSE levels of test and it should be replaced [3,8].

2.5.2 Retests After Structural Modification

After the seismic clips were installed to improve the rigidity of the draw-out units and the defective spring in the Size 5 starter was replaced, the MCC was tested again with the same devices and test setup as shown in Fig. 2.3(b). The fan cooler motor controller, which was concurrently tested with the MCC during the initial tests, was now removed. The sequence in the initial tests was essentially repeated here, and the same test table ZPA's as those used in the initial tests for both the OBE and SSE levels were also duplicated in the retests. For runs in the F-B and vertical (X-Y) axes the order was as follows:

(1) Three OBE runs and one SSE run with the devices de-energized.

(2) Two OBE and two SSE runs with the devices energized.

The runs in the S-S and vertical (Z-Y) axes were then conducted as follows:

(1) Three OBE runs with devices de-energized, and then two OBE runs with the devices energized.

(2) Two SSE runs with the devices energized, and then one SSE run with the devices de-energized.

Figures 2.10 and 2.11 show a comparison of the TRS and the bucket response spectrum at the Size 5 starter in the X- and Y-direction during the X-Y axes runs. Similarly, Figs. 2.12 to 2.13 show the spectrum comparison in the Z- and Y-direction during the Z-Y axes runs. Comparing Figs. 2.10 to 2.13 to the corresponding spectra previously shown in Figs. 2.6 to 2.9 suggests that the addition of the seismic brackets to the buckets did not materially change the dynamic characteristics of the bucket response except at the very high frequency range for which the structural modification appeared to produce somewhat higher response. Both series of tests indicated that the Size 5 starter significantly amplified the high frequency contents of the test table motions in all three axes.

The Size 2 to 5 starters and the two feeder breakers were then removed from the vertical column. Three Size 1 reversing controllers, used for motor-operated valves, were mounted to the vertical column and the tests continued. The bucket response of one of the Size 1 starters was now monitored. In both the X-Y and Z-Y axes runs, the sequence was as follows:

(1) Three OBE runs with the devices de-energized.

(2) One OBE run, energizing all "forward" contactors, and then another OBE run, energizing all "reverse" contactors.

(3) One OBE run, energizing the "reverse" contactors, and then another SSE run with the devices de-energized.

(4) One SSE run, energizing both the "forward" and "reverse" contactors three times each to simulate operating conditions.

Figures 2.14 to 2.17 show the 3% damping TRS and the spectrum for the bucket response motion on the Size 1 controller for the third SSE level run in both the X-Y and Z-Y axes [8]. From these figures it can be seen that the Size 1 controller responded like a rigid body in both the vertical and horizontal directions, except for certain amplification at the high frequency range (exceeding 30 Hz) in the horizontal response.

No chattering was observed during the tests of the MCC with the three Size 1 controllers. For runs including the Size 2 to 5 controllers and the two feeder breakers, a few anomalies were observed but were determined not to affect the safety function of the equipment for the following reasons [3,7]:

(1) During the first X-Y axes SSE run, one normally-open (NO) and one NC auxiliary contact on the Size 4 controller chattered at the 2 msec threshold. Circuit analysis determined that the auxiliary contacts are used only for control room indicator lights and the chatter could at most result in momentary flickering of these lights. Momentary actuation of indicating lights during a seismic shaking, with the contacts and indicating lights returning to proper status on cessation of the seismic motion, was judged to have no unacceptable impact on plant safety.

(2) During the second X-Y axes SSE run, one NC contact chattered with the Size 2 reversing controller de-energized. The effect of this chatter has been analyzed and determined to present no degradation of any safety function. The reason for this conclusion is that all safeguards initiation signals are sealed-in until manually reset. Therefore, if the NC contact chattered and momentarily caused a motor-operated valve to stop for a small fraction of a second, it would immediately resume travel as directed by the safeguards initiation signal.

The above analyses confirmed that the MCC column performed its required safety function during the retests although two anomalies were detected.

From the previous discussions of the test results we can qualitatively summarize the seismic response characteristics of the MCC vertical column as follows:

- The structural frame of the MCC column is essentially rigid, with the vertical natural frequency substantially exceeding 50 Hz and the horizontal natural frequency exceeding 30 Hz.

  The dynamic characteristics of the structural frame is about the same in both horizontal directions due to the square plan dimension and the two-dimensional bracing at the top of the vertical column.

- Based on the bucket response spectrum, the draw-out unit with Size 1 starter exhibited essentially rigid behavior in both the vertical and horizontal axes, with some amplification of the horizontal motion for frequencies exceeding 30 Hz. The draw-out unit with the Size 5 starter had a fundamental frequency of about 12 and 9 Hz in the F-B (X-) and S-S (Z-) axes, respectively, and a fundamental frequency exceeding 50 Hz in the vertical axis. In any case, significant amplification of the high frequency motion was observed in all three axes.

- The bucket response characteristics are essentially linear with the level of the test table ZPA, up to at least about 1.7g in the horizontal direction.

2.6 Seismic Capability

Based on the test results discussed previously, we estimated the minimum seismic capability of the MCC column as follows:

$(\check{A}_V)_{min}$ - A base motion ZPA equal to 1.1g because the vertical frequency of the MCC column exceeds at least 50 Hz and the MCC may be practically considered to be rigid in the vertical direction. This base motion ZPA capability is applicable to the MCC both with and without adding the seismic clips to the draw-out units, based on the observation that this structural modification only enhanced the seismic performance of the devices for vibrations in the F-B (X-) direction. The fact that no relay chattering was ever detected in anyone run in the Z-Y axes, whether or not the seismic clips were added, further confirms the validity of the previous conclusion.

$(\overset{\vee}{A}_H)_{min}$ - A response spectrum for the base motion that has a ZPA of 1.7g, because the devices may have a horizontal frequency as low as 9 to 12 Hz. The idealized minimum capability spectrum for a 3% damping is shown in Fig. 2.18. It represents the idealized mean TRS based on the upper and lower bound TRS envelopes for all the SSE level qualification tests, as shown in Fig. 2.19. This minimum horizontal ZPA capacity of 1.7g is for the MCC with the addition of the seismic clips.

For the commercial standard MCC vertical column, i.e. without the addition of the seismic clips to the draw-out units, the minimum horizontal seismic capability may be inferred from the results of the initial tests. During the initial tests in the X-Y axes, excessive F-B movements of the draw-out units and chattering of the NC contactors were noted in the SSE runs, but no chattering was ever detected in the OBE runs except for the Size 5 controller with the defective spring. Thus we judge that the minimum horizontal base ZPA capability of the MCC column would lie between the OBE and the SSE test table ZPA, i.e. between 1.2g and 1.7g. To estimate the minimum ZPA capability we will assume that the SSE test ZPA of 1.7g corresponds to a 50% probability of failure at a 95% confidence limit. With random variability assumed to be $\beta_r = 0.09$ (based on the observations discussed in Section 1.5), we back calculate the ZPA corresponding to a 5% probability of failure at the same 95% confidence limit to be 1.4g. This is our estimated minimum horizontal ZPA capability for the commercial standard MCC vertical column. The minimum capability spectrum associated with the 1.4g ZPA is equal to 1.4/1.7 = 0.85 times the horizontal capability spectrum for the structurally modified MCC column that is shown in Fig. 2.18.

To estimate the fragility of the MCC vertical column, we use the same assumptions previously adopted for the plant-specific fragility evaluation of the other Diablo Canyon plant electrical components [2]. The only exception is that the fragility descriptor will be represented by both the ZPA and ASA of the base motion for the component where, as previously mentioned in Section 1, the ASA is the average spectrum acceleration for 2% damping and from 4 to 16 Hz. The assumptions for the current fragility evaluation are, therefore:

(1) The base motion for the MCC may be adequately represented by either the ZPA or the ASA. Since the TRS is associated with a 3% damping, the ASA is determined by first averaging the TRS from 4 to 16 Hz and then increasing the average TRS by a factor of 1.2. The factor 1.2 was suggested by BNL to account for the increase in average spectrum acceleration with damping decreasing from 3% to 2% (see Ref. 6).

(2) The minimum seismic capability, expressed by either the ZPA or ASA of the base motion, is associated with a maximum failure probability of 5% with a 95% confidence. This is the HCLPF base ZPA or ASA.

(3) The probability distribution of the fragility is log-normal and the associated modeling uncertainty and random variability is $\beta_u = 0.18$ and $\beta_r = 0.09$, respectively, for both the ZPA and ASA, although the variability for ASA is expected to be higher than that for the ZPA.

(4) The horizontal ASA fragilities of both the commercial standard and structurally modified motor control centers are proportional to the corresponding ZPA fragilities, with the same proportional factor.

Consistent with these assumptions, our estimate of the median seismic capability and the pertinent variability is shown in Table 2.1, in which A and S denote the median ZPA and ASA fragility, respectively.

Figures 2.20(a) and 2.20(b) show the horizontal seismic fragility for the commercial standard and structurally enhanced MCC columns, respectively, the fragility of the former being about 0.85 times that of the latter.

The vertical seismic fragility is the same for both the commercial standard and modified MCC columns, as shown in Fig. 2.21. The ratio of the ASA to ZPA capacity is about 3.5 and 2.4 for the horizontal and vertical direction, respectively.

2.7 Comparison with MCC Demonstration Tests

In its Phase I demonstration test program, LLNL conducted a fragility evaluation for a three-column Westinghouse Five-Star motor control center [1]. The configuration of a Five-Star MCC vertical column is very similar to that of the Type W MCC vertical column considered in the Diablo Canyon qualification tests. Various anchoring conditions were considered in the LLNL tests of the Five-Star MCC, including the one in which each vertical column was anchored at the base with 4 bolts and braced at the top. Relays of both the reed and armature types, from various manufacturers, and Westinghouse starters of Sizes 2 (both reversing and non-reversing), 3 and 4 were devices mounted on the MCC. A total of 56 runs were performed, 43 of which were biaxial random motion test (vertical plus one horizontal axis). The shaker table ZPA's ranged from about 0.9g to 2.5g, and in those biaxial tests the vertical TRS was essentially identical to the horizontal TRS. Chatter of contacts was monitored during each test, and functional failure was defined at the first sign of a contact chattering.

The top-braced commercial standard MCC of the Type W may be compared to the top-braced Five-Star MCC that was used in the LLNL demonstration tests. The correlation in the seismic fragility between the two motor control centers may be summarized in the following:

(1) With the top bracing, no structural damage was ever observed during the demonstration tests of the Five-Star MCC and during the qualification tests of the Type W MCC while chatter of the contacts was detected in both series of tests. This result verified our judgmental ranking of the seismic failure modes for the MCC, namely, functional failure is the prevailing mode of seismic failure.

(2) Both the qualification tests of the Type W MCC and the demonstration tests of the Five-Star MCC consistently showed that the motor control centers are more vulnerable to F-B motions than to S-S and vertical motions. Thus the horizontal seismic capacity of the MCC is governed by its capacity for F-B vibrations.

(3) The LLNL demonstration tests for the top-braced MCC were conducted at five levels of shaker table ZPA, i.e. 1.0, 1.3, 1.4, 1.8, and 2.1g. On the basis of the shaker table ZPA at which contact chatter was detected, the horizontal (F-B) seismic capacities of the Size 2 to Size 4 starters may be ranked in the following descending order: (a) Size 3 starter: no contact chatter occurred at any of the five test table ZPA levels, (b) Size 4 starter: chatter of contact was detected at the shaker table ZPA of 1.8g and higher, (c) Size 2 starter: chatter occurred at a shaker table ZPA of 1.3g and higher. The same ranking applies to the Size 2 to Size 4 starters mounted on the commercial standard Type W MCC, based on results from the qualification tests. For the F-B tests, none of these starters experienced contact chattering during all OBE level runs (shaker table ZPA = 1.2g) and the first two SSE level runs (shaker table ZPA was only 1.1g and did not reach the full SSE level); in the remaining four SSE level runs (shaker table ZPA = 1.7g), the Size 3 starters did not chatter, the Size 4 starters experienced contact chattering during one run, and the Size 2 starters experienced contact chattering during three runs. Thus, as far as the Size 2 to 4 starters are concerned, the consistency in seismic performance between the two top-braced commercial standard motor control centers may be concluded as follows:

- Ranking of the seismic capacity of the MCC-mounted starter, in terms of the MCC base ZPA and in descending order, is Size 3, 4, and 2.

- At a base ZPA of 1.8g and higher for the Five-Star MCC, both the Size 2 and 4 starters chattered while the Size 3 starters did not. The same performance was observed for the Size 2 to 4 starters on the Type W MCC at a base ZPA of 1.7g.

(4) For the Five-Star MCC, the results from the demonstration tests showed that the ratio of the median to HCLPF seismic capacity is essentially the same for both the relays and starters, being about 1.56 (see Table 5-1, Ref. 1). This is consistent with the corresponding ratio we adopted in the fragility evaluation of the Type W MCC, being about 1.56 based on the assumed variabilities of $\beta_u = 0.18$ and $\beta_r = 0.09$. In other words, the demonstration test of the MCC confirmed the reasonableness of the median-to-HCLPF capacity ratio we assumed for the Type W MCC. In addition, the demonstration tests established that the β_u derived from the test data was typically 2 to 3 times the β_r, which confirmed the reasonableness of the values of β_u and β_r we estimated for the Type W MCC.

(5) According to Item (3) above, test results for both the Five-Star and Type W MCC consistently showed that Size 2 starters governed the minimum seismic capacity of the MCC. According to Ref. 1, the demonstration tests estimated the capacity of the MCC-mounted Size 2 starters, in terms of the local device ZPA, to be 2.5g and 3.9g for the HCLPF and median level, respectively. Based on the test data, an average amplification factor for ZPA from the MCC base to the device locations may be taken to be 2.1. Thus the horizontal seismic capacity of the Five-Star MCC, in terms of ZPA at its base, may be deduced from the local device ZPA capacity of the Size 2 starters to be: 2.5g/2.1 = 1.2g for HCLPF capacity; and 3.9g/2.1 = 1.9g for median capacity. For the commercial standard Type W MCC the corresponding base ZPA capacities were previously estimated to be 1.4g and 2.3g, respectively, which are 20% higher than those for the Five-Star MCC estimated above. Such a discrepancy is expected because of the difference in the criteria for failure. For the Five-Star MCC, the first sign of a contact chatter was defined as a functional failure whereas for the Type W MCC the chatter of a contact was not considered a functional failure if, through circuit analysis, the chatter did not impair the required safety function of the controlled load. These different bases for defining functional "failure" will be referred to as failure criteria (2) and (1), respectively, in subsequent discussions. That is, the more conservative failure criterion (2) was used in the fragility study of the Five-Star MCC while failure criterion (1) has been consistently adopted in our fragility evaluation of the electrical components installed in the Diablo Canyon Nuclear Plant. Recall that the capacity for the commercial standard Type W MCC was estimated on the basis of our judgmental assumption that the 1.7g ZPA on the TRS corresponds to a median capacity associated with the 95% confidence level. The seismic capacity would have been lower had we based our evaluation on failure criterion (2) and simply taken the 1.2g ZPA on the TRS for the OBE level qualification tests to be the HCLPF capacity, thus giving a 1.9g median capacity. This example illustrates that when the more conservative failure criterion (2) was used as the evaluation basis the seismic capacity of the Type W MCC would be essentially equal to that of the Five-Star MCC based on the same

failure criterion (2). Thus, we conclude that the horizontal seismic capacities of the two top-braced motor control centers are consistent with each other, the difference being due to the use of a different criterion of functional failure.

Table 2.2 summarizes the comparison of the horizontal seismic capacities between the two top-braced MCC columns. For the Type W MCC, the fragilities based on both failure criteria are listed. The capacity under failure criterion (1) was presented in Section 2.6, and the capacity under failure criterion (2) was estimated in Item (5) above. The ASA capacity for failure criterion (2) was estimated assuming the same ASA/ZPA capacity ratio as that for failure criterion (1), i.e. 3.5 for the horizontal axis. For the Five-Star MCC, the ASA capacity is equal to the average 5% damping TRS estimated from Ref. 1, increased by a factor of 1.35 to account for the adjustment in ASA for damping decreasing from 5% to 2% (see Ref. 6).

The correlation in the dynamic response characteristics between the Five-Star and Type W motor control centers, each with top bracing, is discussed in the following:

(1) According to Table 4-1 from Ref. 1, the resonance frequency of the top-braced Five-Star MCC was about 12 Hz in the F-B axis, and it contained Size 2 to Size 4 starters. For the top-braced Type W MCC, which contained Sizes 2 to 5 starters, the F-B resonance frequency was about 11 to 12 Hz also.

For the Type W MCC containing only the three Size 1 starters the F-B resonance frequency exceeded 30 Hz, which was expected because the Size 1 starter is much lighter than the larger size starters. From the previous observations we conclude that the F-B resonance frequency of both top-braced motor control centers would be around 11 to 12 Hz when they contain starters of Size 2 or larger, and would be higher than 12 Hz when they contain fewer or only Size 1 starters.

A discussion for the correlation in the S-S resonance frequency is not feasible since Ref. 1 did not provide this information for the Five-Star MCC. However, we believe, by judgments, that a conclusion similar to that for the F-B axis is also reasonable for the S-S frequency.

Regarding the local resonance frequency for the draw-out units (i.e. the bucket frequency), it is not identifiable from the test results for both top-braced motor control centers. Our observation is that the bucket frequency is very high, exceeding 30 Hz.

(2) The LLNL demonstration tests showed that the addition of the mounting screws to the draw-out units did not materially improve the seismic performance of the MCC so far as contact chattering is concerned, nor modified the dynamic response of the MCC. For the

seismic qualification test of the Type W MCC, the addition of the seismic clips to the draw-out units did not materially modify the dynamic response characteristics, either, although it reduced the extent of contact chattering to to an acceptable limit. This suggests that the occurrence of chatter depends more on the intensity of motion than on the frequency response of the contact element.

2.8 Comparison with BNL Study of MCC Fragility

Table 3.2 of Ref. 6 presents the results of the BNL study of generic horizontal seismic fragility of motor control centers from five different manufacturers that are commonly installed in nuclear plants. The fragility, expressed in both ZPA and ASA, is based on failure criterion (2), i.e. occurrence of contact chatter is defined as a failure. Two methods were used in the statistical analysis of the test data. Method (1) is the method of moments, and Method (2) is the method of maximum likelihood. The two methods gave results that were not significantly different from each other. They are listed in Table 2.1 for comparison with the corresponding seismic fragilities of the Type W MCC. The comparison is discussed in the following:

(1) Regarding the variability, the BNL results suggest that our assumed value of $\beta_u = 0.18$ and $\beta_r = 0.09$ appears to be reasonable for the ZPA capacity but somewhat underestimated for the ASA capacity. This, of course, is anticipated because our current study is for one plant-specific MCC column only.

(2) Regarding the ZPA capacity, the BNL result is about one-half and two-thirds of the value we estimated for the Type W MCC under failure criteria (1) and (2), respectively. Note that the basis for the fragility study by BNL corresponded to failure criterion (2). Regarding the ASA capacity, the BNL result is about one-third and one-half of the corresponding ASA capacity we estimated for the Type W MCC under failure criteria (1) and (2), respectively. Again, such difference in the estimated capacity is anticipated because our current study was for only one top-braced Type W MCC column while the BNL study was for freestanding columns from several manufacturers.

In summary, the outcome of the above comparison between the BNL generic horizontal fragility for free-standing motor control centers and the plant-specific horizontal fragility for the top-braced Type W MCC is anticipated. As previously discussed in Item (1), the variability we assumed in our evaluation of the Type W MCC is somewhat lower than the corresponding result from the BNL study. To examine the sensitivity of the median capacity to the value of the variability, we re-computed the median capacity for the Type W MCC based on our previously estimated HCLPF horizontal capacity and on the variability from the BNL study. The results are shown in Table 2.3. The larger variability produced a median capacity that is higher than the corresponding one in Table 2.2,

which was based on $\beta_u = 0.18$ and $\beta_r = 0.09$. This is because the ratio of the median to the HCLPF capacity is proportional to the variability.

Table 2.1 Seismic fragility for the Westinghouse Type W motor control center (single column).

	Standard Commercial[1] Configuration		Structurally Modified[2]	
	$\hat{A}^v$	$\hat{S}^v$	$\hat{A}^v$	$\hat{S}^v$
Horizontal (g)[3]	2.3	8.0	2.6	9.1
Vertical (g)[3]	1.7	4.1	1.7	4.1
β_u	0.18		0.18	
β_r	0.09		0.09	

Notes:

1. Standard commercial configuration, top bracing added.
2. Seismic clips added to draw-out units.
3. $\hat{A}^v$ = median capacity based on ZPA

   $\hat{S}^v$ = median capacity based on ASA

Table 2.2 Comparison of horizontal seismic fragility for various motor control centers.

	Type W (Current Study)		Five-Star (LLNL Tests)		Generic (BNL Study)	
Failure Criterion[1]	Criterion (1)		Criterion (2)		Criterion (2)	
Top bracing?	Yes	Yes	Yes	Yes	No	
Seismic clips?	Yes	No	No	No	No	
A_{oH} (HCLPF,g)	1.7	1.4	1.2 [2]	1.2 [3]	0.8 [6]	0.8 [7]
$\hat{A}_H$ (median,g)	2.6	2.3	1.9	1.9	1.3	1.3
β_u	0.18	0.18	0.18	0.21	0.18	0.24
β_r	0.09	0.09	0.09	0.06	0.10	0.09
S_{oH} (HCLPF,g)	6.0	5.1	4.2 [4]	4.7 [5]	1.7	1.7
$\hat{S}_H$ (median,g)	9.1	8.0	6.4 [4]	7.4 [5]	2.9	3.1
β_u	0.18	0.18	0.18	n/a	0.25	0.31
β_r	0.09	0.09	0.09	n/a	0.06	0.06
S_{oH}/A_{oH}	3.5	3.5	3.5	3.9	2.1	2.1
$\hat{S}_H/\hat{A}_H$	3.5	3.5	3.5	3.9	2.2	2.4

Notes:

1. Criterion (1): Contact chatter not considered as "failure" if circuit analysis shows that the safety function is not impaired.

   Criterion (2): Contact chatter is defined a failure.

2. ZPA of the OBE level TRS taken to be the HCLPF ZPA for failure criterion (2).

(continued on next page)

Table 2.2 (cont.) Comparison of horizontal seismic fragility for various motor control centers.

Notes (cont.):

3. MCC base ZPA fragility is the ZPA fragility at the starter mounting location divided by an estimated amplification factor of 2.1.

4. Based on the same S to A ratio (3.5) as for failure criterion (1).

5. Based on the averaged 5% damping TRS as increased by 1.35 to account for the adjustment from 5% to 2% damping ASA.

6. Statistical analysis by method of moments (see Ref. 6).

7. Statistical analysis by method of maximum likelihood (see Ref. 6).

Table 2.3 Horizontal median capacity of Type W MCC recomputed based on variability from BNL study.

Failure Criterion[1]	(1)		(2)		(2)	
Seismic clips?	Yes		No		No	
A_{oH} (HCLPF,g)[2]	1.7		1.4		1.2	
Method[3]	(1)	(2)	(1)	(2)	(1)	(2)
β_u	0.18	0.24	0.18	0.24	0.18	0.24
β_r	0.10	0.09	0.10	0.09	0.10	0.09
$\hat{A}_H$ (median,g)	2.7	2.9	2.2	2.4	1.9	2.1
S_{oH} (HCLPF,g)[2]	6.0		5.1		4.2	
Method	(1)	(2)	(1)	(2)	(1)	(2)
β_u	0.25	0.31	0.25	0.31	0.25	0.31
β_r	0.06	0.06	0.06	0.06	0.06	0.06
$\hat{S}_H$ (median,g)	10.3	11.0	8.8	9.4	7.2	7.7

Notes:

1. Criterion (1): Contact chatter not considered as "failure" if circuit analysis shows that the safety function is not impaired.

   Criterion (2): Contact chatter is defined a failure.

2. A = fragility based on ZPA

   S = fragility based on ASA

3. Method (1): statistical analysis by method of moments

   Method (2): statistical analysis by maximum likelihood method

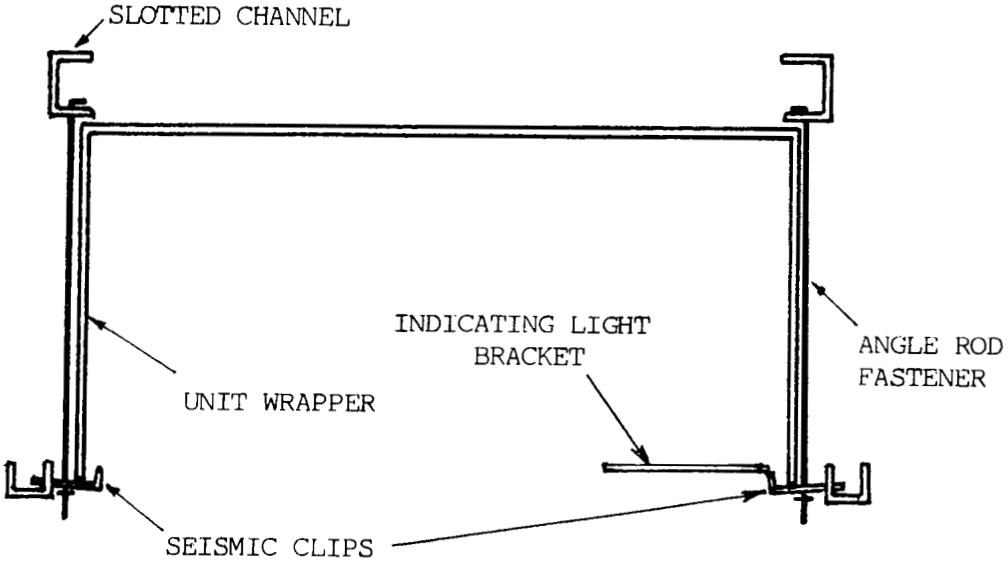

Fig. 2.1. Plan view of the seismic clips for the MCC draw-out units.

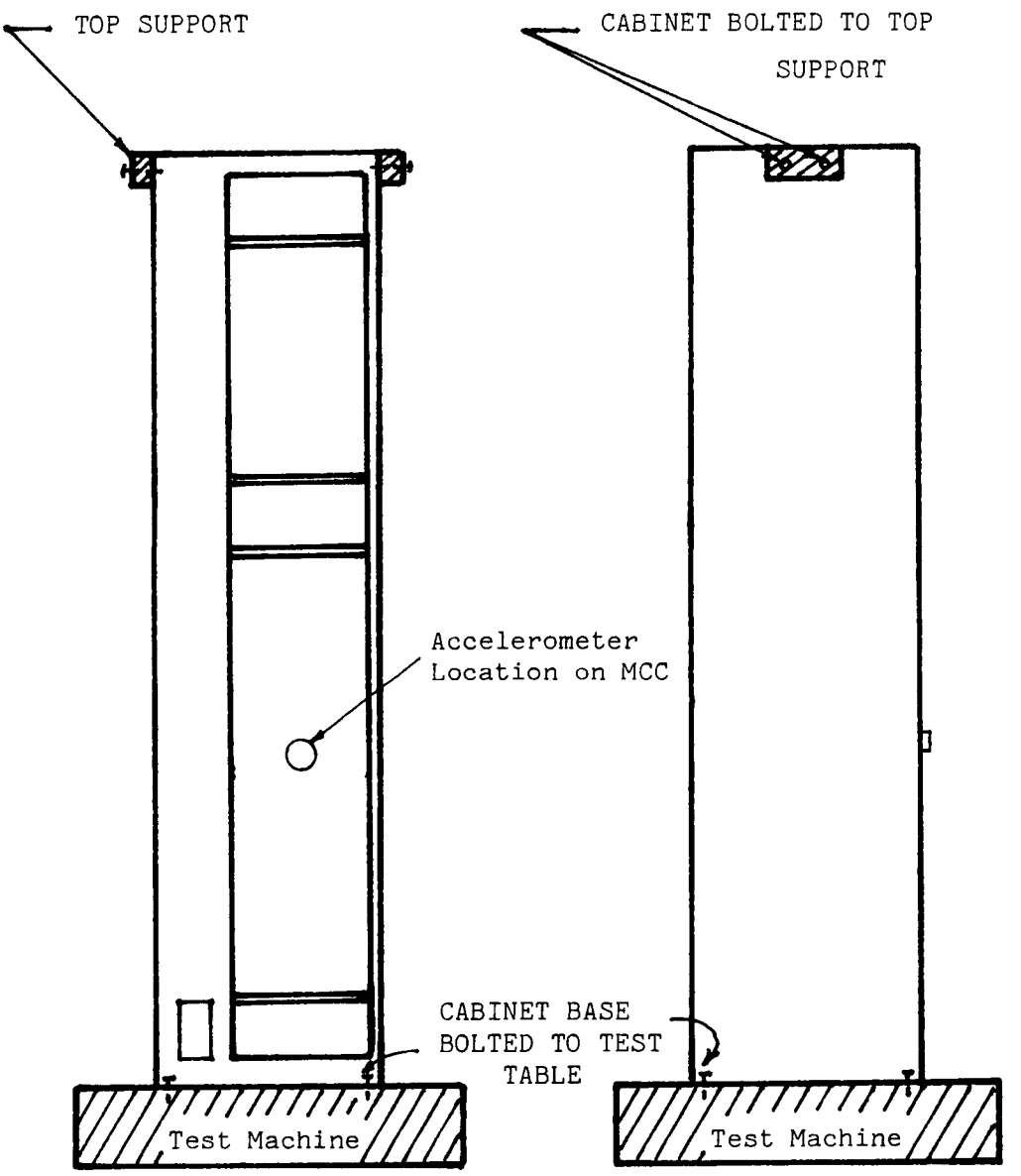

Fig. 2.2 **Test setup for the MCC single vertical column, showing the mounting of the cabinet and bucket response accelerometers.**

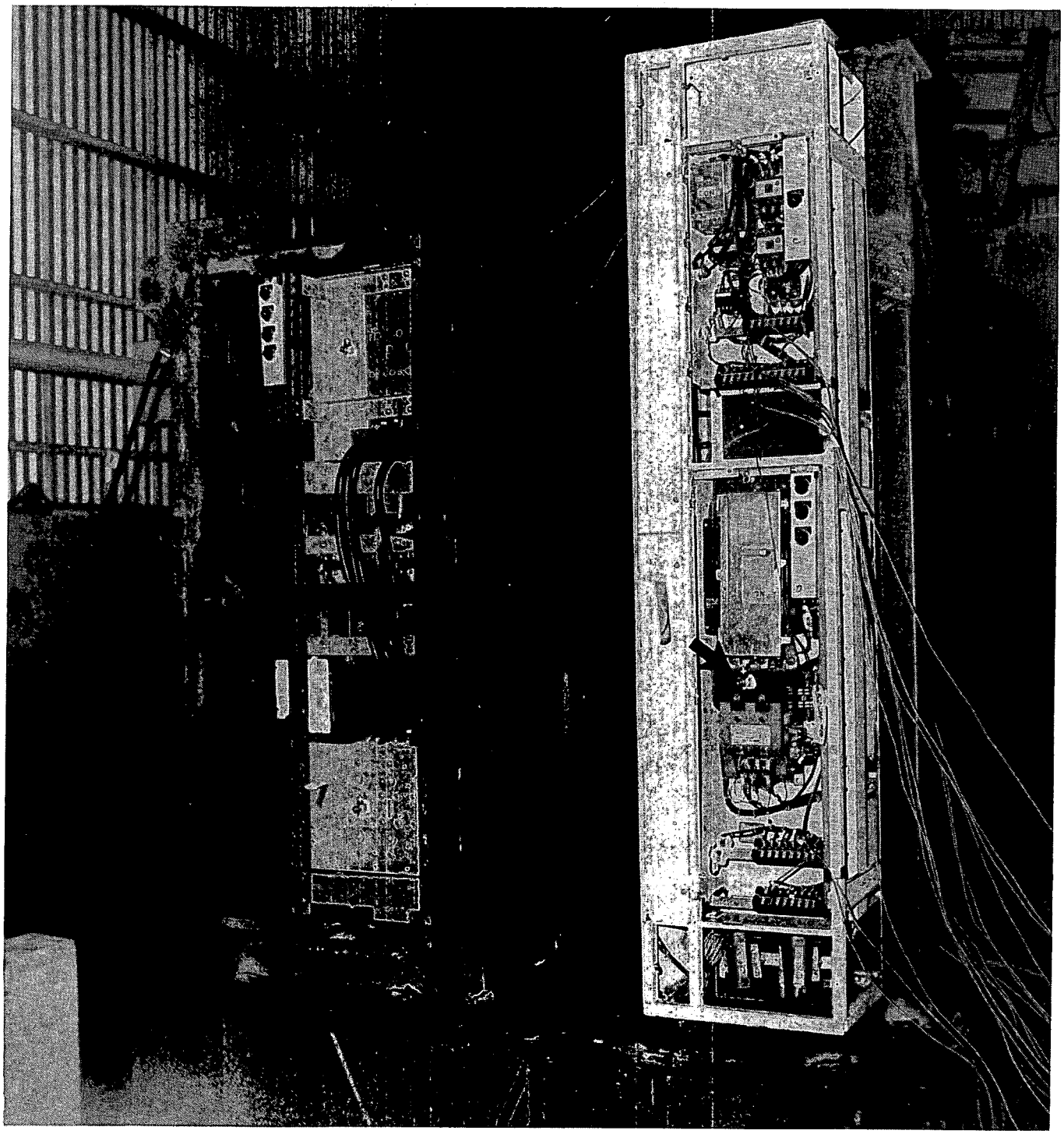

Fig. 2.3(a) Front-to-back and vertical (X-Y) axes setup for initial test of MCC and fan cooler motor controller. Arrow points to accelerometer location.

Fig. 2.3(b) X-Y axes setup for retest of MCC including seismic clips. Top and bottom arrows point to the locations of the seismic clips and the response accelerometers, respectively.

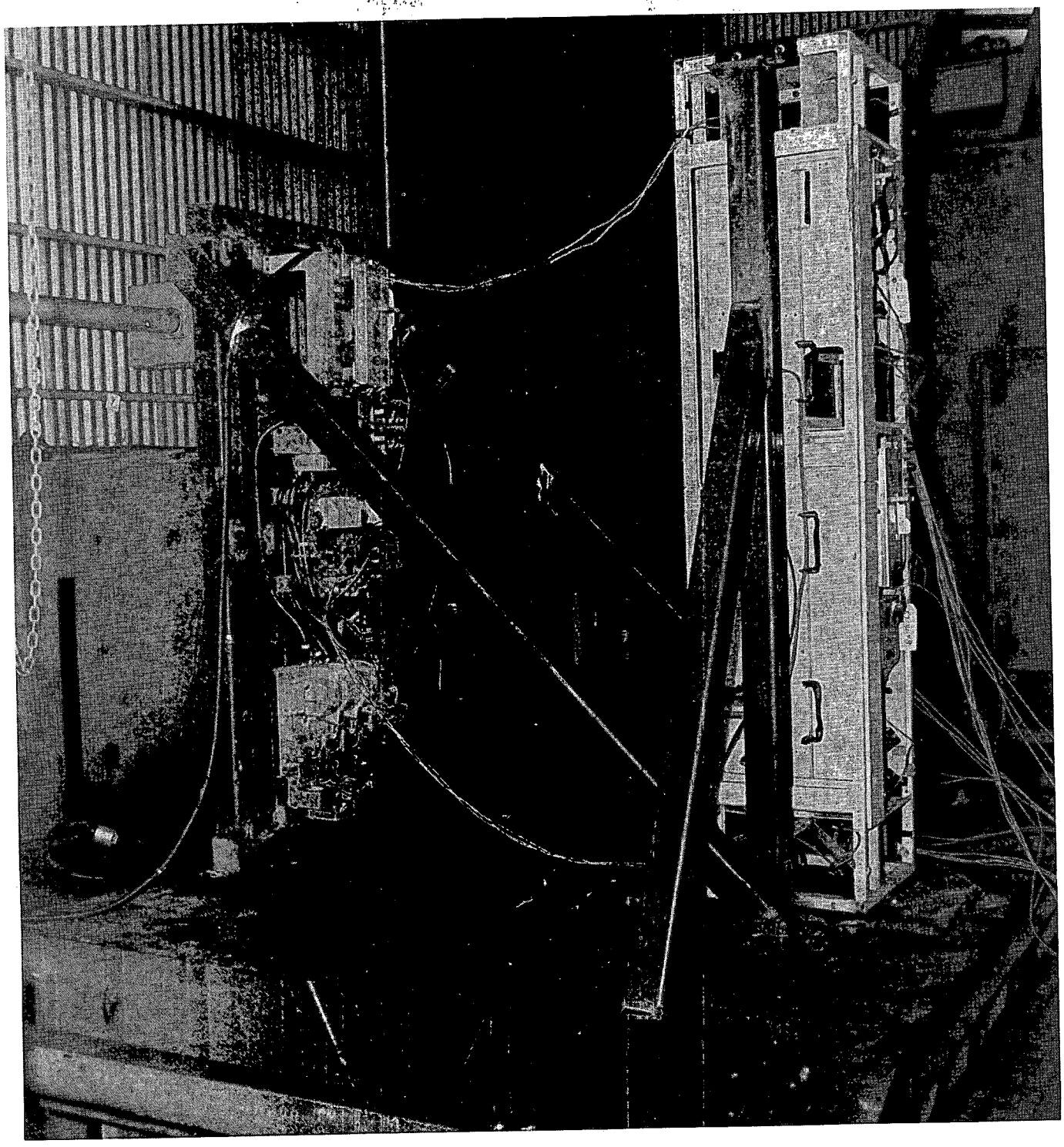

Fig. 2.4 Side-to-side and vertical (Z-Y) axes setup for initial test of MCC and fan cooler motor controller.

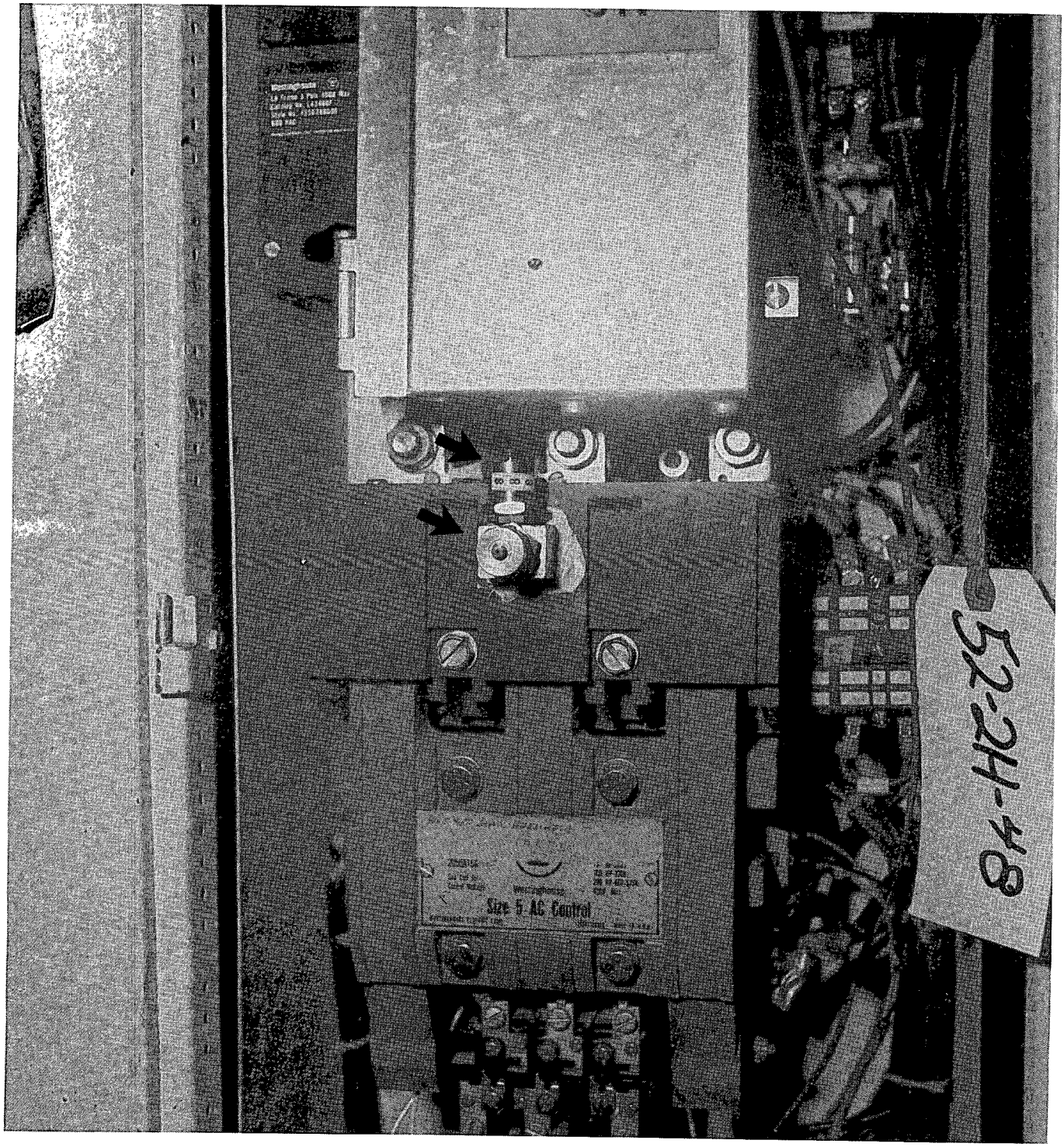

Fig. 2.5 Location of accelerometers on MCC front face.

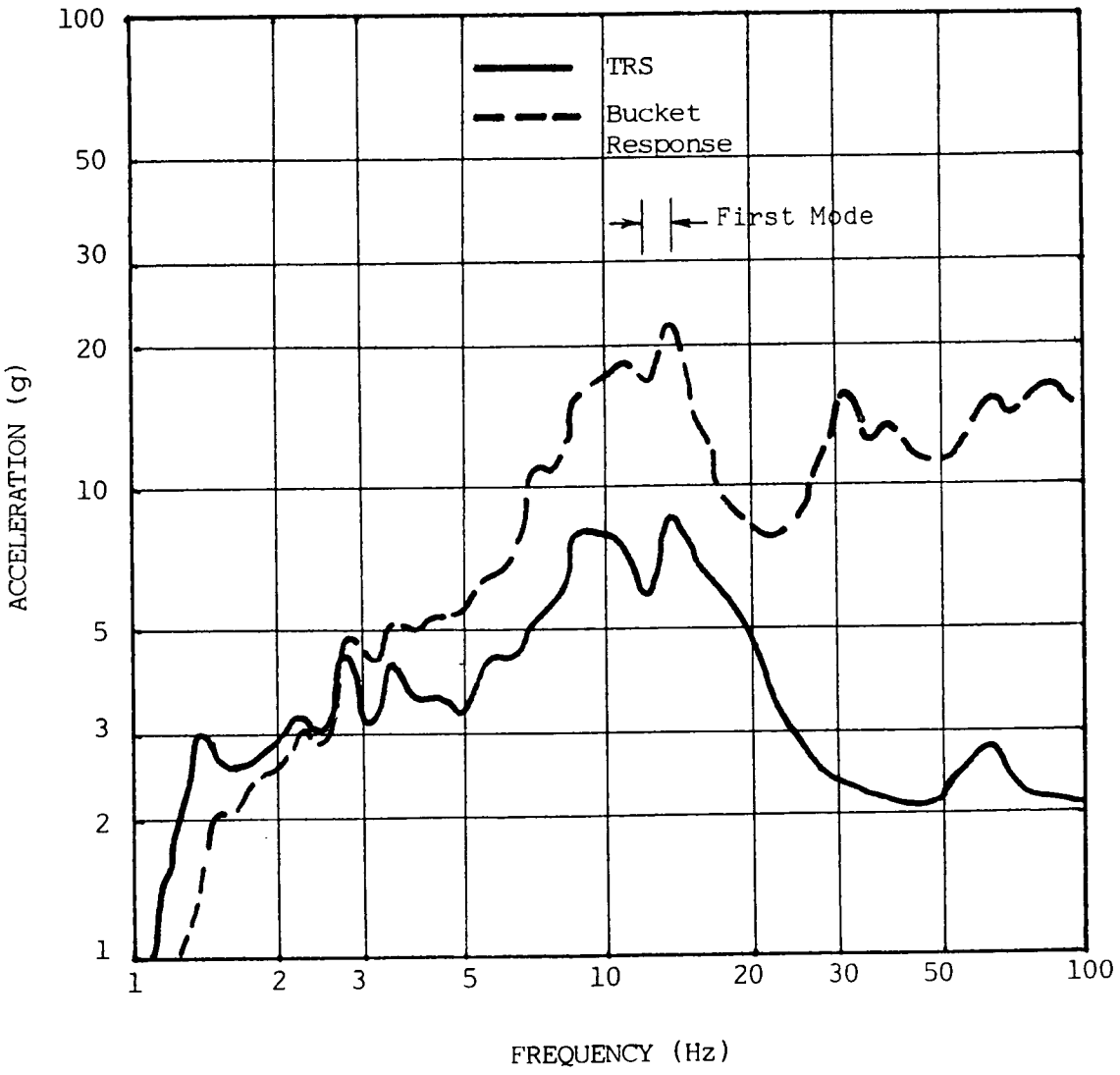

Fig. 2.6 Front-to-back TRS and bucket response spectrum at Size 5 starter during the sixth SSE initial test in the X-Y axes (3% damping, no seismic clips).

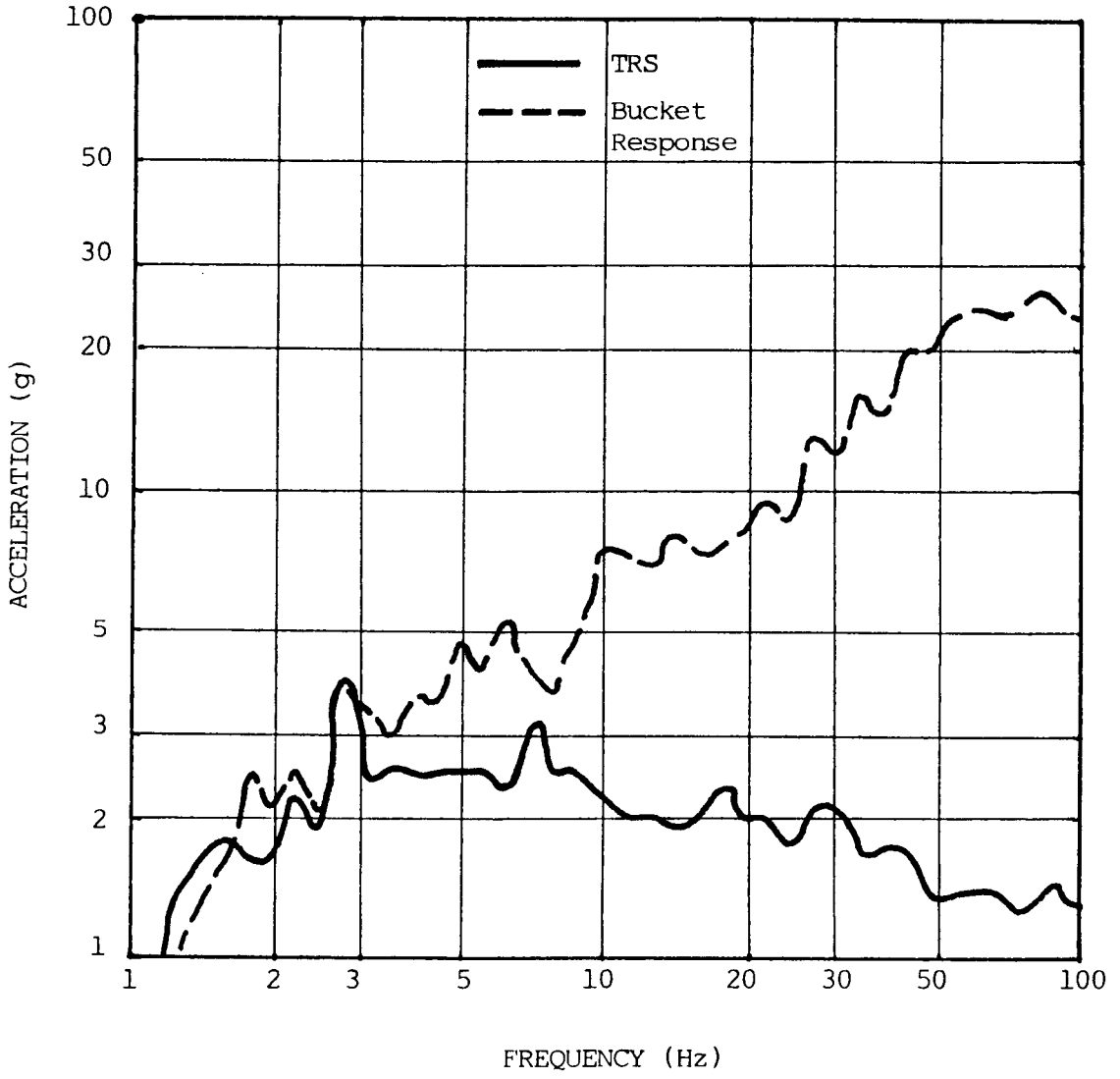

Fig. 2.7 Vertical TRS and bucket response spectrum at Size 5 starter during the sixth SSE initial test in the X-Y axes (3% damping, no seismic clips).

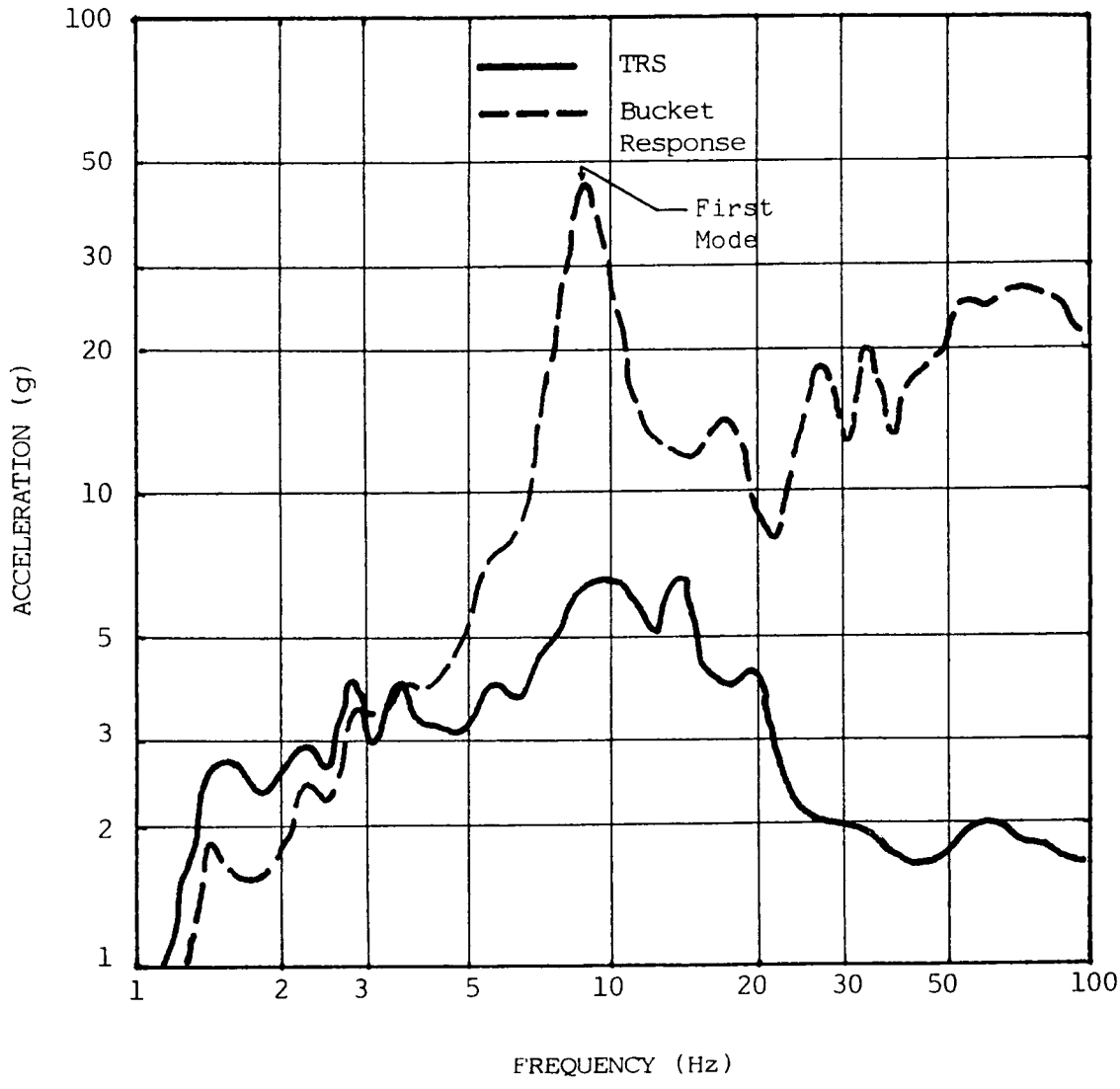

Fig. 2.8 Side-to-side TRS and bucket response spectrum at Size 5 starter during the third SSE initial test in the Z-Y axes (3% damping).

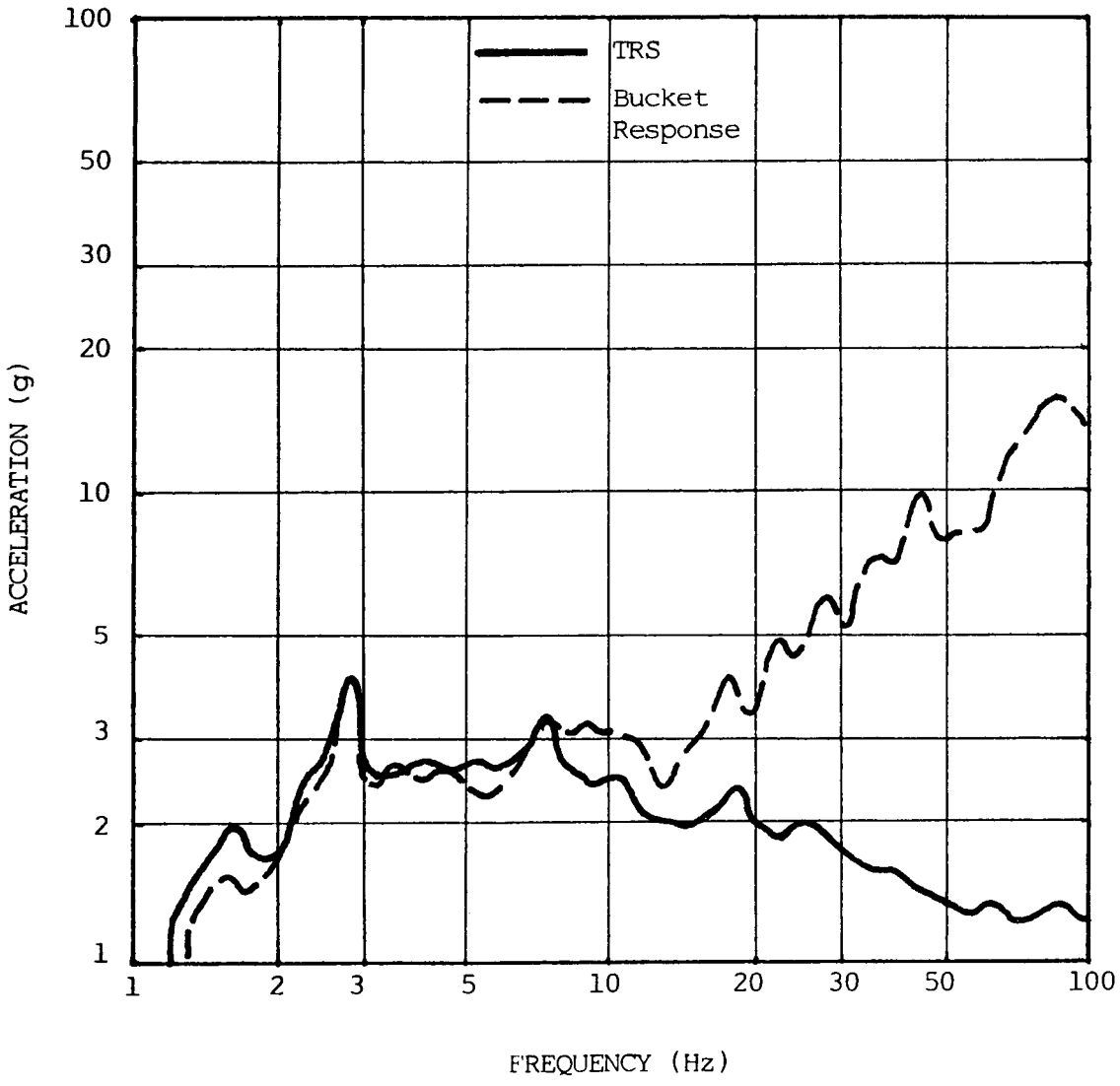

Fig. 2.9 Vertical TRS and bucket response spectrum at Size 5 starter during the third SSE initial test in the Z-Y axes (3% damping).

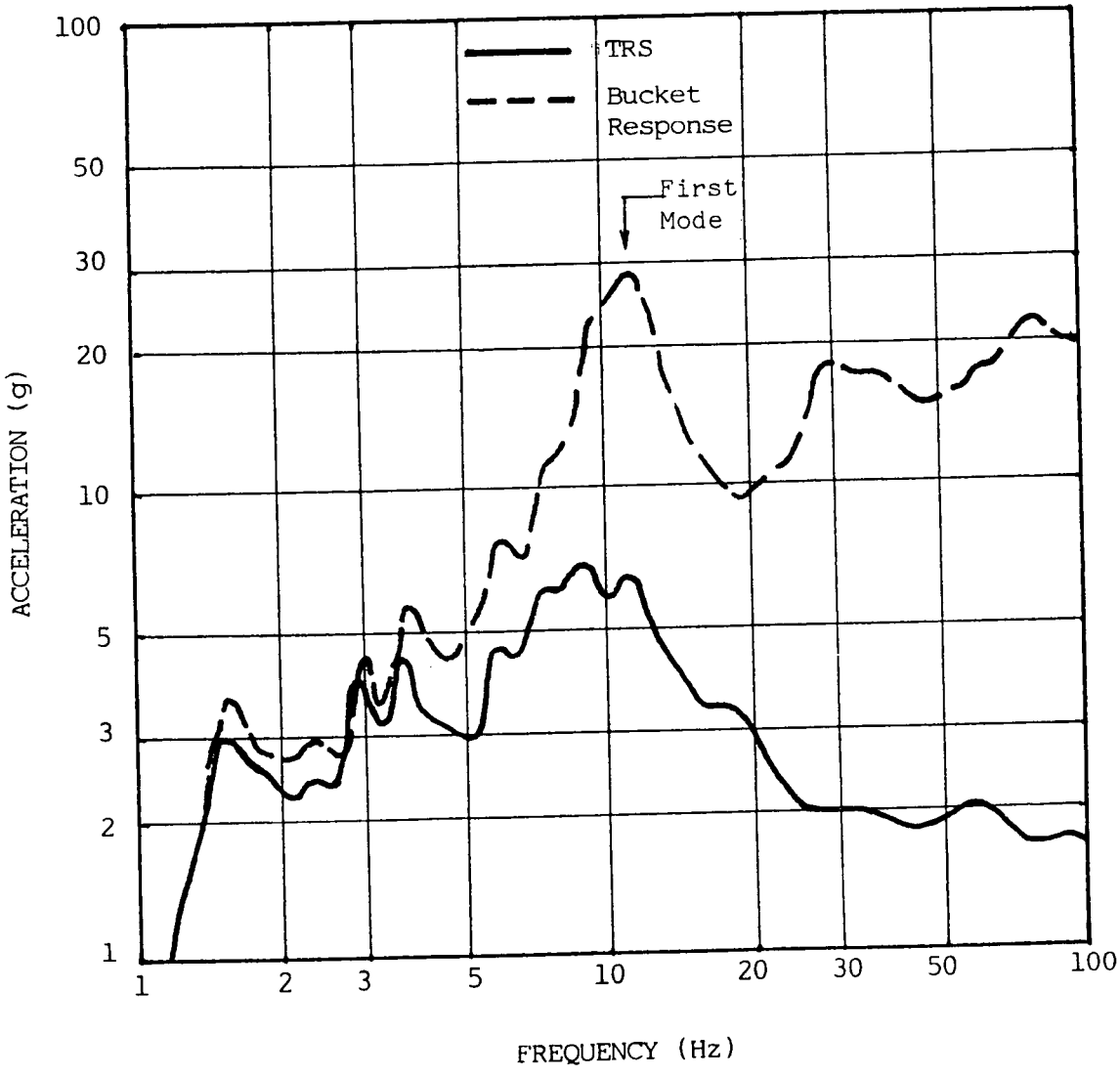

Fig. 2.10 Front-to-back TRS and bucket response spectrum at Size 5 starter during the third SSE retest in the X-Y axes (3% damping, with seismic clips). Compare with Fig. 2.6.

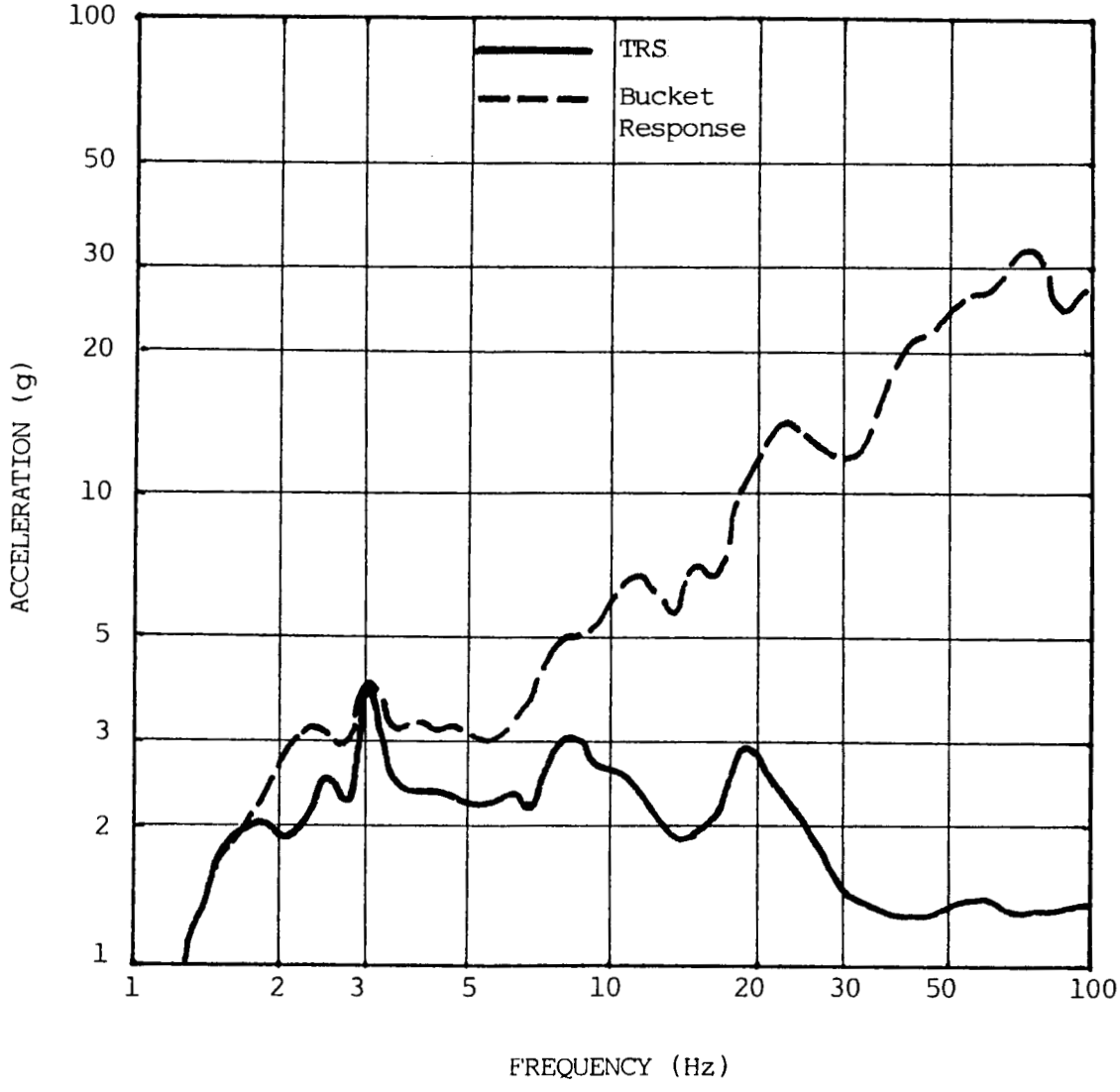

Fig. 2.11 Vertical TRS and bucket response spectrum at Size 5 starter during the third SSE retest in the X-Y axes (3% damping, with seismic clips). Compare with Fig. 2.7.

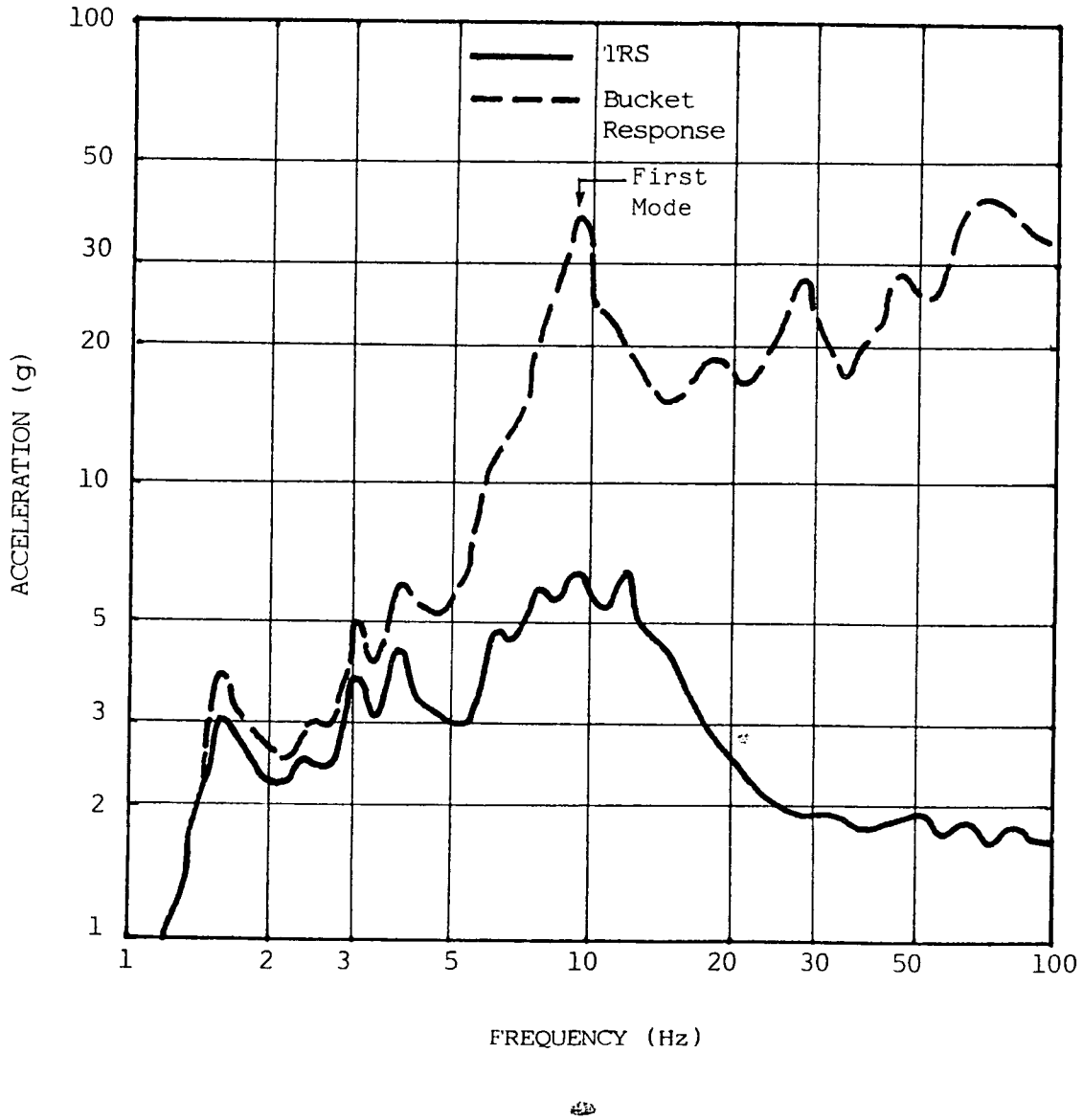

Fig. 2.12 Side-to-side TRS and bucket response spectrum at Size 5 starter during the third SSE retest in the Z-Y axes (3% damping, with seismic clips). Compare with Fig. 2.8.

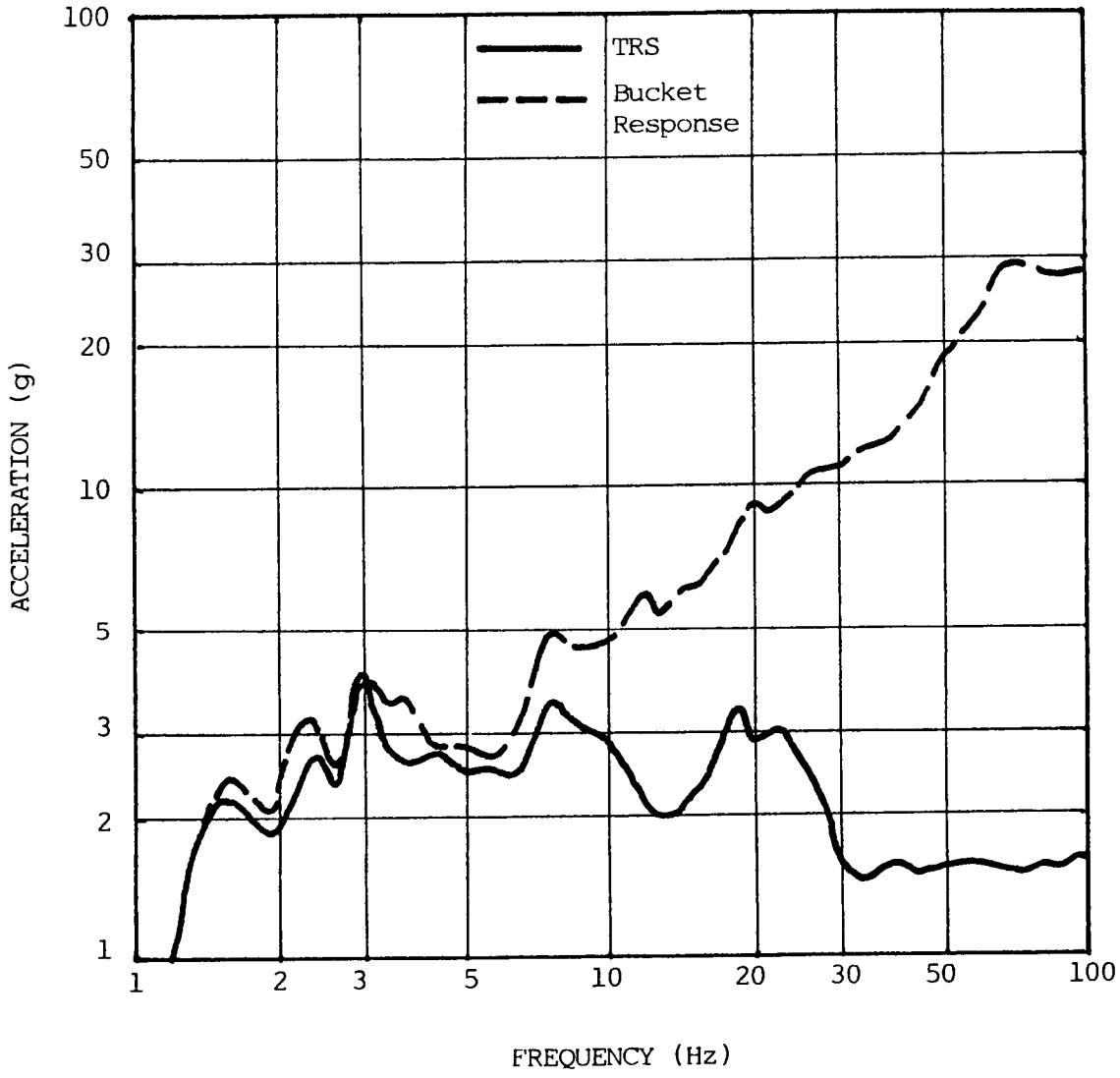

Fig. 2.13 Vertical TRS and bucket response spectrum at Size 5 starter during the third SSE retest in the Z-Y axes (3% damping, with seismic clips). Compare with Fig. 2.9.

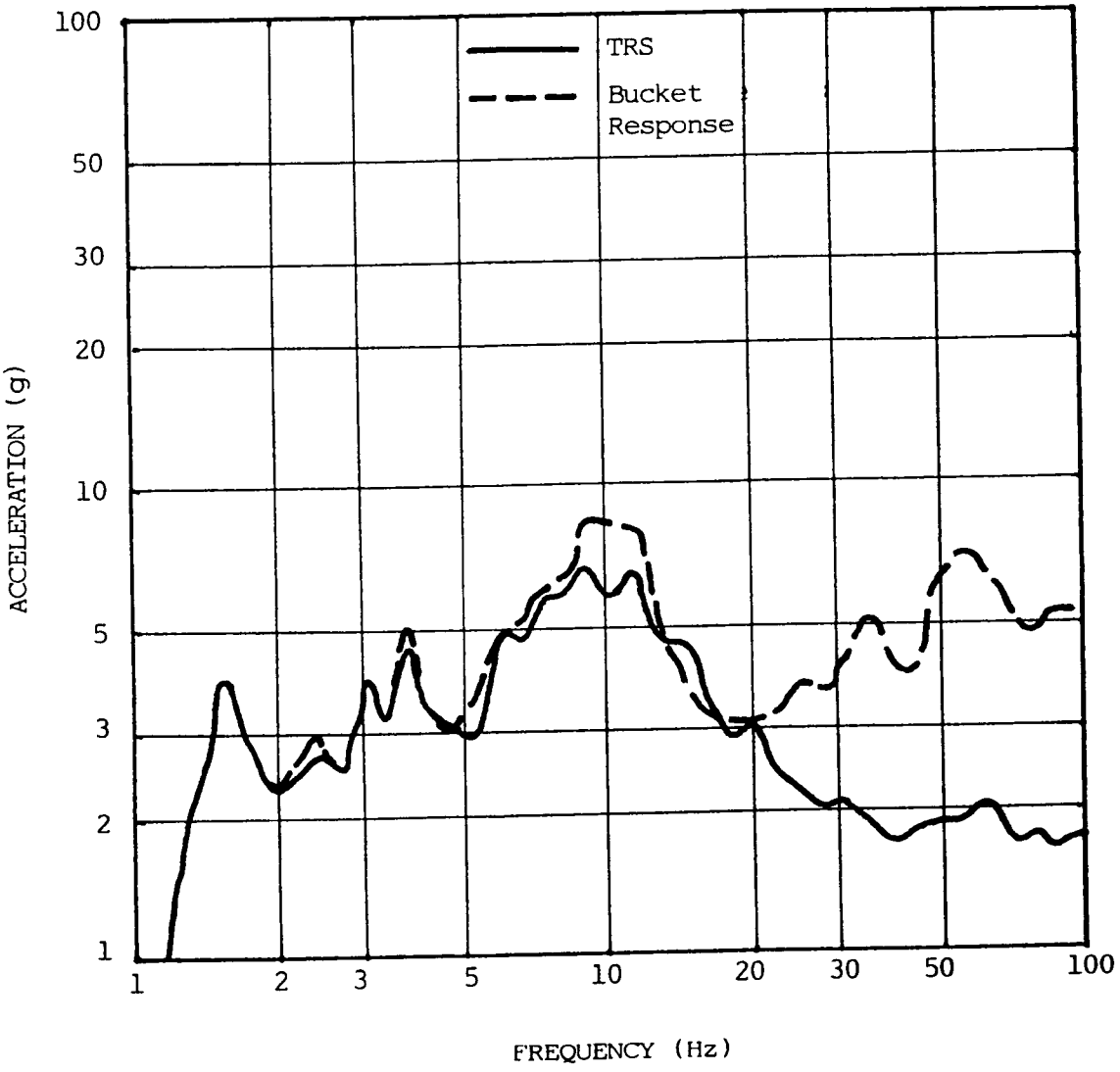

Fig. 2.14 Front-to-back TRS and bucket response spectrum at Size 1 starter during the fifth SSE retest in the X-Y axes (3% damping). Note that Size 2 through Size 5 starters have been removed from the MCC.

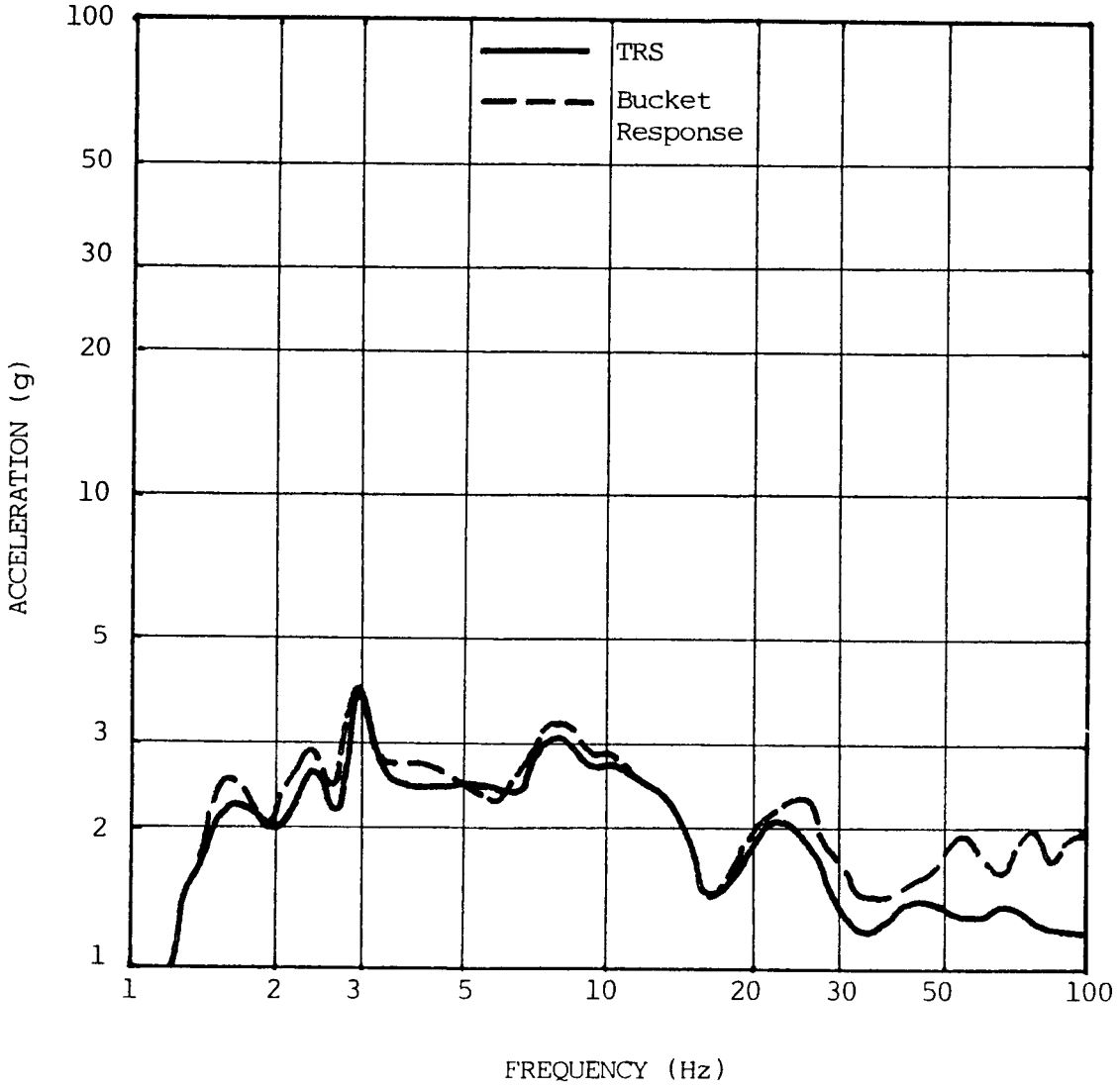

Fig. 2.15 Vertical TRS and bucket response spectrum at Size 1 starter during the fifth SSE retest in the X-Y axes (3% damping). Note that Size 2 through Size 5 starters have been removed from the MCC.

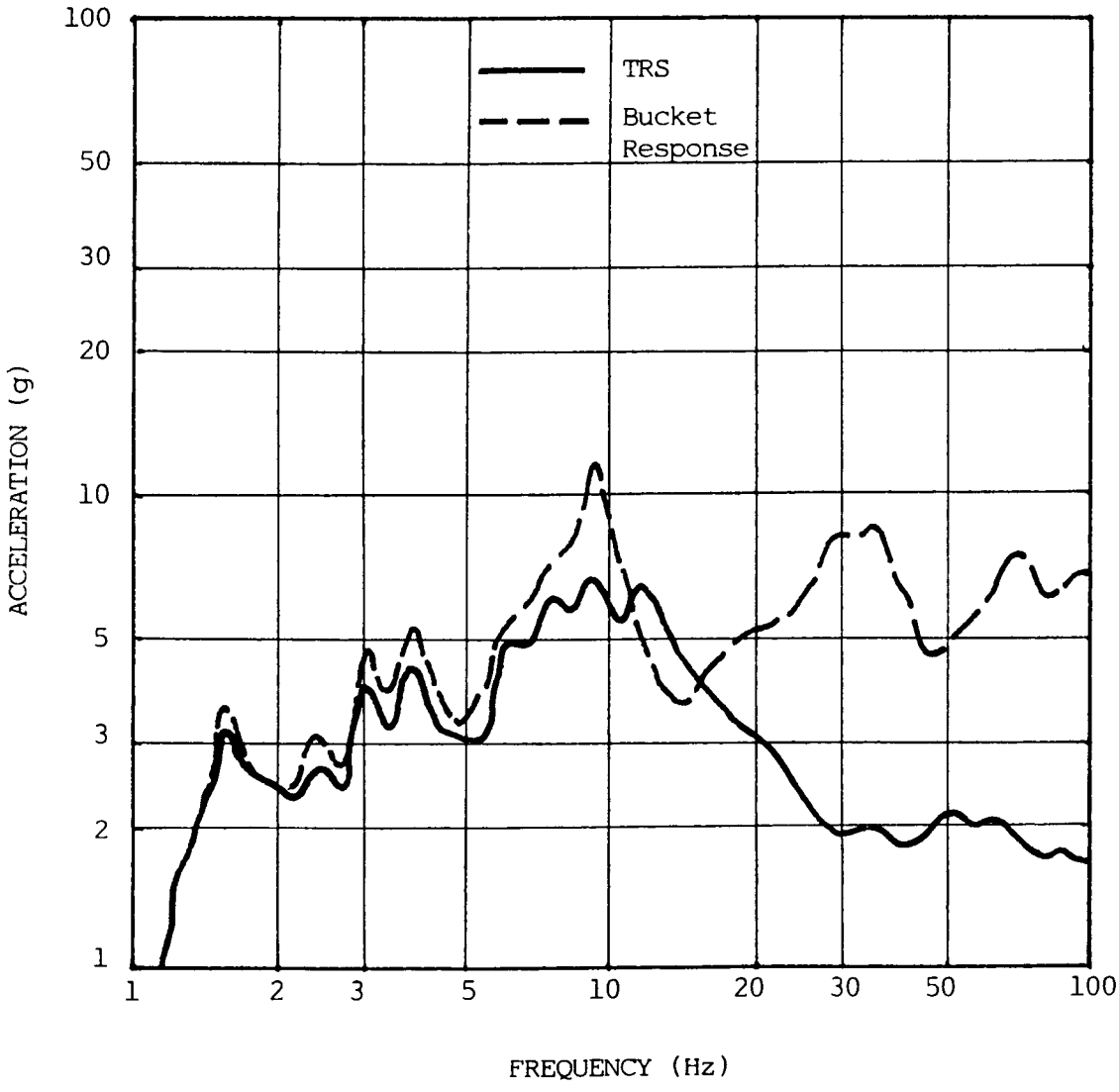

Fig. 2.16 Side-to-side TRS and bucket response spectrum at Size 1 starter during the fifth SSE retest in the Z-Y axes (3% damping). Note that Size 2 through Size 5 starters have been removed from the MCC.

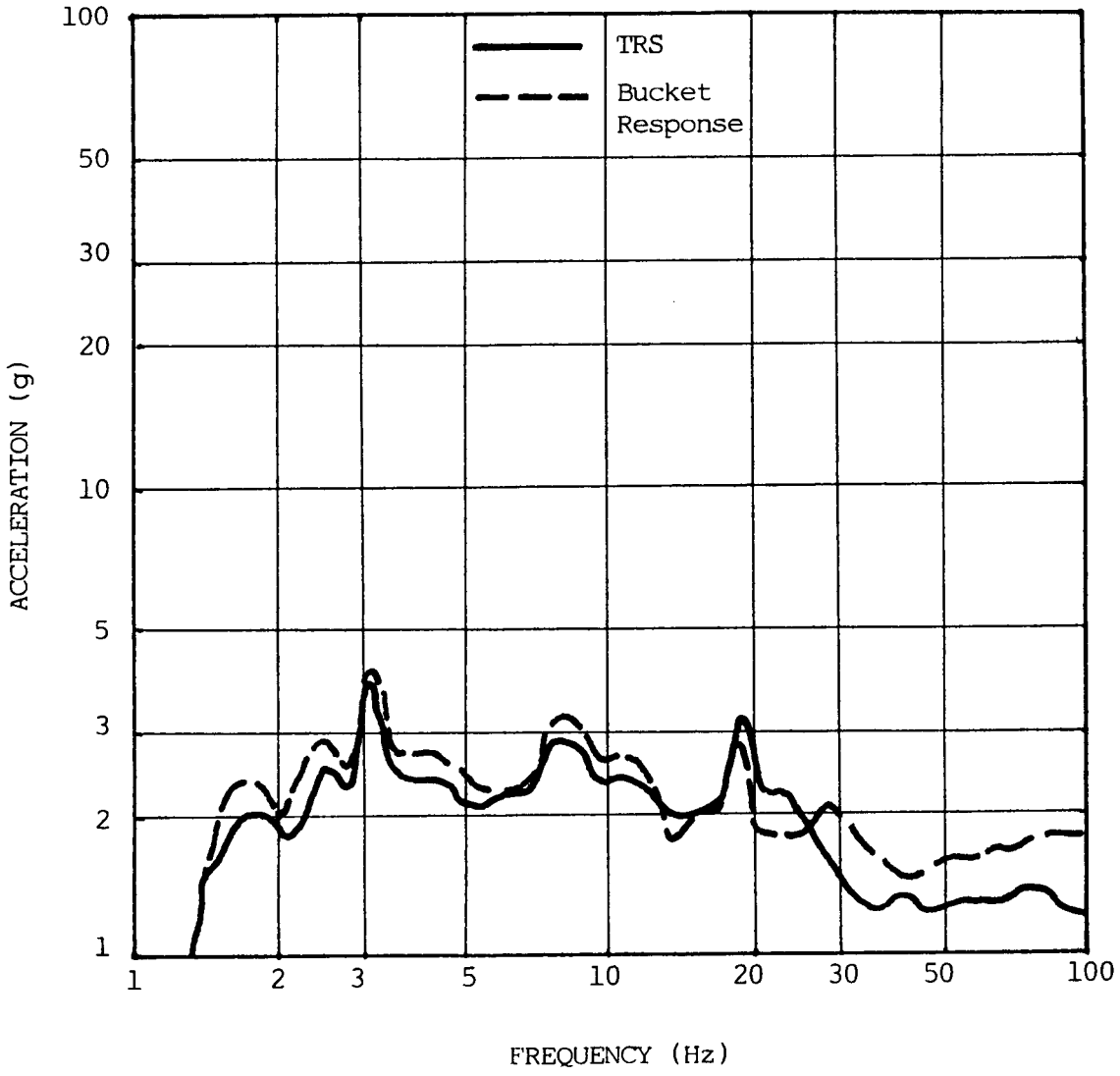

Fig. 2.17 Vertical TRS and bucket response spectrum at Size 1 starter during the fifth SSE retest in the Z-Y axes (3% damping). Note that Size 2 through Size 5 starters have been removed from the MCC.

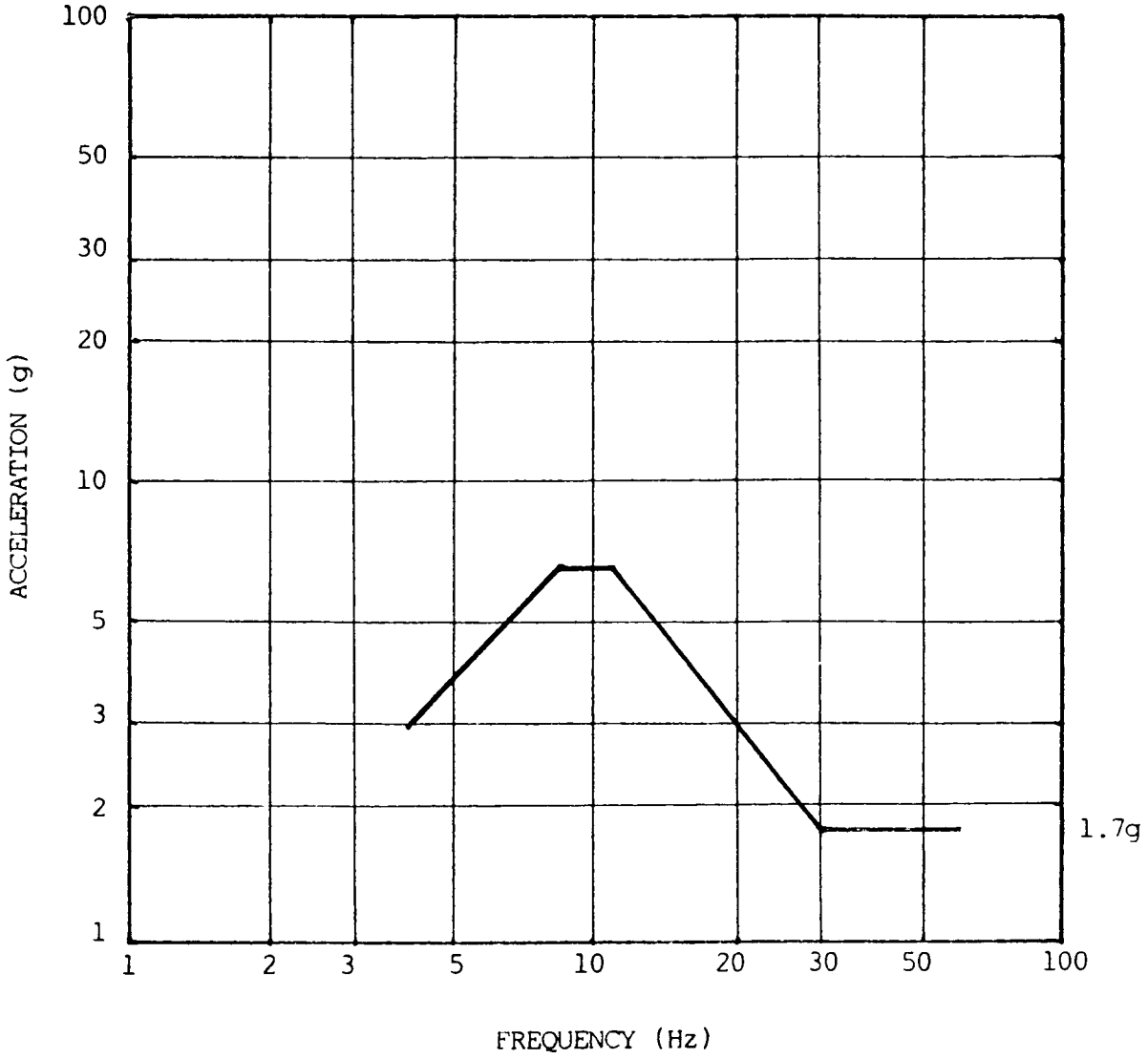

Fig. 2.18 Best-estimate minimum seismic capability of MCC with seismic clips added, expressed as a 3% damping base motion response spectrum in the horizontal direction. Note that the corresponding capacity spectrum for the commercial standard MCC is 0.85 times the spectrum shown.

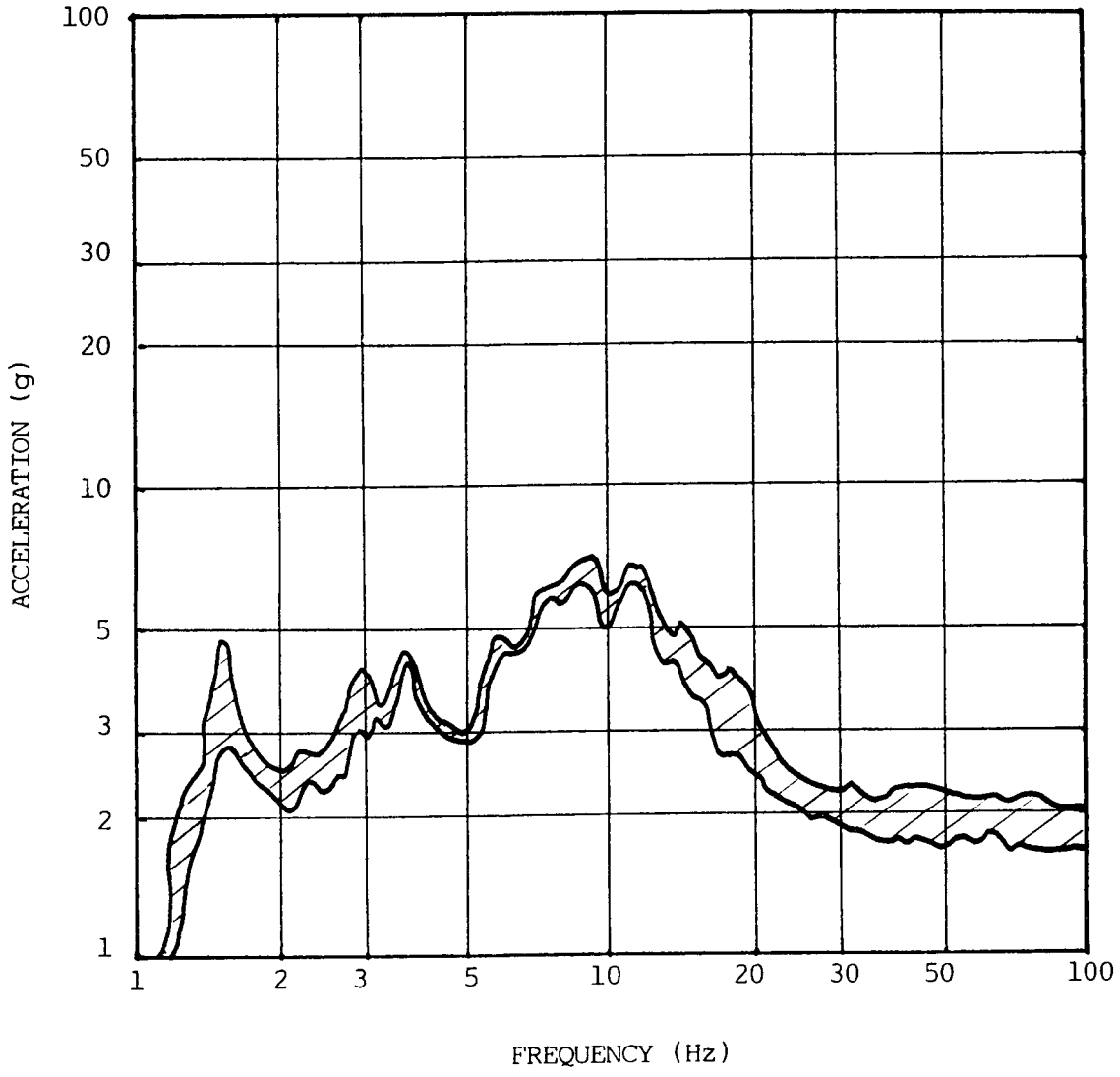

Fig. 2.19 Upper- and lower-bound TRS envelopes for the horizontal SSE tests (3% damping).

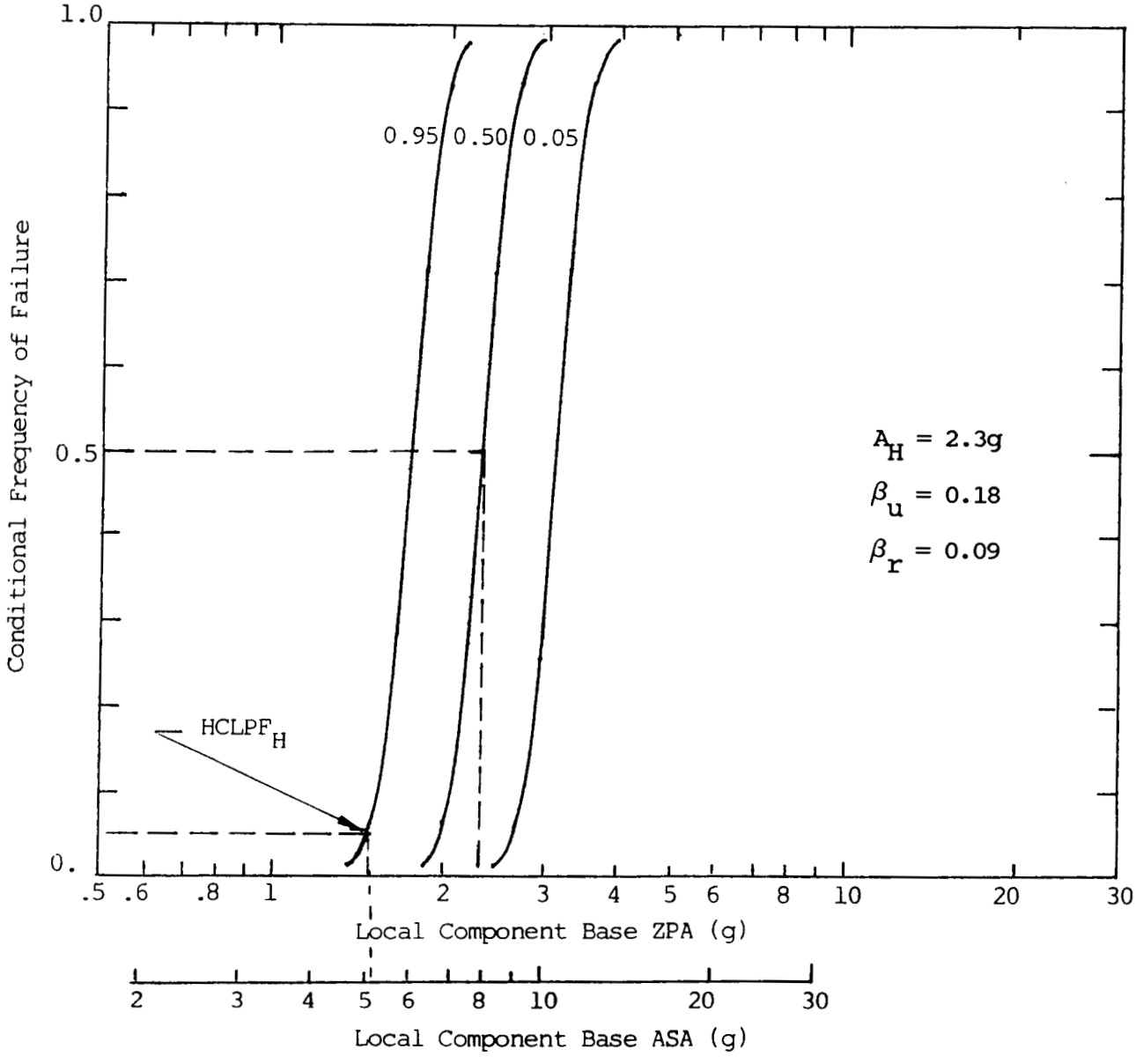

Fig. 2.20(a) Horizontal seismic fragility curves for the commercial standard Type W motor control center.

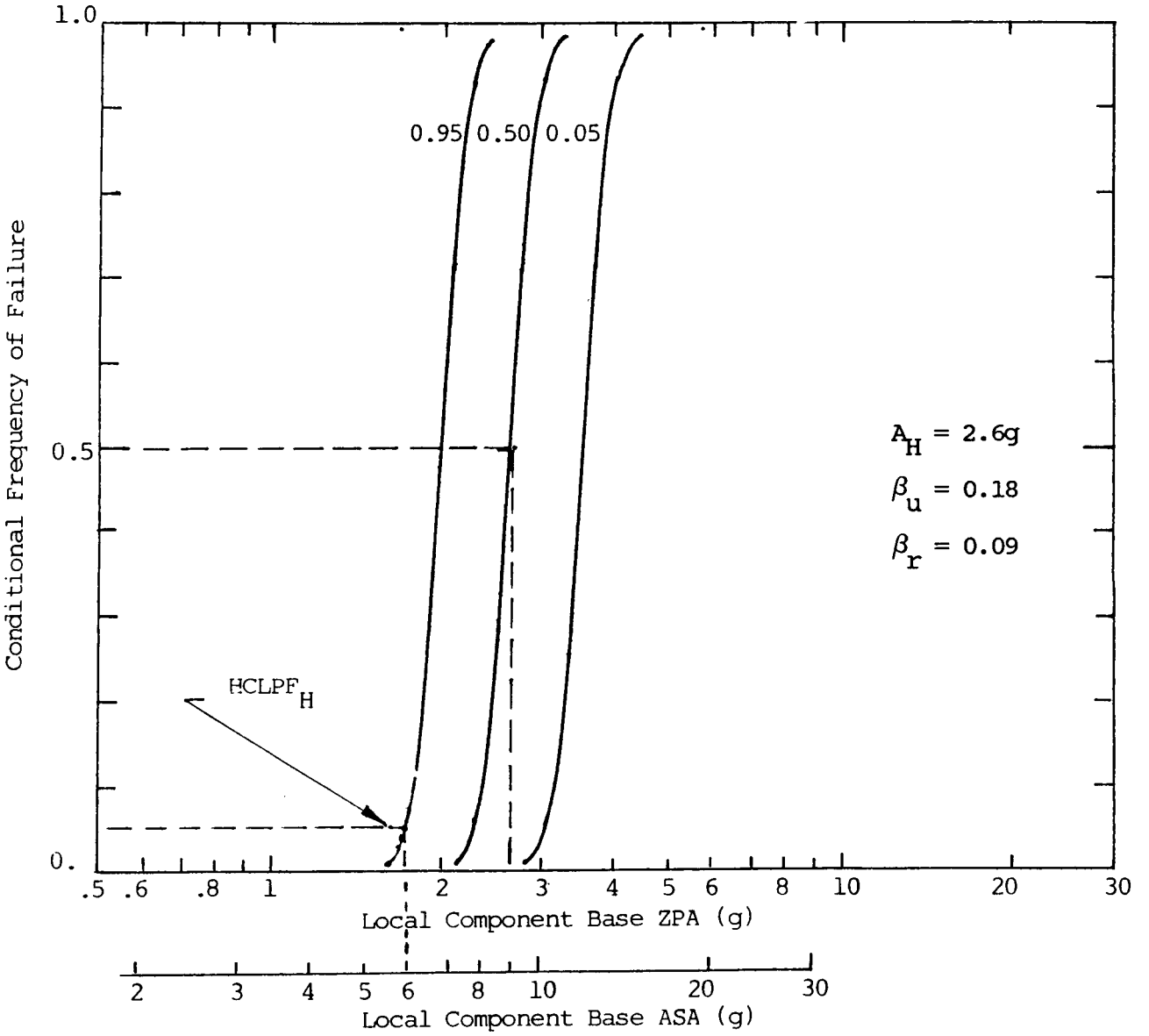

Fig. 2.20(b) Horizontal seismic fragility curves for the Type W MCC with seismic clips added.

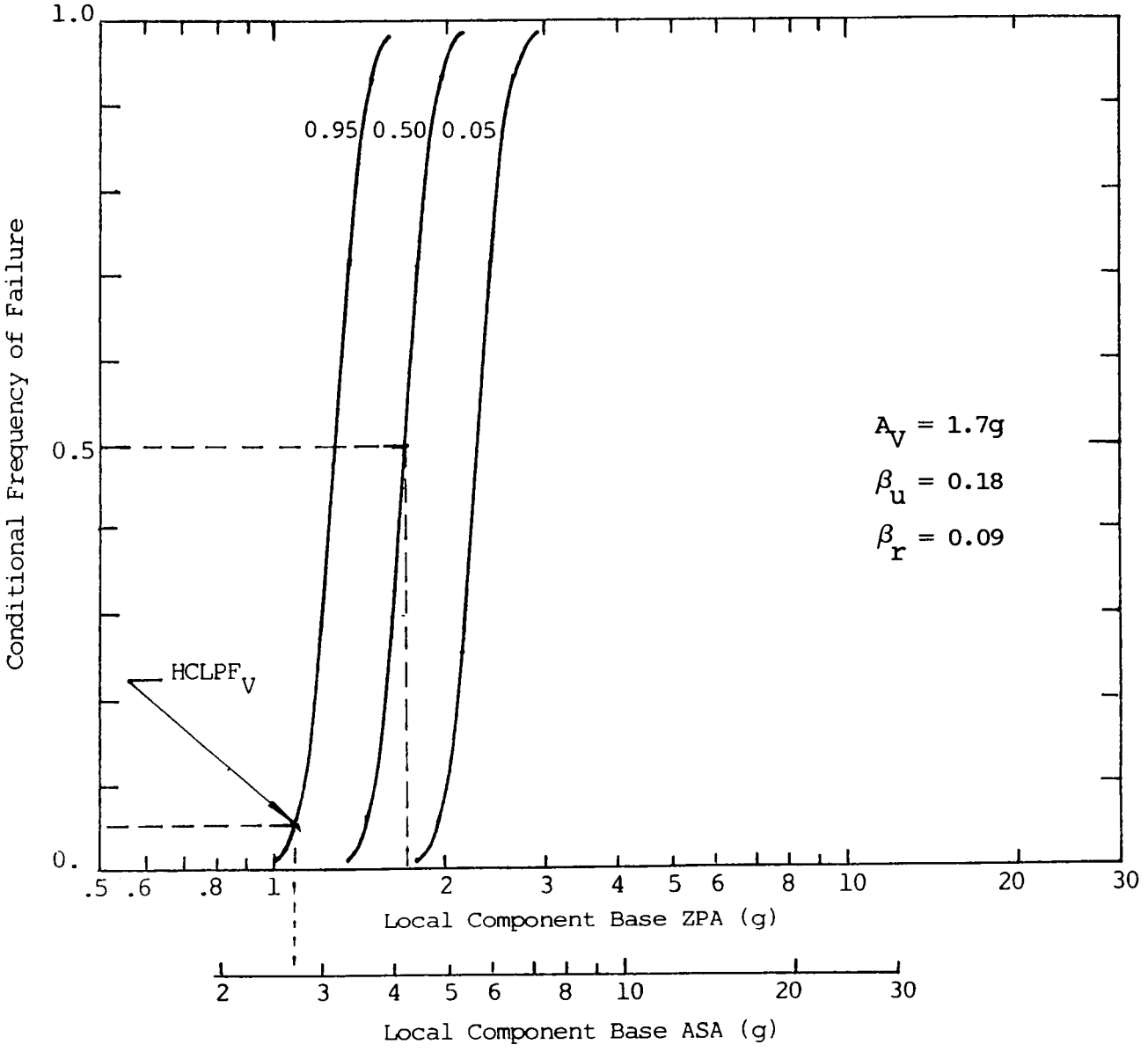

Fig. 2.21 Vertical seismic fragility curves for the Type W MCC with and without seismic clips.

3. FAN COOLER MOTOR CONTROLLER

3.1 Description of Equipment

The fan cooler motor controller (FCMC) is a two-speed circuit breaker type combination motor controller. The complete controller is an integral part of the vital load center in the Diablo Canyon nuclear power plant as described in Section 10.3.25 of Ref. 3. The high- and low-speed contactors are of NEMA Size 6 and Size 5, respectively. In the plant the devices are mounted in full-height sections of the vital load center. There are a total of five controllers, two on Bus F, two on Bus G, and one on Bus H.

3.2 Safety Function

The safety function of the controller is to control the flow of power to the reactor containment fan cooler motors. Upon receiving a Safety Injection Signal (SIS), all fans are to run at low speed. That is, upon the SIS, the FCMC should be able to switch all operating fans from the high- to the low speed, and to start non-operating fans to run at low speed as well. To achieve such required function during and after an earthquake, the circuit breaker must be capable of remaining closed, the low-speed controller must be capable of closing and staying closed for 15 to 25 seconds after receiving the SIS, and the time-delay relay must be capable of picking up and timing out.

3.3 Seismic Failure Modes

In accordance with the dynamic test qualification data shown in Refs. 3, 7, and 8, the devices were typically rigidly mounted on the rigid supporting steel frame during the tests to simulate the in-plant mounting at the vital load center, and the structural failure mode is less likely than the functional failure mode during earthquakes. Our ranking of the seismic failure modes is as follows:

(1) Spurious chatter of the high-speed contactors (NEMA Size 6) while the fan cooler motors are running at low speed upon the initiation of the SIS. An inadvertent closing of the high-speed contactors while the motors are running on low speed could damage the motor and hence caused a functional failure; this is the reason mechanical interlocks were installed on the controllers in order to enhance their seismic performance.

(2) Inadvertent opening of the circuit breaker during and after the earthquakes.

(3) Inadvertent opening of the low-speed controller after receiving an SIS.

(4) Failure of the time-delay relay in picking up and timing out.

(5) Structural failure in the device or in its mounting.

3.4 Modifications to Improve Seismic Performance

According to the test results, contact chatter was observed only in the controller from Unit 2 because it is mechanically different from that from Unit 1. To assure uniform operating characteristics, however, mechanical interlocks have been installed on all Unit 1 and Unit 2 fan cooler motor controllers. This enhancement measure would prevent the occurrence of any inadvertent closing of the high-speed contactors when the fan cooler motors are running at low speed after receiving the SIS. No other enhancement has been applied to the fan cooler motor controllers.

3.5 Seismic Qualification

Two fan cooler motor controllers, one each from Units 1 and 2, were mounted on the same test fixture for concurrent dynamic test qualification. Two series of tests were conducted. The initial series of tests were conducted concurrently with the Type W MCC single column on one common shaker table, as shown previously in Figs. 2.3 and 2.4. This was done for testing convenience and was believed not to affect any conclusion about the performance of the MCC or the fan cooler motor controller. During the initial series of tests, two pairs of accelerometers, one horizontal and one vertical sensor in each pair, were used to record the dynamic response of the controllers. The tests were conducted at both the OBE and SSE levels. During the second series of tests, only the SSE runs were made because enough OBE runs had already been made during the initial tests and no functional or structural anomalies were ever observed. In addition, two pairs of accelerometers were mounted on each of the Unit 1 and 2 fan cooler controllers this time, giving a total of four response readouts rather than only two as was the case in the initial tests. Because the second series of tests were equally representative of the qualification testing while giving more response readouts, they were taken as the basis for our fragility evaluation.

In the second series of tests, the fan cooler motor controllers were tested concurrently with the auxiliary relay panel on the same shaker table. Again, this was done for convenience of the qualification testing and was believed not to affect the performance of either the fan cooler motor controllers or the auxiliary relay panel. The shaker table motions were biaxial, one axis in the front-to-back (X-) or side-to-side (Z-) direction and the other in the vertical direction. Figures 3.1 and 3.2 show the front and back views, respectively, of the test setup for the second series of tests. The Unit 2 controller was mounted on the front face of one vertical frame, the Unit 1 controller on the back face of another vertical frame. The two steel frames were rigidly connected back-to-back with each other. Each steel frame was formed from two 4x4x1/4-inch vertical steel tubes that were about 20 inches apart from each other in the side-to-side plane and welded to steel U-channels at both the top and bottom. The bottom U-channels were rigidly attached to the shaker table, and the top of the square tubes was rigidly braced from the shaker table in the front-to-back

(F-B) direction. Each controller was bolted to two 1-1/2 inch vertical angles with 1/4-inch bolts, using the in-service bolt holes, and the angles were then welded to the vertical square tubes in the steel frame. This setup simulated the in-service mounting condition in the plant.

The accelerometers for monitoring the device response were mounted at Locations 1 and 2 on the Unit 2 controller, and Locations 3 and 4 on the Unit controller. Figures 3.1 and 3.2 show the accelerometers at Location 1 and Locations 2 to 4, respectively. The local mounting details are shown in Figs. 3.3 to 3.6.

To monitor the operability of the fan cooler controller during and after each test, a 440VAC, three-phase power source was connected to the input of the breaker. One phase was connected in series with the breaker and starter "F" contacts, one phase in series with the starter "S" contacts, and the third phase for powering the switches of the mechanically interlocked starters. The outputs were connected to 6VAC stepdown transformers and monitored on a direct readout recorder. The seismic tests were conducted with the "F" starter energized and the "S" starter deenergized, and then with the states of both starters reversed. The normally-open (NO) and normally-closed (NC) contacts of the starters were connected to a chatter detector and monitored for contact changes-of-state of duration two milliseconds or greater. Proper operation of the various devices were also visually monitored prior to and upon completion of each test. Figure 3.7 shows the wiring diagram for monitoring the operability of the controllers.

The controllers were subjected to four F-B and vertical runs at the SSE level, and then five runs at the same SSE level in the side-to-side and vertical axes. The averaged shaker table ZPA, i.e. ZPA on the TRS, was about 1.7g for the horizontal motions and 1.4g for the vertical motions for the SSE level runs. Figures 3.8 to 3.11 compare the 3% damping TRS to the controller response spectra from the fourth SSE run in the F-B and vertical (X-Y) axes. Similarly, Figs. 3.12 and 3.13 compare the TRS to the controller response spectra for the side-to-side motions from the fifth SSE run in the side-to-side and vertical (Z-Y) axes; the spectrum comparison for the vertical motions is omitted here because it is similar to that from the SSE run in the X-Y axes. An examination of the spectrum comparison indicates that the resonance frequency in the F-B axis was about 13 Hz for the Unit 1 and 2 controllers. In the vertical axis, the resonance frequency may be identified as at about 18 Hz, but with only a small amplification. This suggests that the controllers are effectively rigid as far as vertical seismic response is concerned. In the side-to-side axis, Figs. 3.12 and 3.13 indicate that the resonance frequency was about 13 Hz for both controllers, which was the same as the resonance frequency for both controllers in the F-B axis. In summary, the fan cooler controllers from both Units 1 and 2 may be considered flexible for horizontal motions and essentially rigid for vertical motions.

For all four X-Y and five Z-Y runs at the SSE level, the devices changed state on command as required during the tests. No chatter was observed on any of the energized contactors. The timing of the 42X-2G-1 low-speed contactor auxiliary relays varied slightly, less than 5%, during the test runs from the timing obtained before and after the test, and such minor variation in the timing was considered to have no adverse effect on the required safety function of the low-speed controller operation. Chatter was, however, observed on the deenergized high-speed contactor 42-2G-1/HIGH with the low-speed contactor both energized and deenergized. Normally, spurious chatter of a motor controller contactor would not adversely affect the connected motor or the contactor itself. But, in the case of the two-speed fan cooler motors, spurious chatter of the the high-speed contactor, while the motors are running on low speed, could cause damage to the motors. For this reason, mechanical interlocks were installed on the fan cooler motor controllers in order to prevent the possibility of high-speed contactor closing when the motors are operated at low speed. Although chatter was detected only on the Unit 2 controller, which is mechanically different from the Unit 1 controller, interlocks were installed on all Unit 1 and 2 fan cooler controllers to maintain uniform operation features.

From the previous discussions of the test results, we can summarize the seismic response characteristics of the fan cooler motor controllers as follows:

(1) The controllers are flexible for horizontal vibrations, with a resonance frequency at about 13 Hz in the F-B axis. In the vertical axis, both controllers are essentially rigid.

(2) Chatter was consistently detected on the high-speed contactor of Unit 2 controller at deenergized state with the low-speed contactor both energized and deenergized. In order to prevent possible damage to the motors when running at low speed, mechanical interlocks were installed to the controllers from Units 1 and 2. This was a positive improvement to the operability of the controllers and hence no further qualification tests were needed.

3.6 Seismic Capability

Based on the tests results discussed previously and the fact that the moving armatures all move in the horizontal direction only, we judge that the fan cooler controllers are more sensitive to horizontal than to vertical input motions at the base. In addition, we will assume that the controllers have a 50% chance of functional failure, with a 95% confidence, for a commercial standard fan cooler controller without the mechanical interlock and subjected to the 1.7g ZPA horizontal base motion. With the mechanical interlock installed, we assume that the 1.7g horizontal base ZPA becomes the horizontal HCLPF ZPA. On the other hand, we will assume that the vertical direction HCLPF base ZPA is 1.4g for both the commercial standard and modified controllers.

Based on the above observations and assumptions, we estimate the minimum seismic capabilities of the fan cooler motor controllers as follows:

$(\check{A}_V)_{min}$ - Because the fan cooler controllers have been shown by tests to be essentially rigid, their minimum seismic capability can be sufficiently represented with a base motion ZPA of 1.4g. This minimum base ZPA capability applies to the controllers both with and without the installation of the mechanical interlocks because the modification was primarily needed for improving the seismic performance of the controllers for horizontal vibrations.

$(\check{A}_H)_{min}$ - The minimum seismic capability is different for the controllers with and without the installation of the mechanical interlocks. With the modification, the minimum horizontal seismic capability may be expressed as a 3% damping response spectrum of the base motion, as shown in Fig. 3.14. The base spectrum has a ZPA of 1.7g, which corresponds to the HCLPF base ZPA we previously assumed for the controllers with the modification.

For controllers without the mechanical interlocks, the previous assumption that the 1.7g base ZPA corresponds to a probability of failure of 50% with a 95% confidence gives the HCLPF level to be approximately 0.85 x 1.7g = 1.4g, assuming a random variability of $\beta_r = 0.09$. It is a reasonable estimate because during all OBE runs conducted for the first series of qualification tests the average ZPA on the TRS was about 1.3g and chatter of the high-speed contactor was not detected. The capacity for the commercial standard fan cooler controller, expressed in a response spectrum, is therefore equal to 0.85 times the capacity spectrum for the modified controller as shown in Fig. 3.14.

The fragility evaluation for the fan cooler motor controller will be based on the same assumptions that were applied to the MCC, with both the ZPA and ASA representing the alternate fragility descriptor. The median ZPA and ASA capacities, A and S, respectively, are listed in Table 3.1.

Figures 3.15 and 3.16, respectively, show the horizontal seismic fragility curves for the commercial standard and the modified fan cooler controllers. The vertical seismic fragility curves are the same for both, as shown in Fig. 3.17. The ratio of ASA to ZPA capacity is 3.5 for the horizontal fragility, which is the same as that for the Type W MCC, and 1.9 for the vertical fragility.

Table 3.1 Median seismic fragility of fan cooler motor controller

	Standard Commercial Configuration		Structurally Modified (with mechanical interlock)	
	$\breve{A}$	$\breve{S}$	$\breve{A}$	$\breve{S}$
Horizontal (g)	2.6	9.1	2.3	8.0
Vertical (g)	2.2	4.2	2.2	4.2
β_u	0.18		0.18	
β_r	0.09		0.09	

Notes:

$\breve{A}$ = median capacity based on ZPA

$\breve{S}$ = median capacity based on ASA

Fig. 3.1 Setup for FCMC and auxiliary relay panel during second series of tests. The Unit 1 FCMC is at the front, that from Unit 2 at the back.

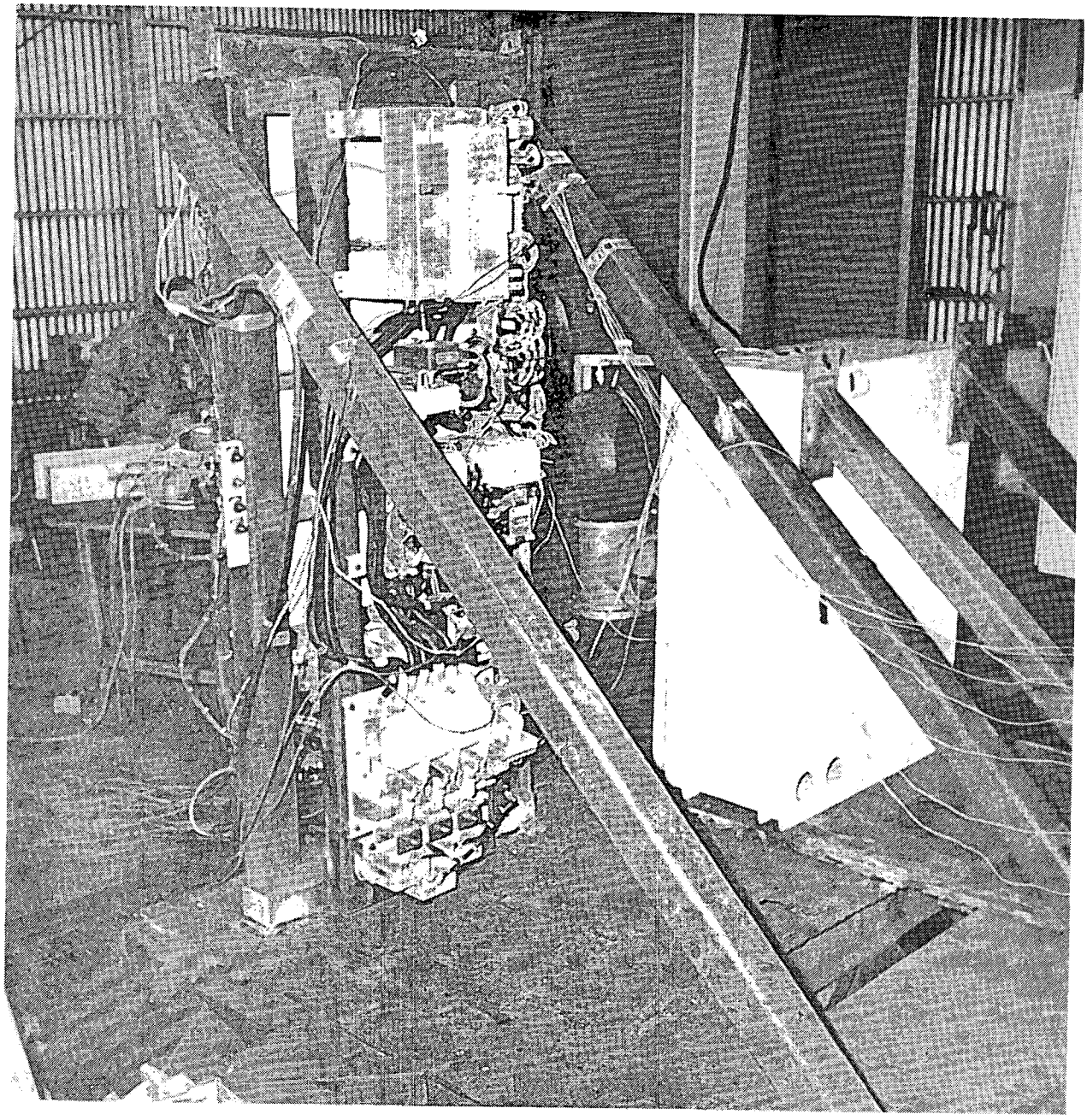

Fig. 3.2 Rear view of setup for FCMC and auxiliary relay panel for second series of qualification tests.

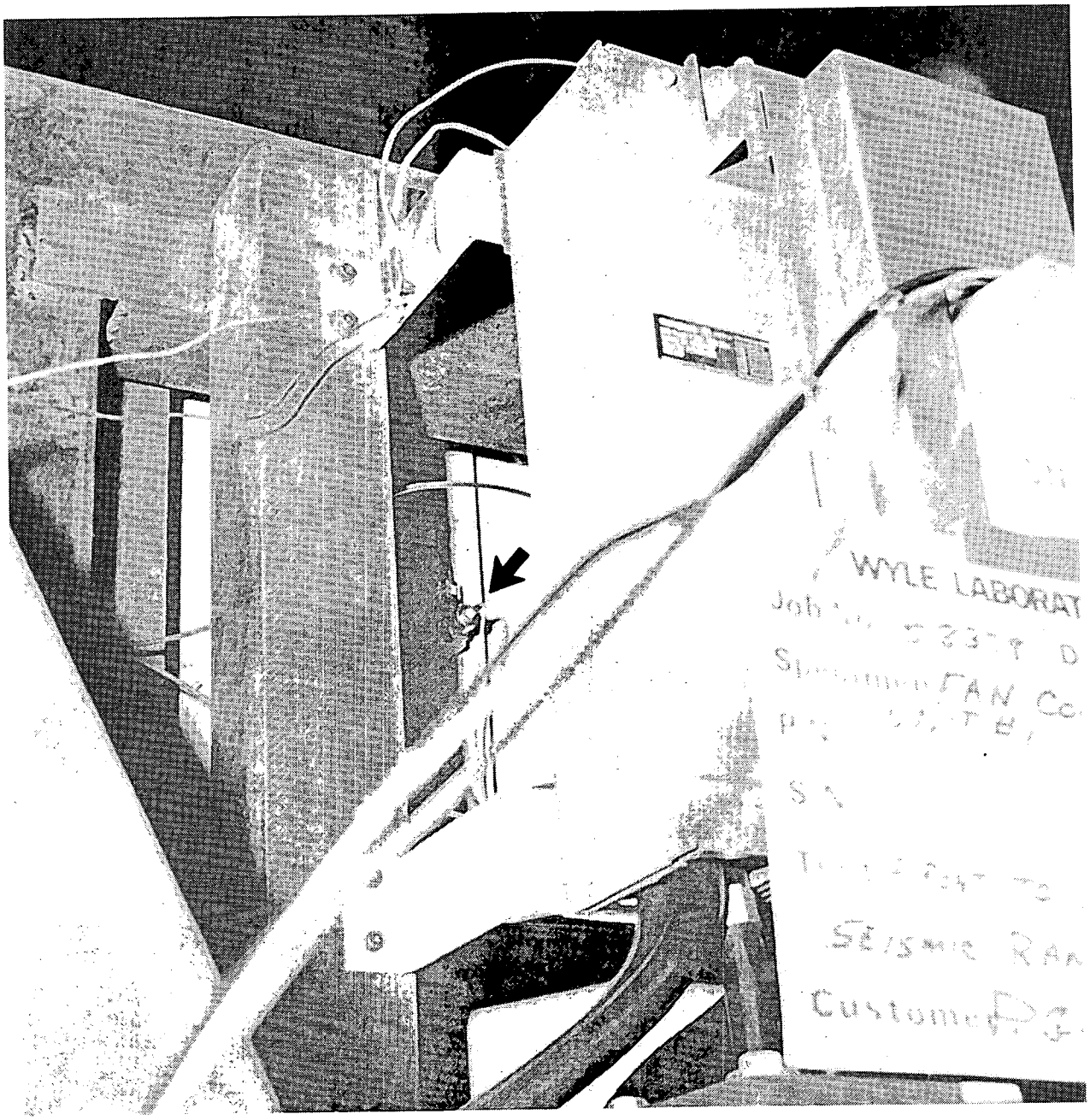

Fig. 3.3 Accelerometer Location 1 on Unit 2 FCMC.

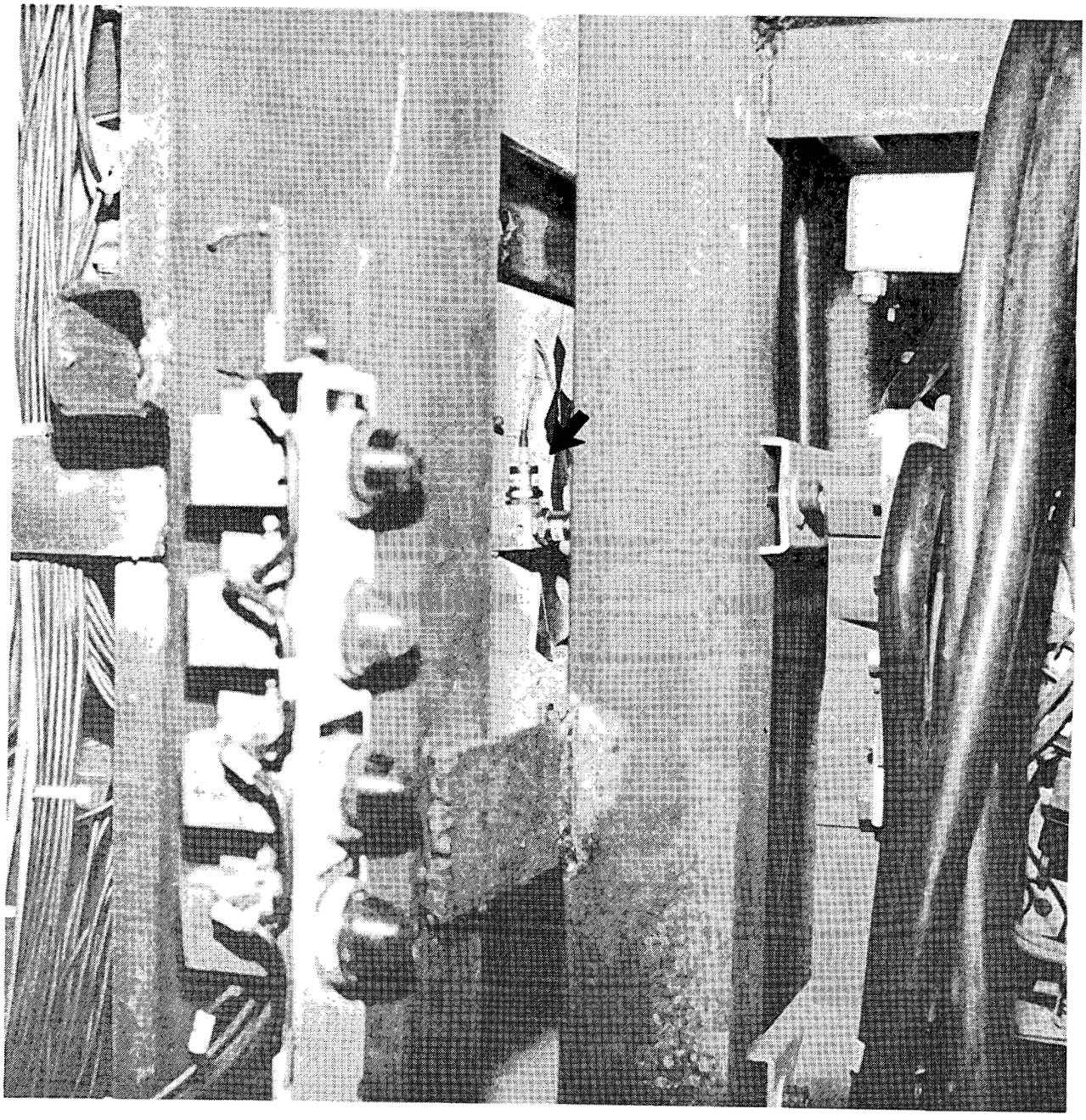

Fig. 3.4 Accelerometer Location 2 on Unit 2 FCMC.

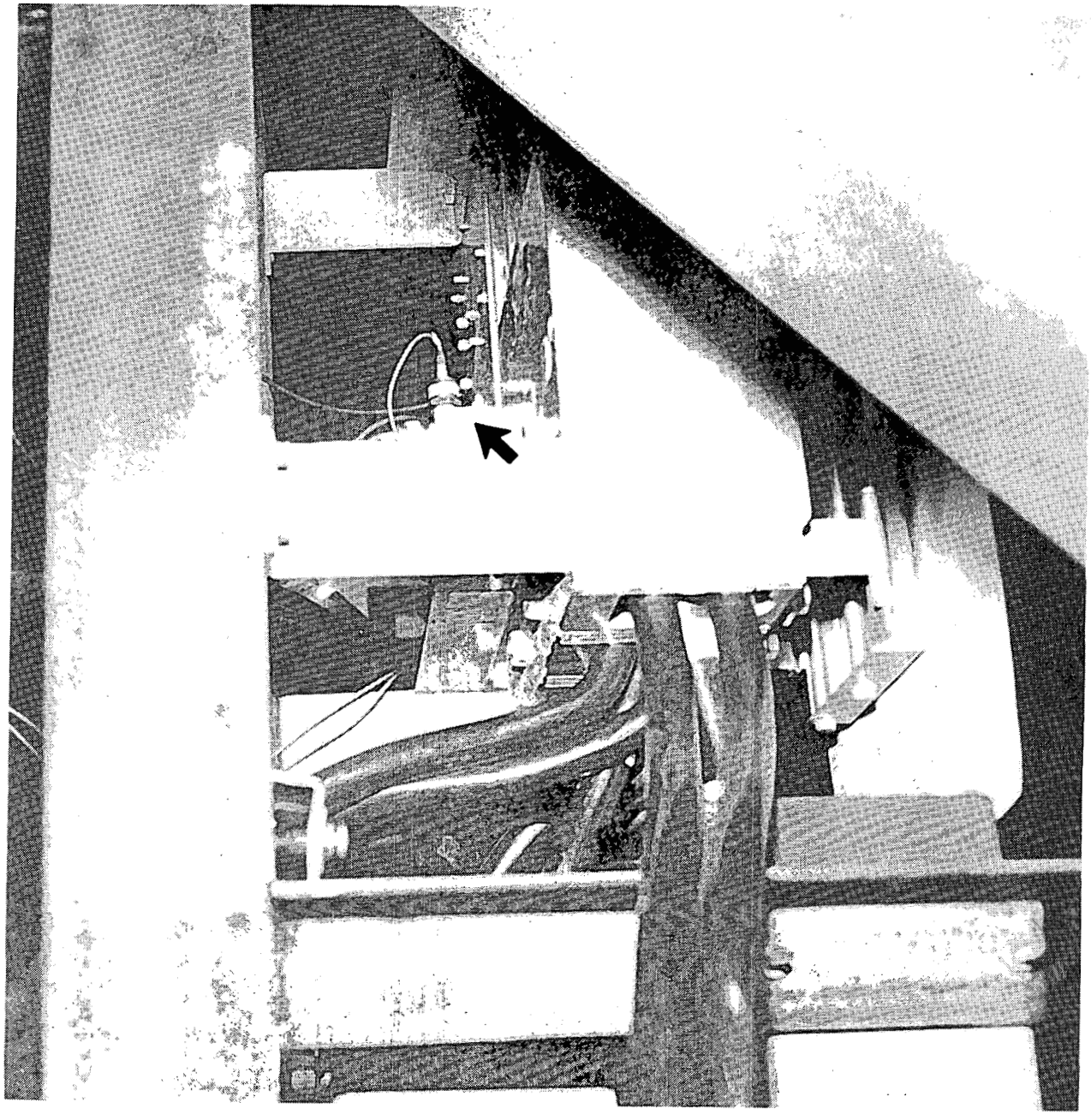

Fig. 3.5 Accelerometer Location 3 on Unit 1 FCMC.

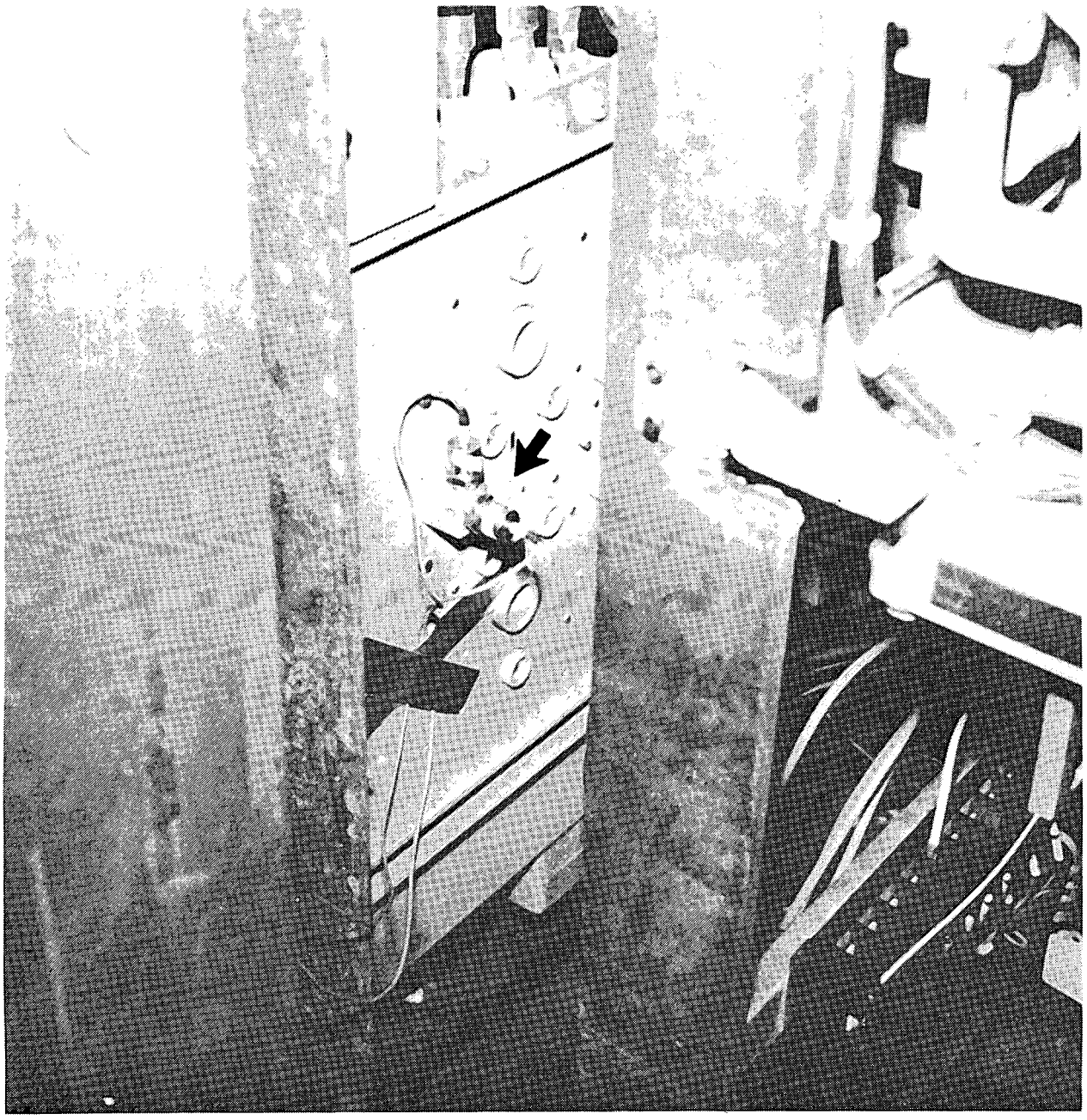

Fig. 3.6 Accelerometer Location 4 on Unit 2 FCMC.

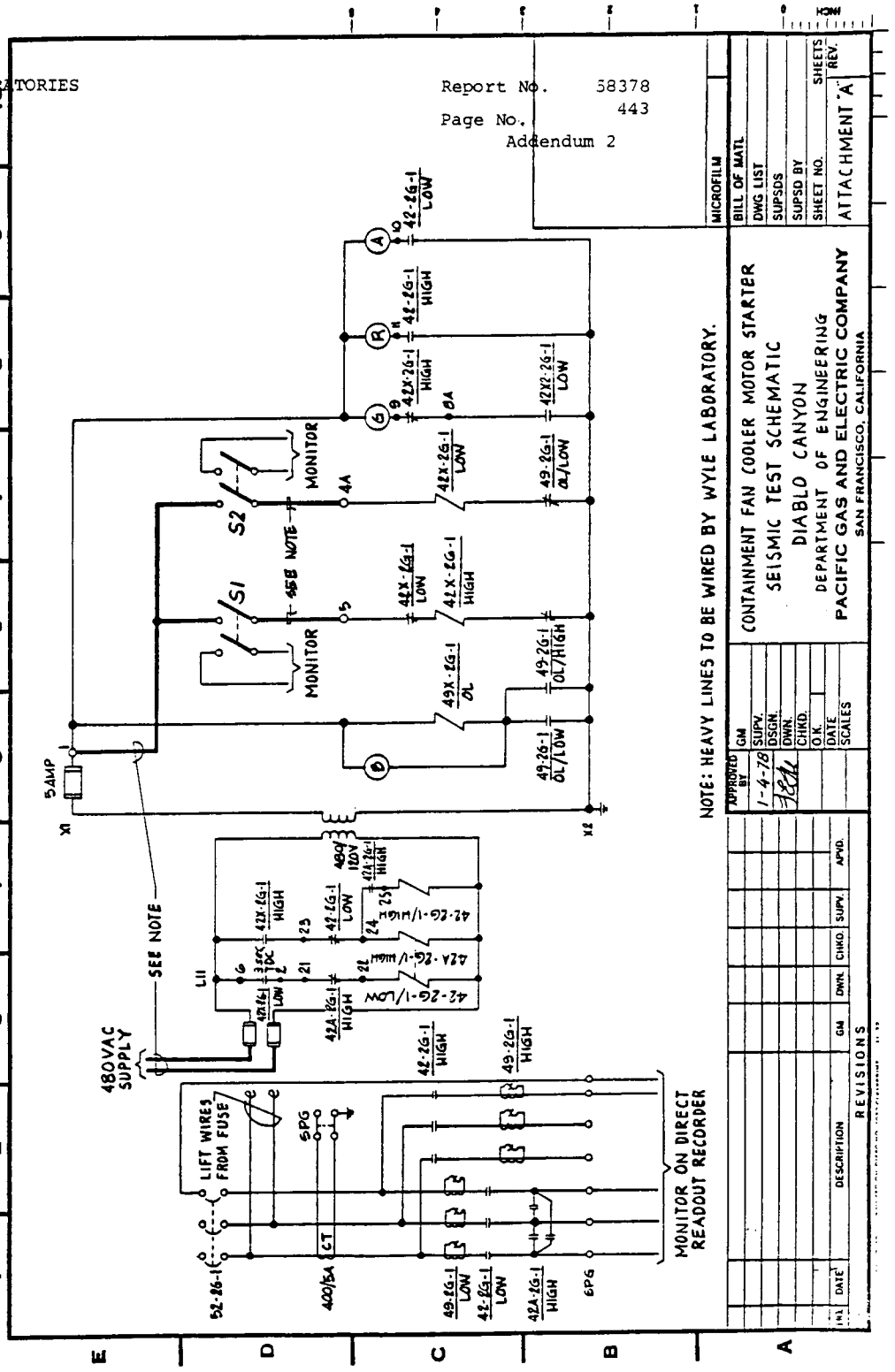

Fig. 3.7 Wiring diagram for FCMC tests.

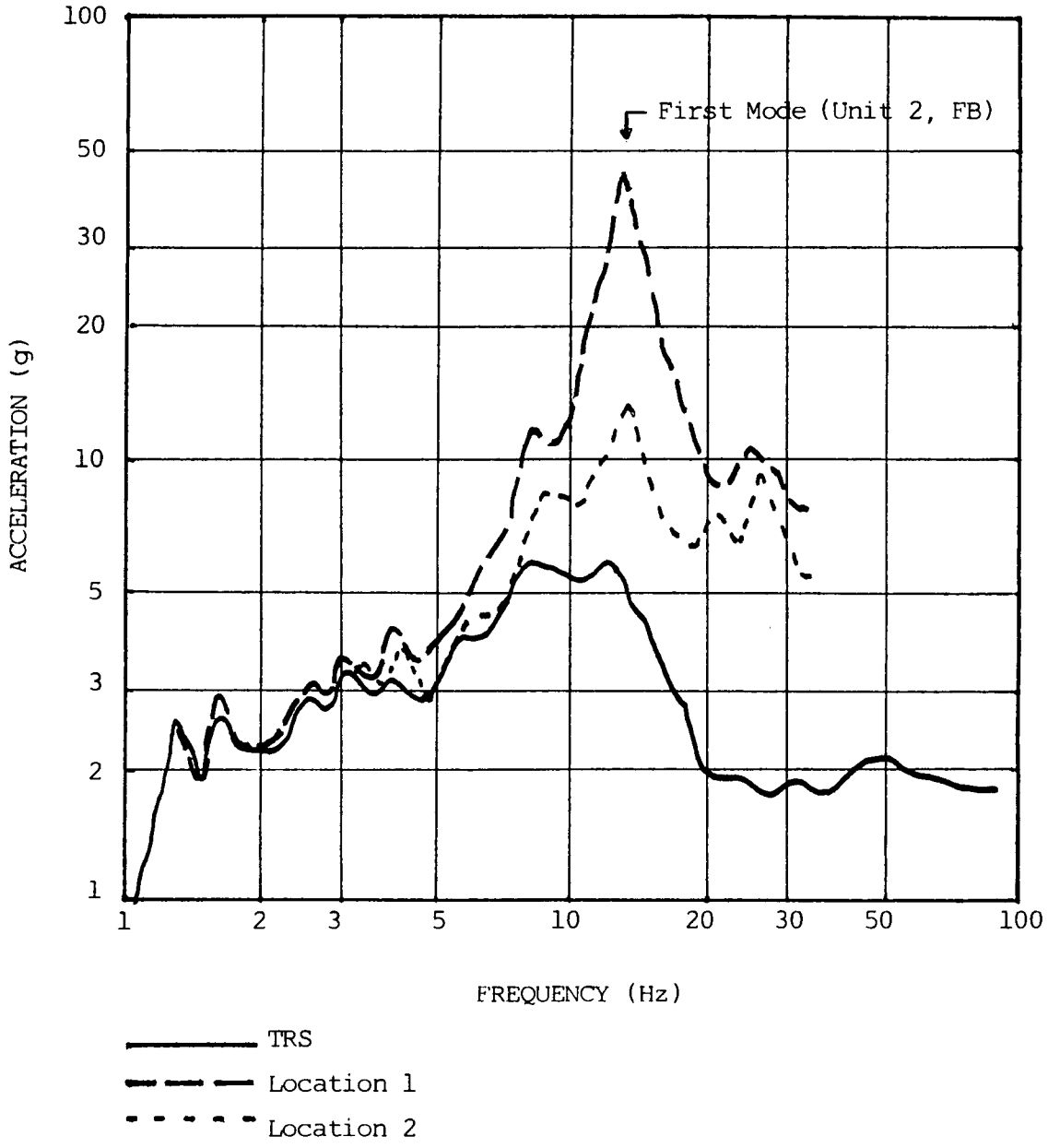

Fig. 3.8 Front-to-back response spectra at Locations 1 and 2 on the Unit 2 FCMC for the fourth SSE test in the X-Y axes (3% damping).

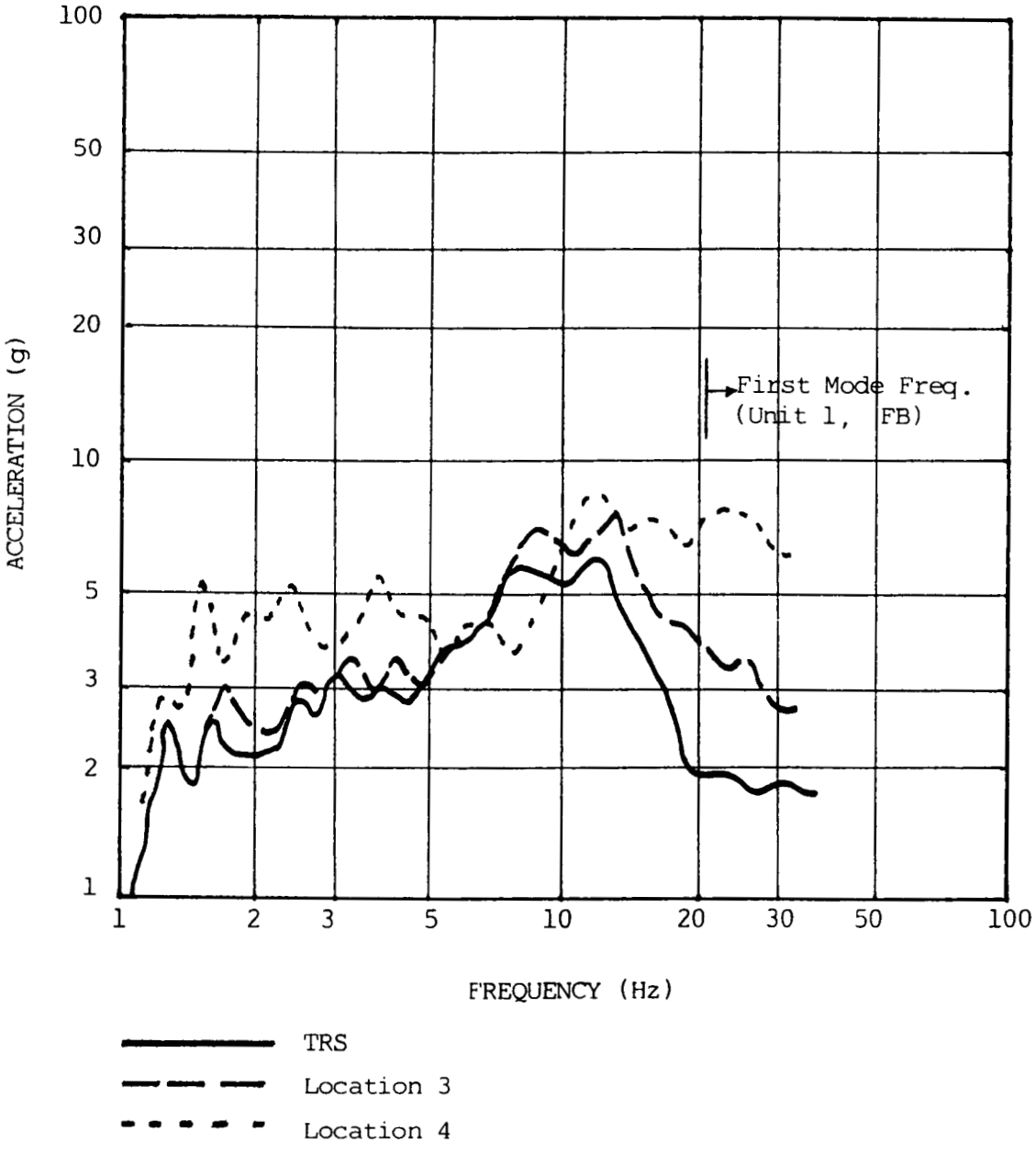

Fig. 3.9 Front-to-back response spectra at Locations 3 and 4 on the Unit 1 FCMC for the fourth SSE test in the X-Y axes (3% damping).

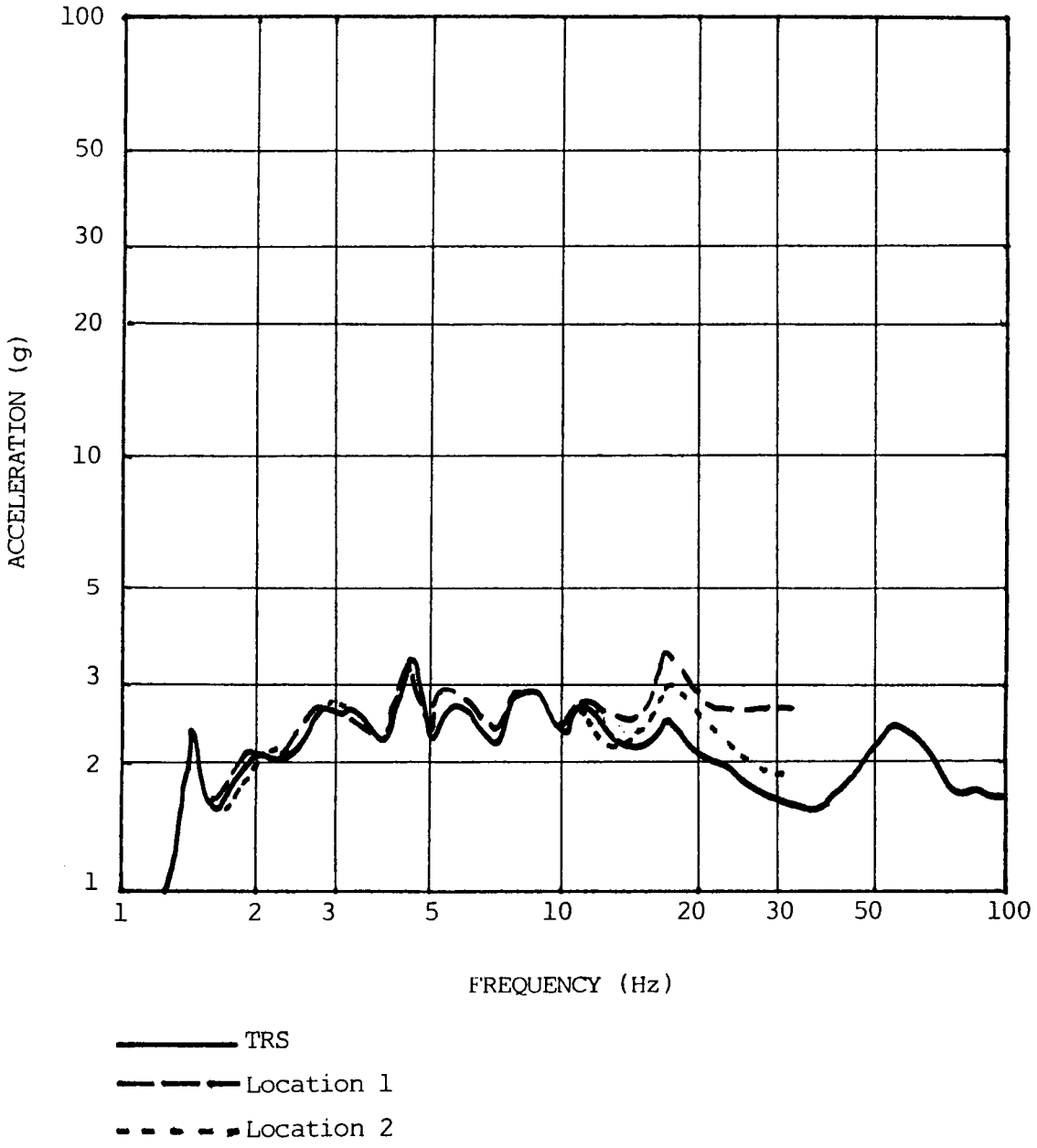

Fig. 3.10 Vertical response spectra at Locations 1 and 2 on the Unit 2 FCMC for the fourth SSE test in the X-Y axes (3% damping).

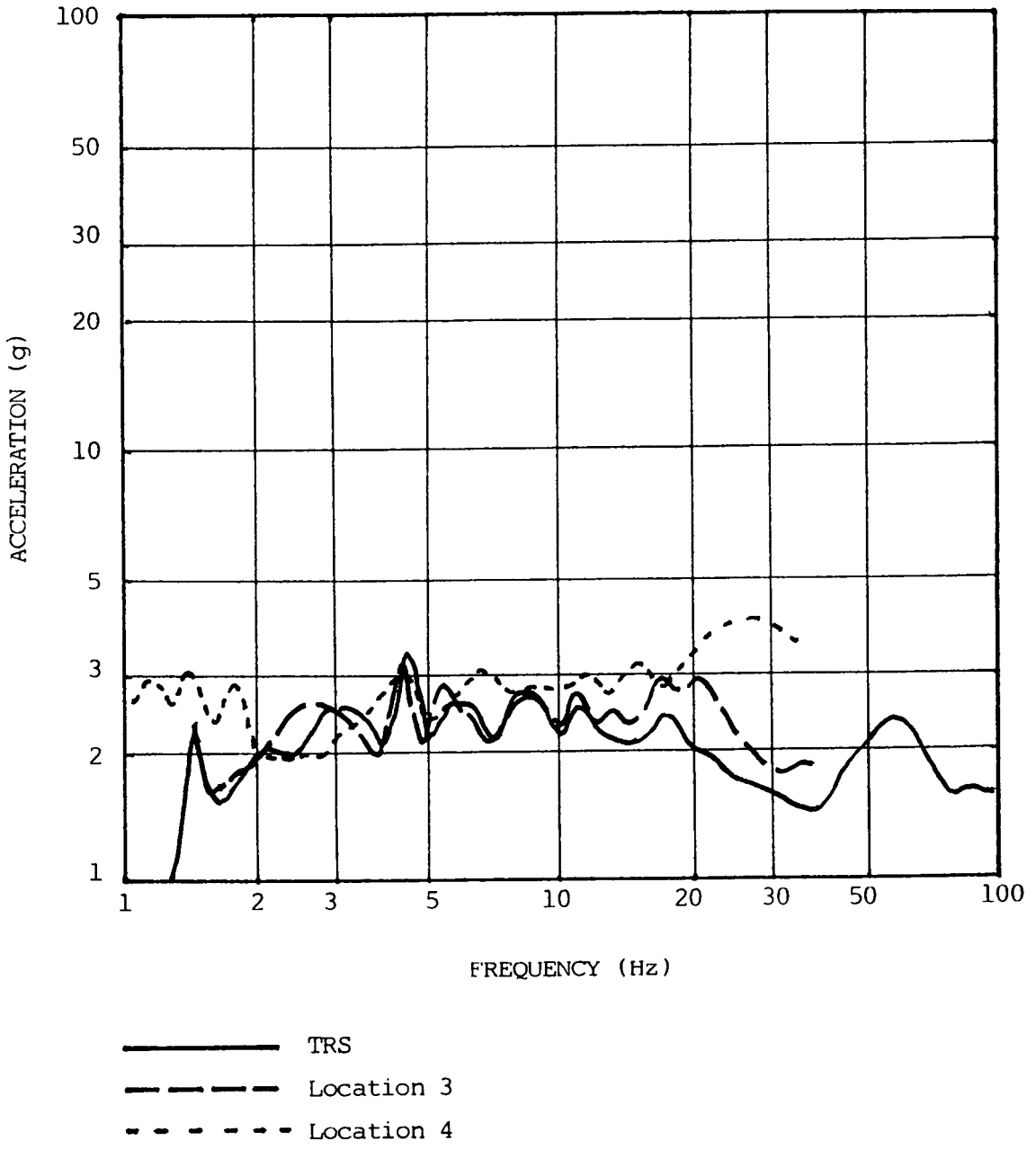

Fig. 3.11 Vertical response spectra at Locations 3 and 4 on the Unit 1 FCMC for the fourth SSE test in the X-Y axes (3% damping).

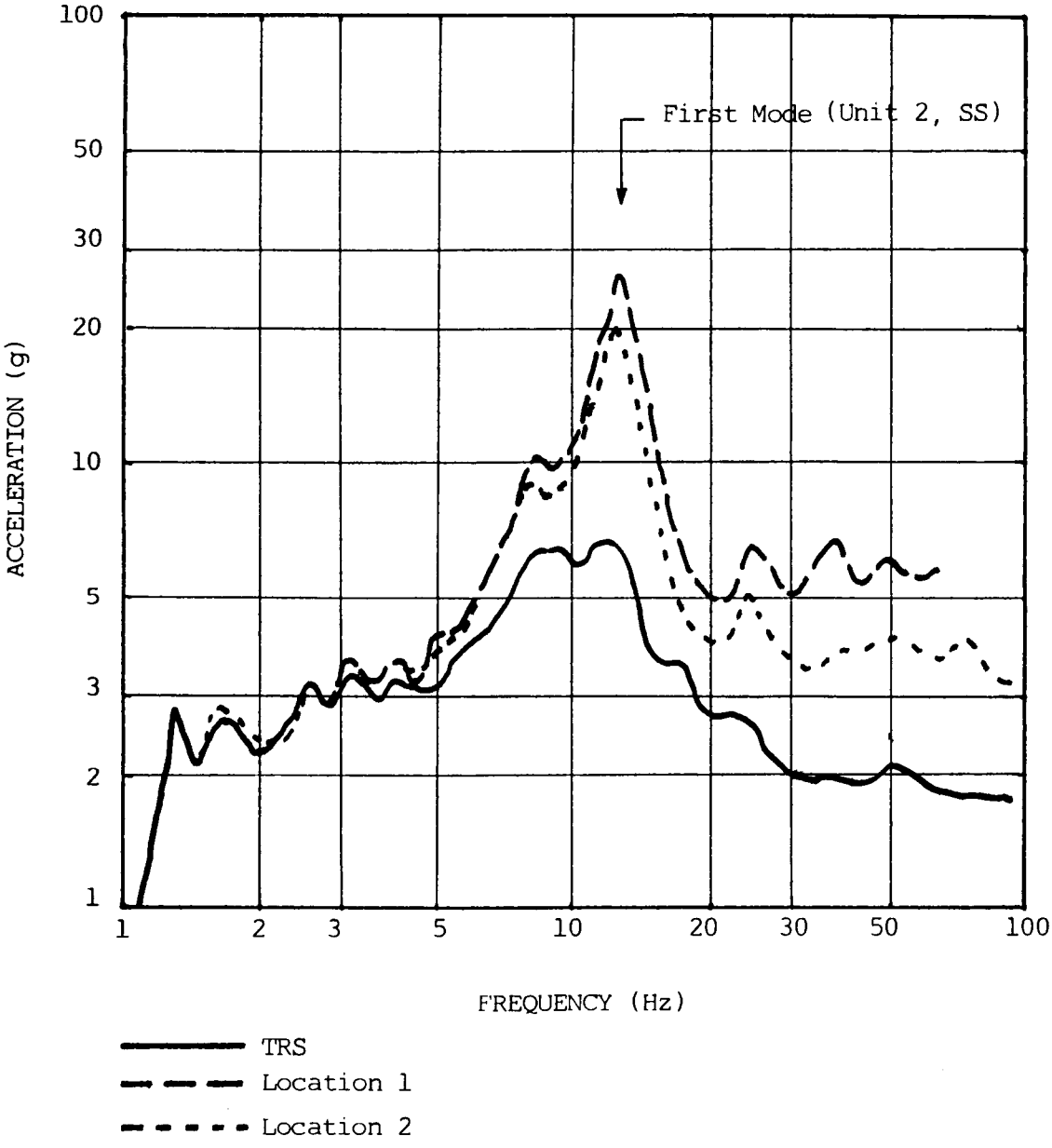

Fig. 3.12 Side-to-side response spectra at Locations 1 and 2 on the Unit 2 FCMC for the fifth SSE test in the Z-Y axes (3% damping).

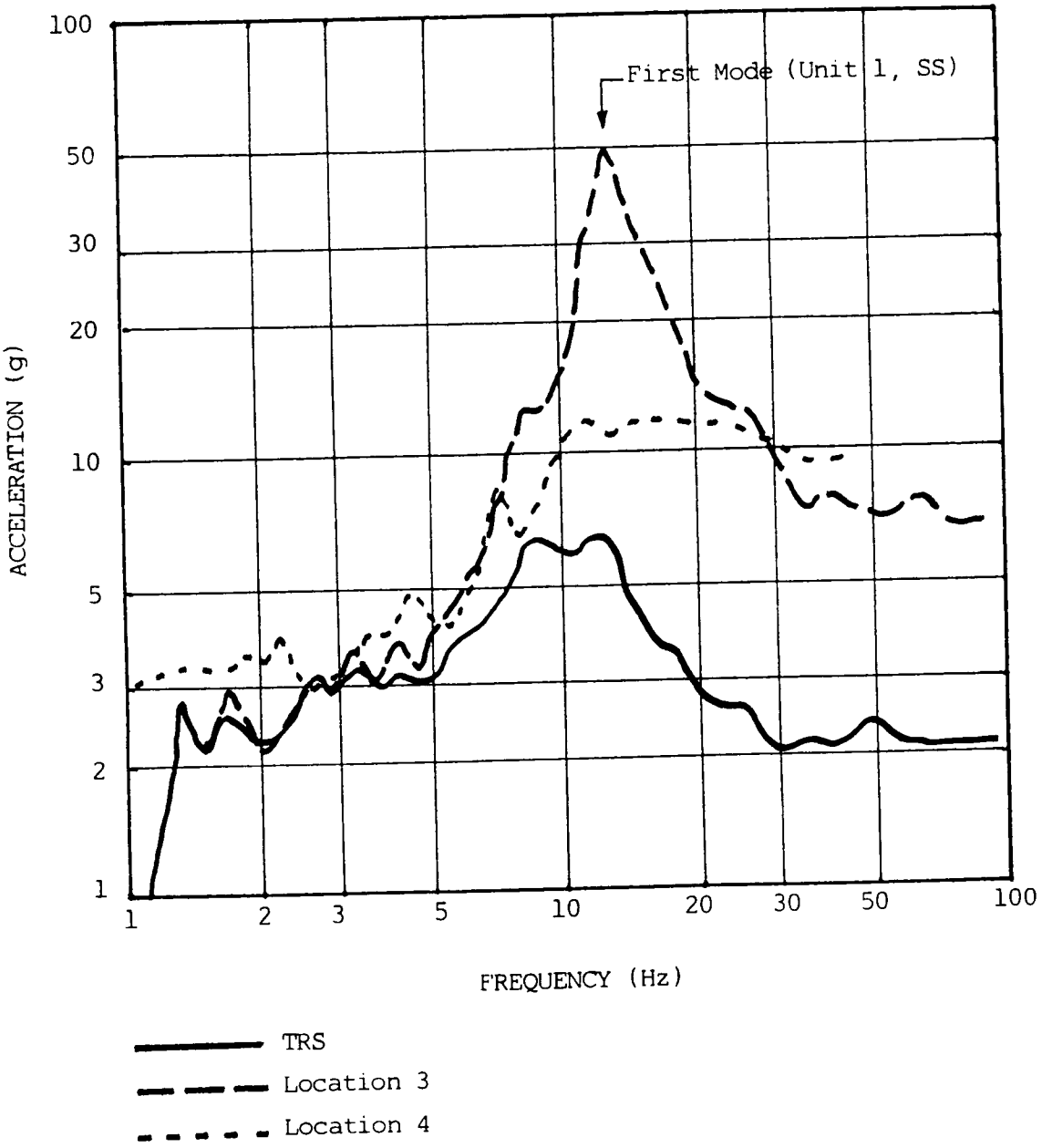

Fig. 3.13 Side-to-side response spectra at Locations 3 and 4 on the Unit 1 FCMC for the fifth SSE test in the Z-Y axes (3% damping).

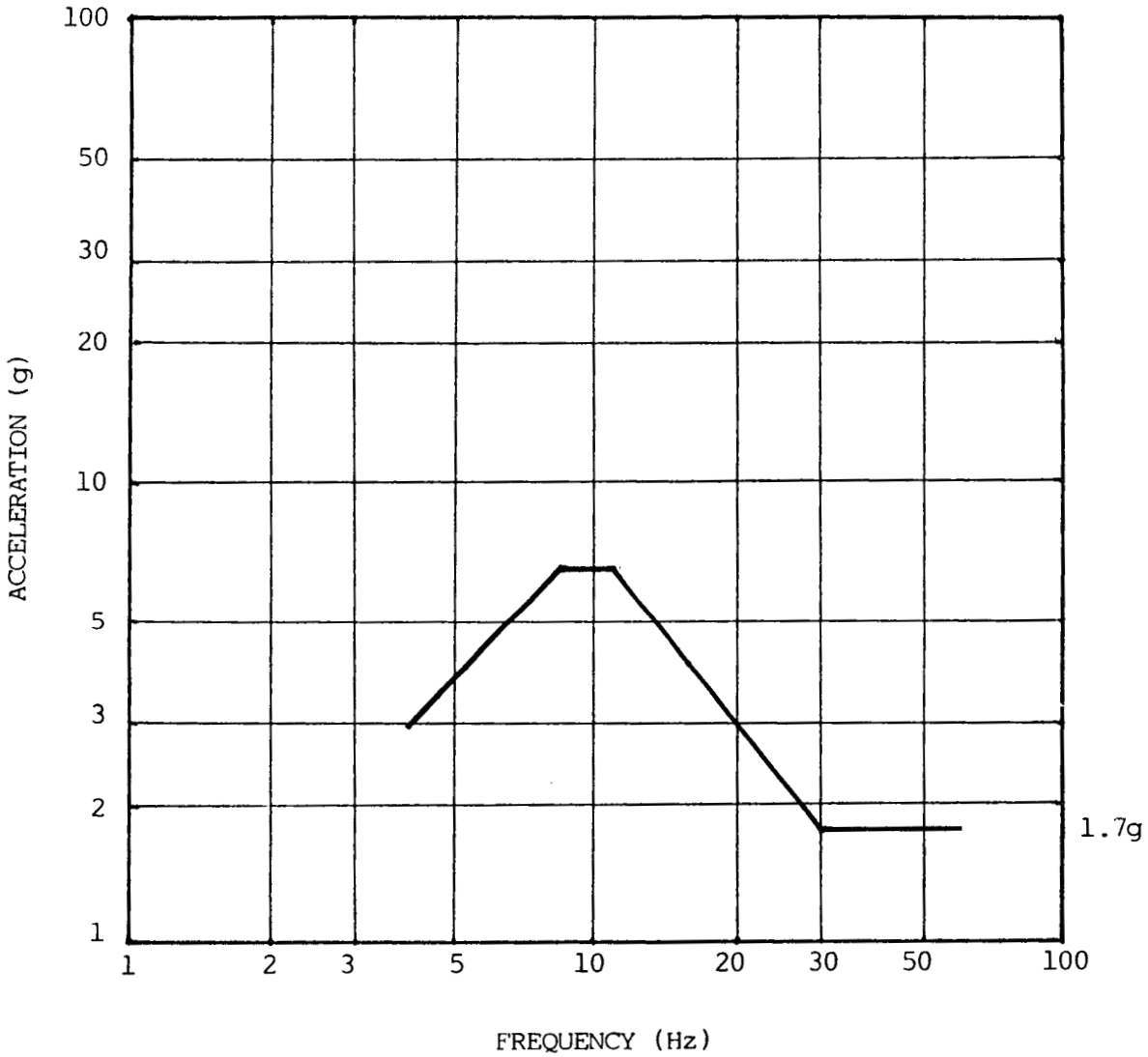

Fig. 3.14 Best estimate minimum seismic capability of FCMC with mechanical interlocks installed, expressed as a 3% damping base motion spectrum in the horizontal direction. Note that the capability spectrum for the commercial standard FCMC is 0.85 times the above spectrum.

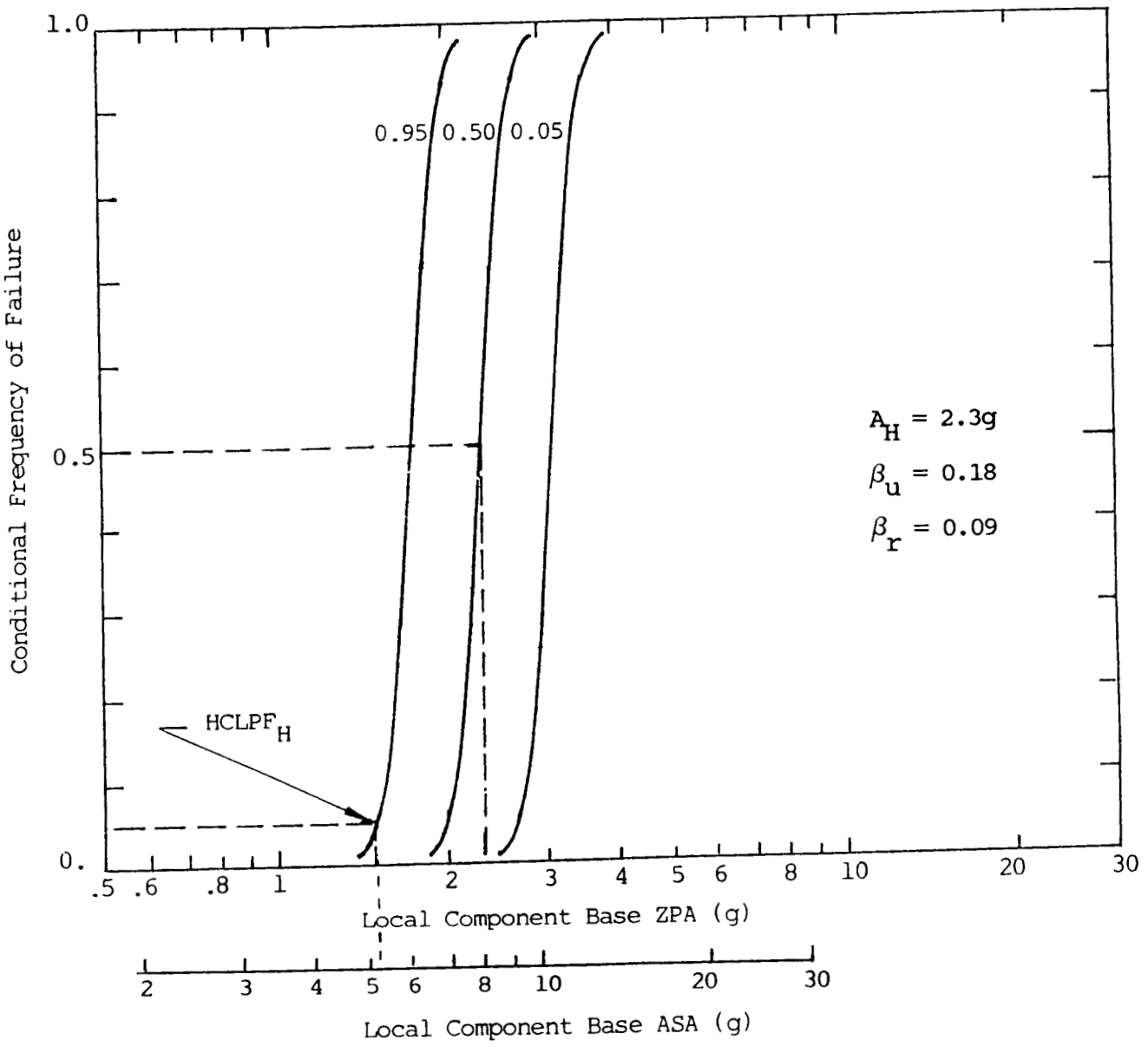

Fig. 3.15 Horizontal seismic fragility curves for the commercial standard fan cooler motor controller.

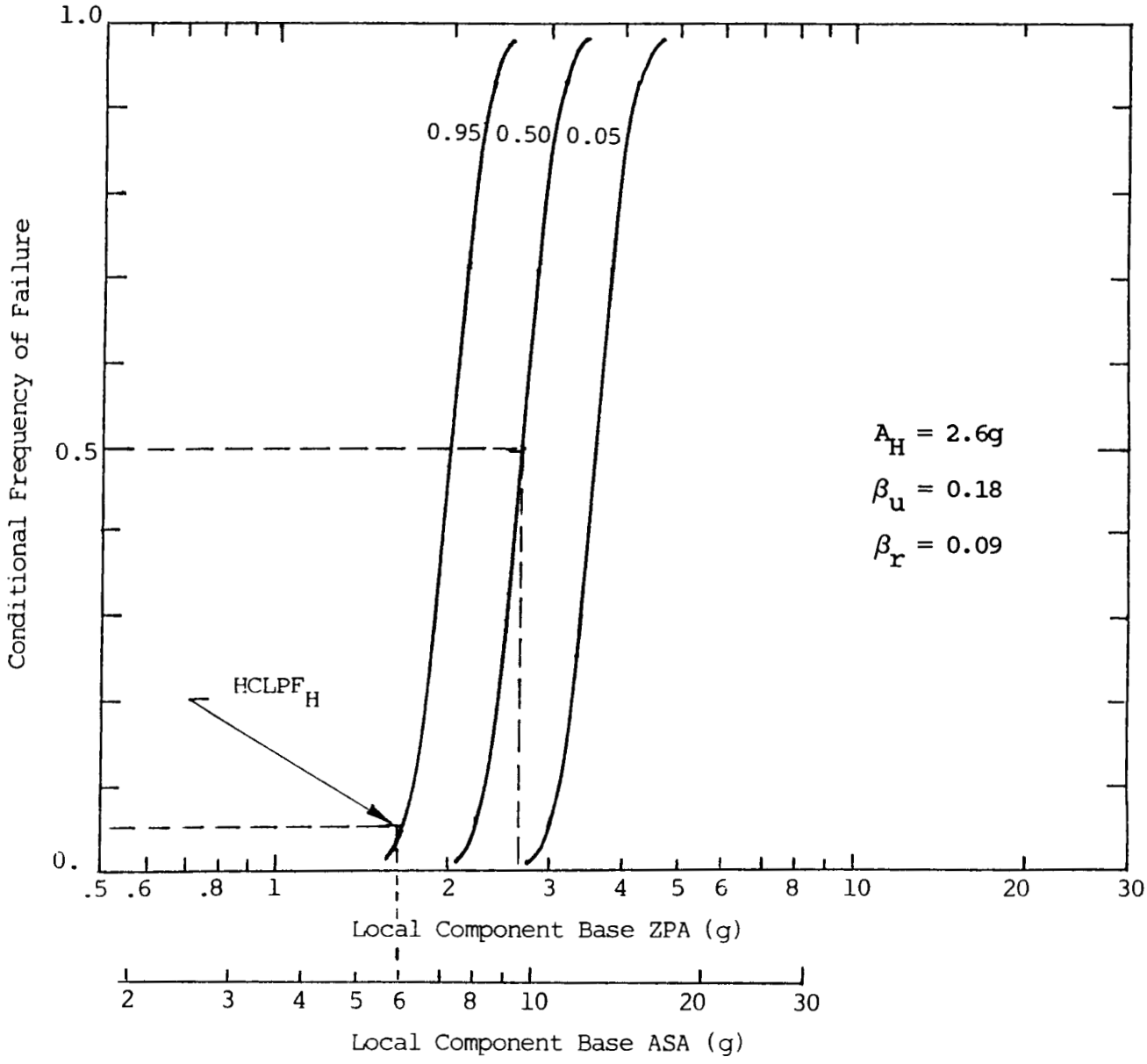

Fig. 3.16 Horizontal seismic fragility curves for the structurally modified fan cooler motor controller.

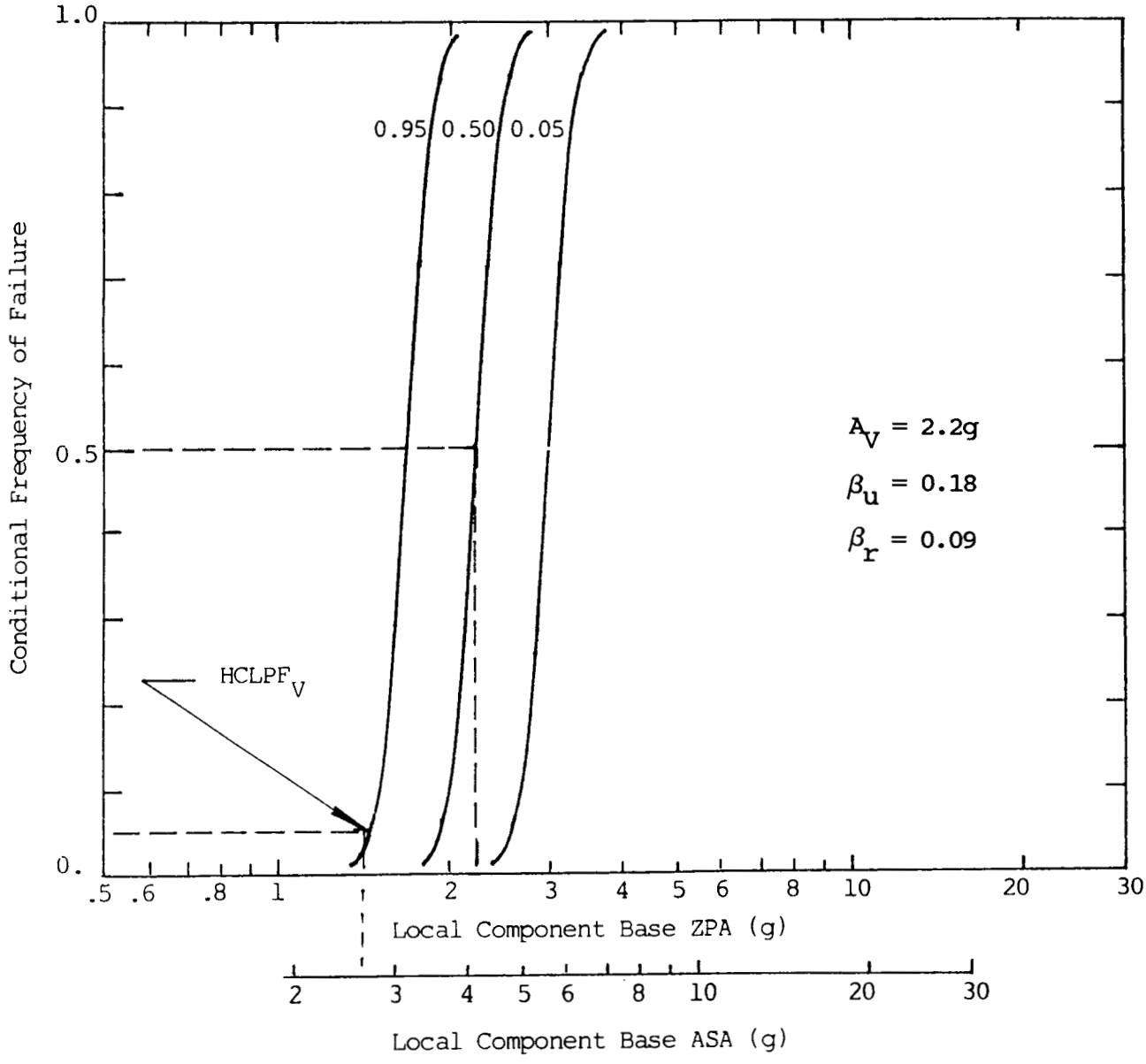

Fig. 3.17 Vertical seismic fragility curves for the commercial standard and structurally modified fan cooler motor controllers.

4. LOCAL STARTERS

4.1 Description of Equipment

The three local starters discussed in this section are in the auxiliary building at the Diablo Canyon plant and are located near their respective controlled loads. They are typically housed in cold-formed sheet metal enclosures that are attached to concrete walls with expansion anchors at its corners. The electrical devices housed in the local starters are nominally the same (i.e. contact-operated motor starters) as those housed in motor control centers. In the local starters, however, the electrical devices whose functionability determines when component "failure" occurs are located much closer to the component mounting point. The devices in a local starter do not therefore see local motions amplified by a complex intermediate structure such as a motor control center cabinet. Consequently, given the fact that we reference fragility to the ZPA (or, alternatively, the ASA) at the component base, we expect local starters to exhibit higher fragility levels than the MCC, even though the internal devices in each component are nominally similar.

Local starters LPF36 and LPF37 are each NEMA Size 1 disconnect switch combination motor controllers weighing approximately 75 pounds. LPG66 is a Size 4 starter weighing about 120 pounds. Figures 4.1, 4.5 and 4.8 show the setup for the qualification tests. Because of similarity in their function, construction and qualification testing, the three local starters will be considered simultaneously in the following discussion.

4.2 Safety Function

The local starters must provide power to their controlled loads on demand. In order to accomplish this required function, the main power contacts must properly operate on demand and remain at the commanded state during and after the earthquakes.

4.3 Seismic Failure Modes

From the results of the qualification tests conducted for the MCC and fan cooler motor controllers, we observed that the starters mounted on these equipment never suffered any structural damage although chattering of contacts sometimes occurred. We therefore rank the seismic failure modes for the local starters in the descending order given below.

(1) Functional failure due to inadvertent change of state of the contactors.

(2) Functional failure of the main power contacts to operate on demand and remain at the commanded state.

(3) Structural failure such that the local starter is disabled.

4.4 Modifications to Improve Seismic Performance

No improvements to any of the three local starters were needed because they all easily withstood the qualification tests at the SSE level without compromise of their required safety function. This was anticipated because the local starters, through the direct rigid mounting to the shaker table, did not experience the amplification of the shaker table motion that the same devices did when mounted on the MCC during the qualification testing of the MCC. In other words, in terms of the local in-cabinet ZPA, the devices were subjected to motions lower than those experienced by the same devices mounted in the Type W MCC during the front-to-back (F-B) test runs.

4.5 Seismic Qualification

For the qualification tests, the local starters were bolted to a rigid test stand using 1/2-inch bolts to simulate the in-service conditions at the plant. The rigid test stand was in turn welded to the shaker table. Accelerometers were attached to the devices to monitor the local device response. Figures 4.1 to 4.4 show the test setup and device response accelerometers for local starter LPF36. Figures 4.5 to 4.7 illustrate the corresponding setup for LPF37, and Figs. 4.8 to 4.9 that for LPG66. Note that both the vertical response of LPF37 and the horizontal and vertical responses of LPG66 were not monitored during the tests.

To monitor the functional operability of the local starters during and after each run, each starter was connected to a 440 VAC one-phase power source. It was then functionally tested by applying 440 VAC to the starter control circuit, connecting the disconnect and starter contact in series, and visually monitoring proper operation prior to and upon completion of the test. During the test the output of the disconnect and starter contacts were connected to a 6VAC stepdown transformer and recorded on a direct readout recorder. The normally-open (NO) and normally-closed (NC) auxiliary contacts were connected to a chatter detector set at a 2 msec threshold. Figure 4.10 shows the wiring diagram for monitoring the function of LPF36, which was typical for local starters LPF37 and LPG66 as well. In addition, visual inspection was conducted to assess the structural integrity of the components at the completion each run.

The seismic tests were conducted in accordance with the guidelines of the 1975 edition of IEEE 344. The test motions were biaxial random motions in either the X-Y (F-B and vertical) or Z-Y (side-to-side and vertical) axis. Five OBE and three SSE runs were conducted in each axis, with the exception that five SSE runs were made for LPF36 in the Z-Y axis. Each run lasted about 30 seconds. During both the OBE and SSE runs, no change of state of the contactor was commanded. The sole exception was the last SSE run for LPF36 in both the X-Y and Z-Y axes, during which the state was switched in order to assure proper operation of the device during a commanded change of state.

The SSE run for LPF36 was conducted in the following manner, starting with the X-Y axis run:

(1) Close disconnect switch.

(2) Run one SSE test with contactor de-energized.

(3) Run one SSE test with contactor energized.

(4) Run last SSE test, first energizing contactor about 10 seconds into the run and then de-energizing the contactor about 10 seconds later.

(5) Rotate the equipment 90 degrees on the shaker table, and repeat the above steps.

(6) Verify proper contactor operation before and after completing each test.

The ZPA of the test motion was about 2g in both the horizontal and vertical directions. Figs. 4.11 and 4.12 show the 3% damping TRS and device response spectrum for the first X-Y axes SSE run, and Figs. 4.13 and 4.14 for the fifth Z-Y axes SSE run.

The SSE runs for LPF37 and LPG66 were conducted in a similar manner. The differences were: (1) only three SSE runs were made in the Z-Y axes, and (2) state of contactor was not switched in the last SSE runs in both X-Y and Z-Y axes. Figs. 4.15 and 4.16 show the horizontal 3% damping TRS and device response spectrum from the third SSE runs in both axes, and Fig. 4.17 shows the vertical TRS from the corresponding runs for LPF37. As previously mentioned the vertical device response spectrum was not available because it was not monitored. For the same reason, only the TRS was available for LPG66, as shown in Figs. 4.18 and 4.19 for the second X-Y and third Z-Y SSE run, respectively. For LPF37 and LPG66, the shaker table ZPA was about 2.0g and 1.1g, respectively, in the horizontal and vertical axes for the SSE runs.

Neither functional failure nor structural damage was detected in any of the qualification tests of the three local starters. Consequently, no modification to the commercial standard local starters was necessary to meet the Hosgri qualification requirements.

Because LPF36 and LPF37 each contain a Size 1 starter, we expected their dynamic response characteristics to be similar although their cabinet configurations are dissimilar. This anticipated consistency is verified upon examining Figs. 4.11 to 4.17:

- The starters appear "rigid" in the side-to-side and vertical directions because no apparent resonance frequency below 33 Hz can be observed.

- The starters appear "stiff", but not rigid, in the F-B axis, with the resonance frequency around 25 Hz.

No direct deduction regarding the dynamic characteristics of local starter LPG66 can be made in the absence of the device response spectrum. From the fact that it contains a Size 4 starter, which is heavier than the Size 1 starter, we judge that LPG66 is more flexible than LPF36 and LPF37, particularly in the F-B axis.

4.6 Seismic Capability

The minimum seismic capacity of the local starters is assumed to correspond to the envelope of the TRS for the various SSE runs.

$(\overset{v}{A}_H)_{min}$ - for LPF36 and LPF37, the minimum horizontal seismic capacity may be represented by the simplified base motion spectrum shown in Fig. 4.20, with a ZPA of 2.0g. For LPG66, the same minimum horizontal seismic capacity may be assumed, as shown in Fig. 4.21.

$(\overset{v}{A}_V)_{min}$ - for LPF36 and LPF37, the minimum vertical capacity is taken to be the same as that shown in Fig. 4.20 for the horizontal direction. This is because the TRS for the SSE runs of LPF36 was about the same in both horizontal and vertical directions. The minimum vertical capacity of LPG66 is taken to be the one shown in Fig. 4.21, having a ZPA of 1.1g.

The seismic fragility of the local starters is estimated on the basis of the following assumptions:

(1) The fragility may be adequately represented by both the ZPA and ASA of the motion at the base of the starter.

(2) The HCLPF ZPA capacity corresponds to the ZPA of the spectrum representing the minimum seismic capacity of the equipment, i.e., Figs. 4.20 and 4.21. Thus, the HCLPF capacity for starters LPF36 and 37 becomes 2.0g for both horizontal and vertical vibrations, and for LPG66, 2.0g and 1.1g for horizontal and vertical motion, respectively. The corresponding HCLPF ASA capacity is 8.0g for local starters LPF36 and LPF37 in both horizontal and vertical directions, and for local starter LPG66 in the horizontal direction. The HCLPF vertical ASA capacity for local starter LPG66 is 2.6g.

(3) The probability distribution of the seismic capacity is log-normal. The associated uncertainty and random variability is taken to be $\beta_u = 0.18$ and $\beta_r = 0.09$ for local starter LPF36 and LPF37, which is consistent with what was previously assumed for other plant-specific electrical components in the Diablo Canyon plant. For local starter LPG66, we assume the same random variability, $\beta_r = 0.09$, but an uncertainty $\beta_u = 0.27$, which is 50% higher than that assumed previously for all other plant-specific

electrical components at the Diablo Canyon plant. Based on the HCLPF horizontal ZPA capacity of 2.0g, the corresponding median ZPA capacity becomes 3.6g when $\beta_u = 0.27$ is assumed. This median ZPA capacity, estimated on the basis of a larger uncertainty, is judged reasonable in view of the amplified response that was experienced by the MCC-mounted Size 4 starter during the LLNL demonstration test and during the PG&E qualification test for the Type W MCC. For example, the median horizontal capacity for the Size 2 starter was about 3.9g, in terms of the local base ZPA of the device, and the corresponding median capacity for the Size 4 starter would, in our judgment, equal or exceed 3.9g (see Ref. 1). Note that the same reasoning is not applicable to local starters LPF36 and LPF37 because Size 1 starters were not included in the LLNL demonstration test and the Size 1 starters included in the PG&E qualification test did not experience as much amplification as that experienced by the larger-size starters.

Based on the above assumptions, the estimated ZPA and ASA median capacities for the local starters ($\hat{A}$ and $\hat{S}$, respectively) are given in Table 4.1. Figure 4.22 shows the corresponding fragility curves for local starters LPF36 and LPF37, Figs. 4.23 and 4.24 the equivalent information for local starter LPG66. The ratio of ASA to ZPA is 4.0 for LPF36 and LPF37 in both the horizontal and vertical directions, and 4.0 and 2.4 for LPG66 in the horizontal and vertical directions, respectively.

Table 4.1 Median seismic fragility of local starters

	LPF36 and LPF37		LPG66	
	$\hat{A}$	$\hat{S}$	$\hat{A}$	$\hat{S}$
Horizontal (g)	3.1	12.4	3.6	14.4
Vertical (g)	3.1	12.4	2.0	4.8
β_u	0.18		0.27	
β_r	0.09		0.09	

Notes:

$\hat{A}$ = median capacity based on ZPA

$\hat{S}$ = median capacity based on ASA

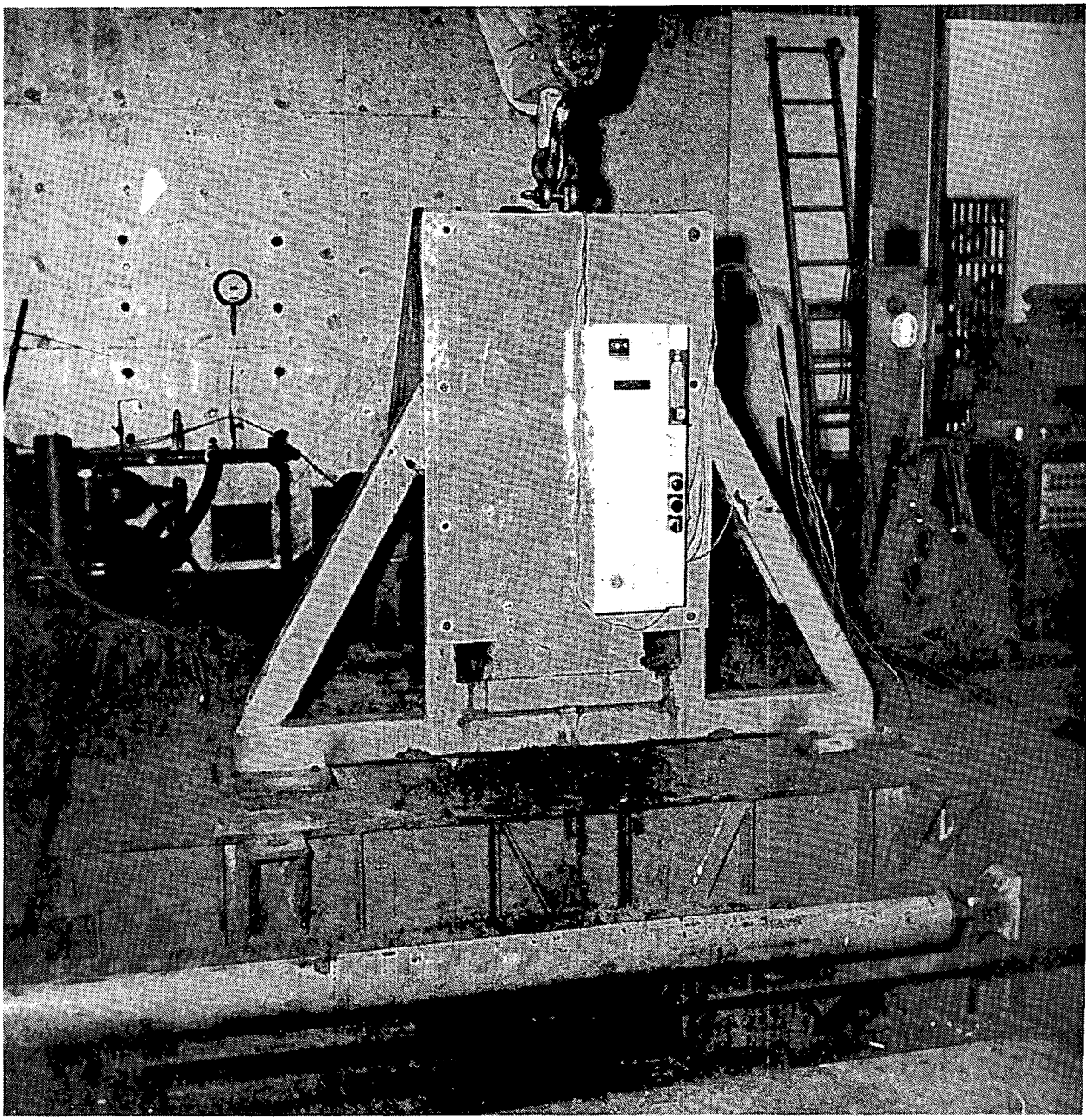

Fig. 4.1 Front-to-back and vertical test setup for local starter LPF36.

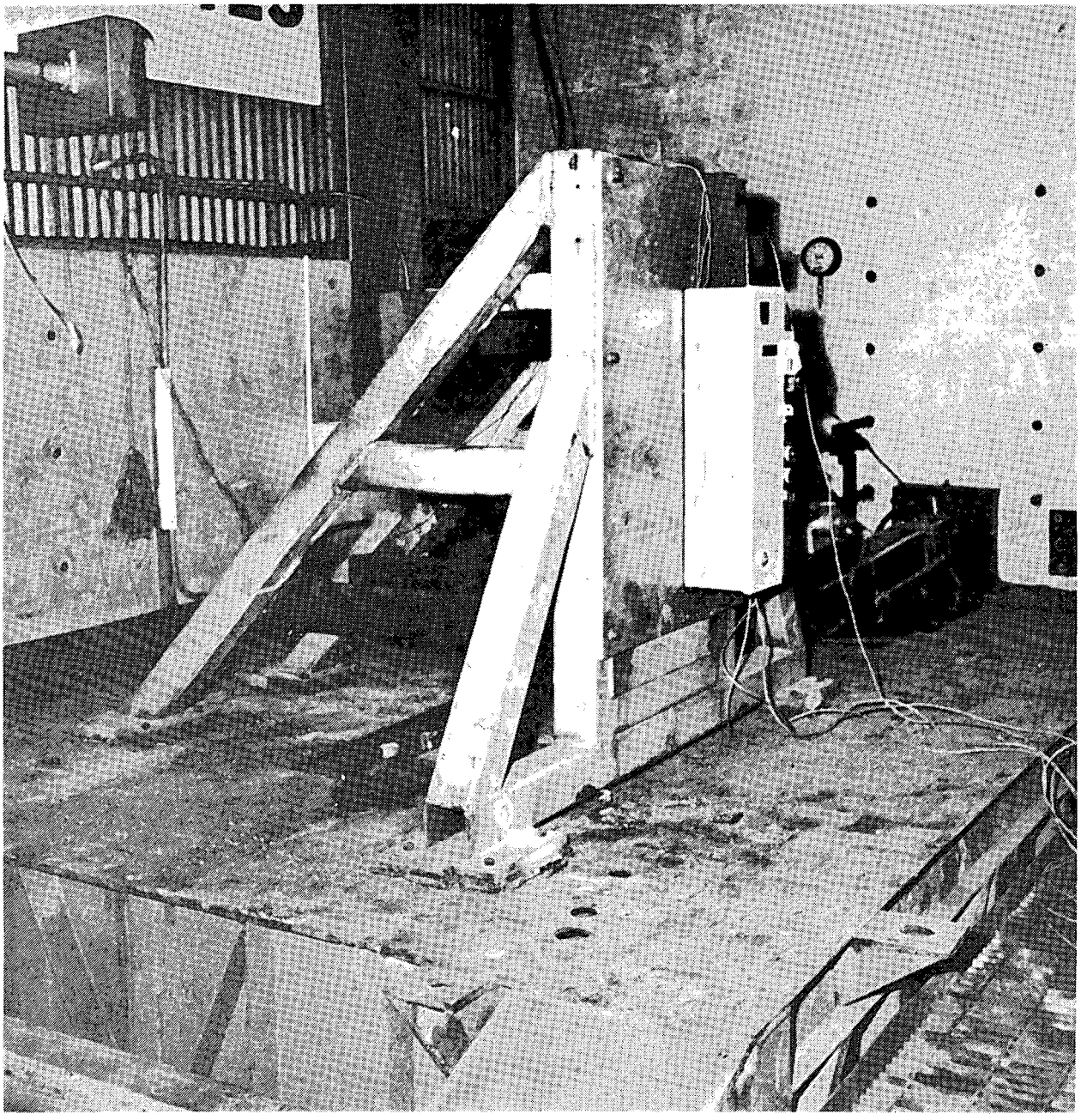

Fig. 4.2 Side-to-side and vertical test setup for local starter LPF36.

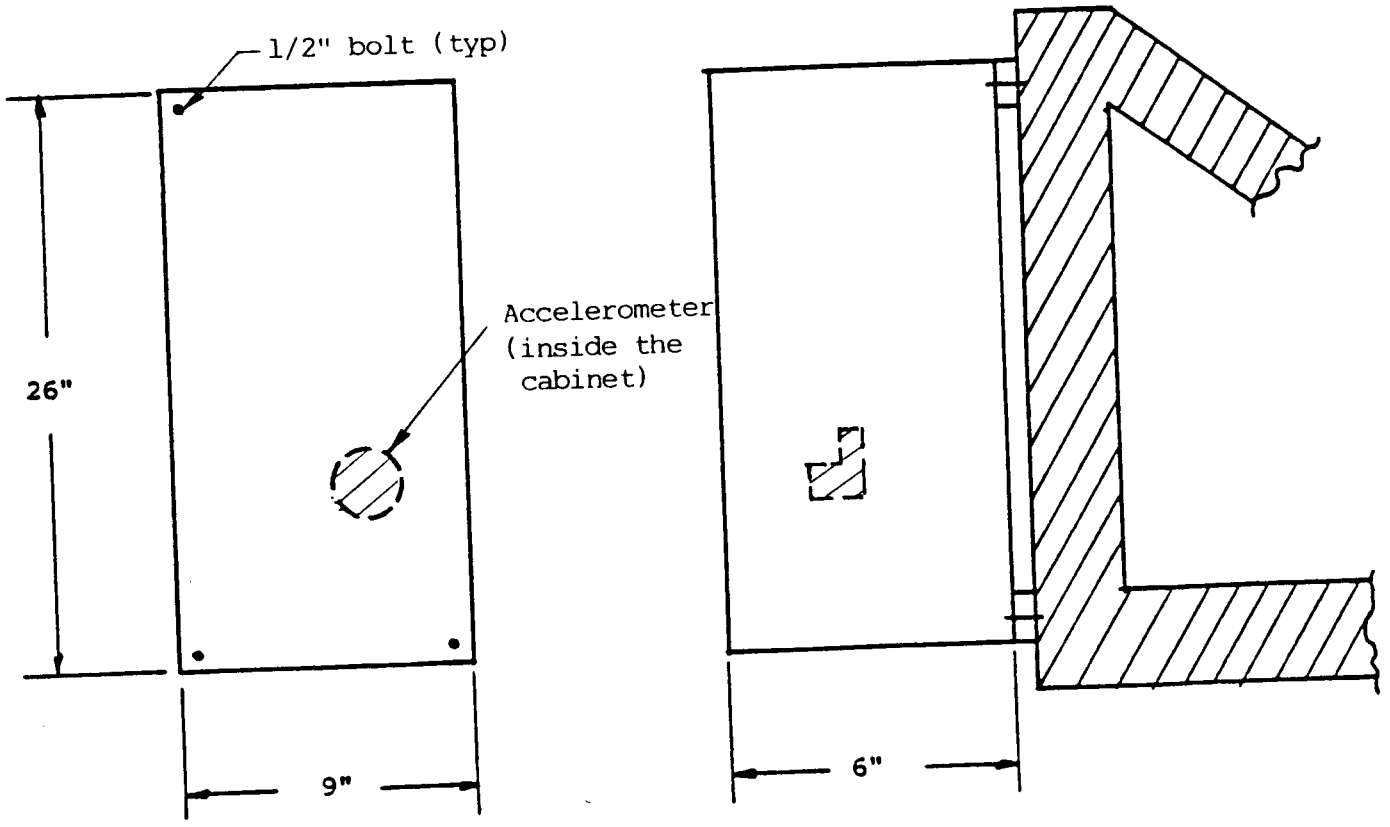

**Four mounting bolts
Fixture support only
near bolts.**

Fig. 4.3 Mounting of local starter LPF36 to test fixture and accelerometer mounted behind cabinet door.

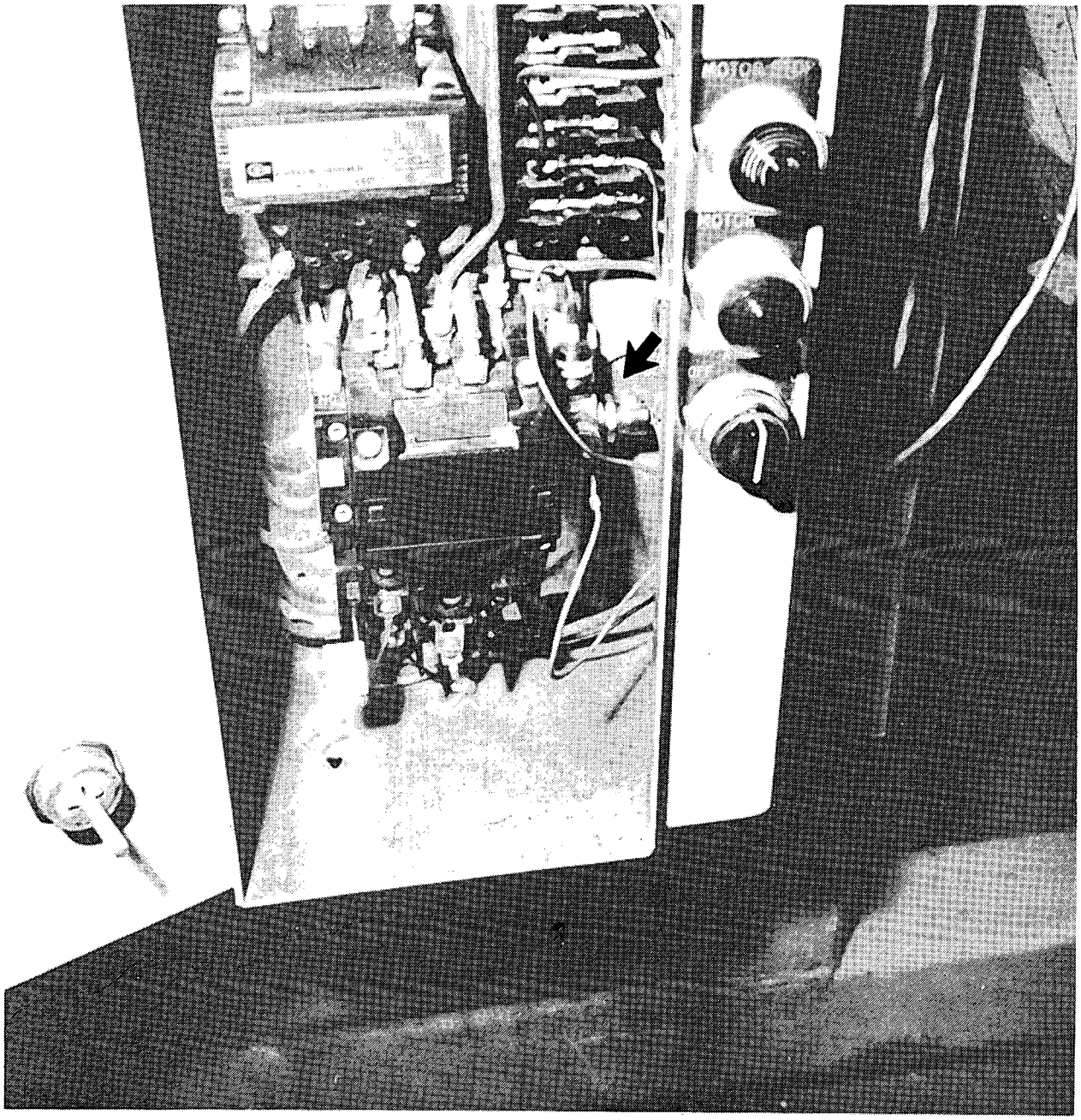

Fig. 4.4 Location of accelerometer on local starter LPF36 with cabinet door removed.

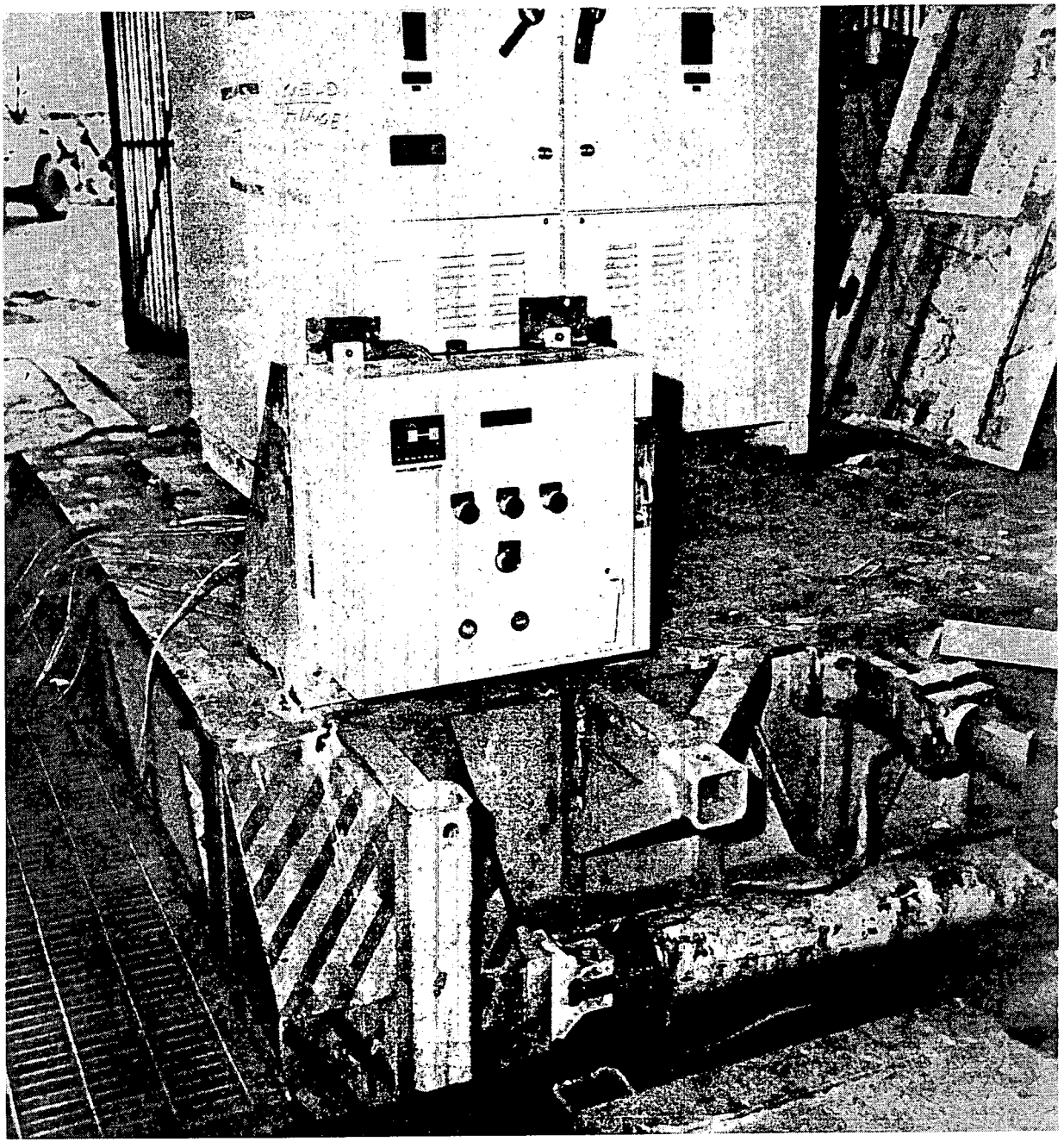

Fig. 4.5 Test setup for local starter LPF37, with a battery charger in the background.

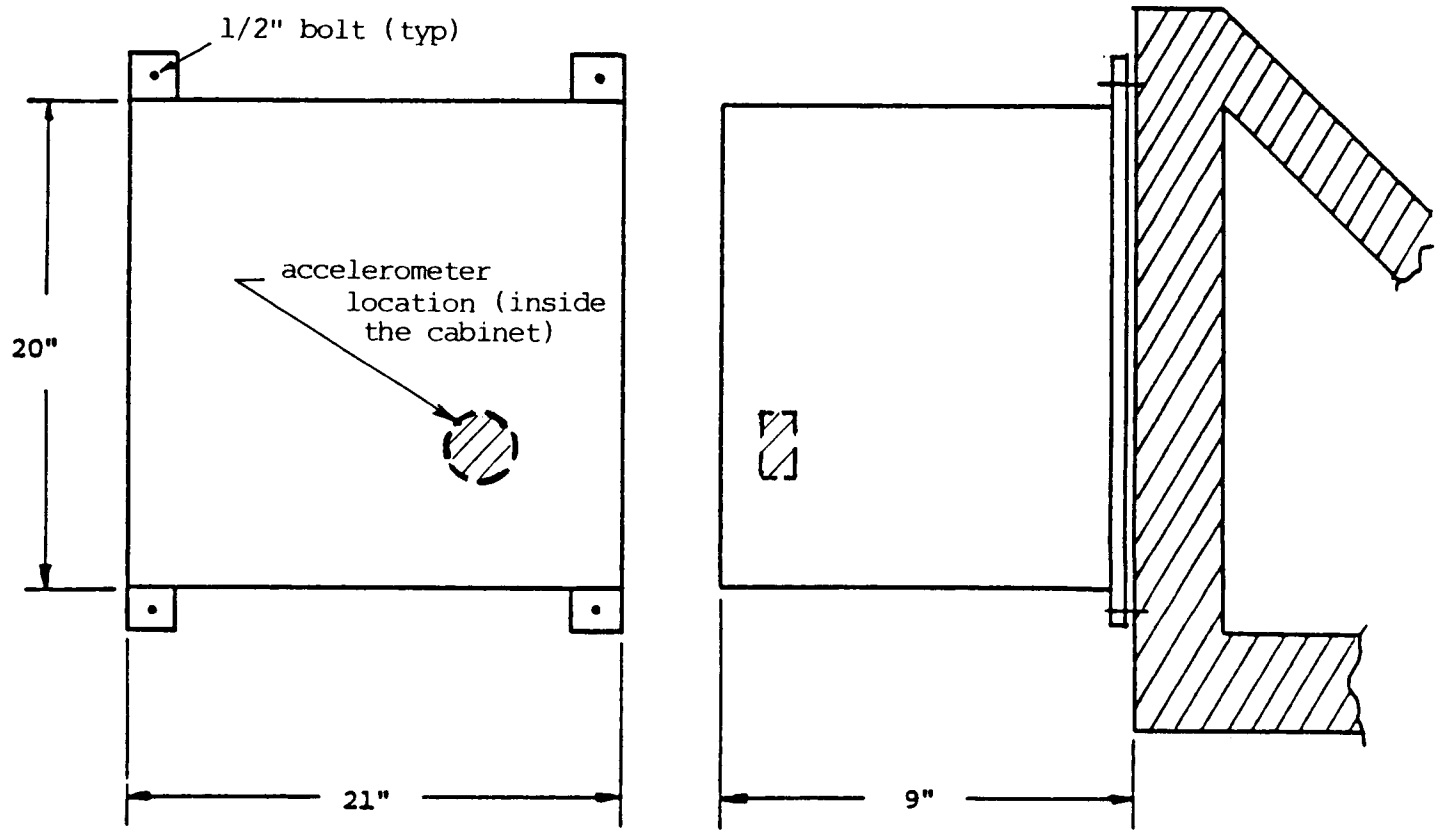

Test specimen bolted to fixture

Fig. 4.6 Mounting of local starter LPF37 to test fixture and location of accelerometer (horizontal only).

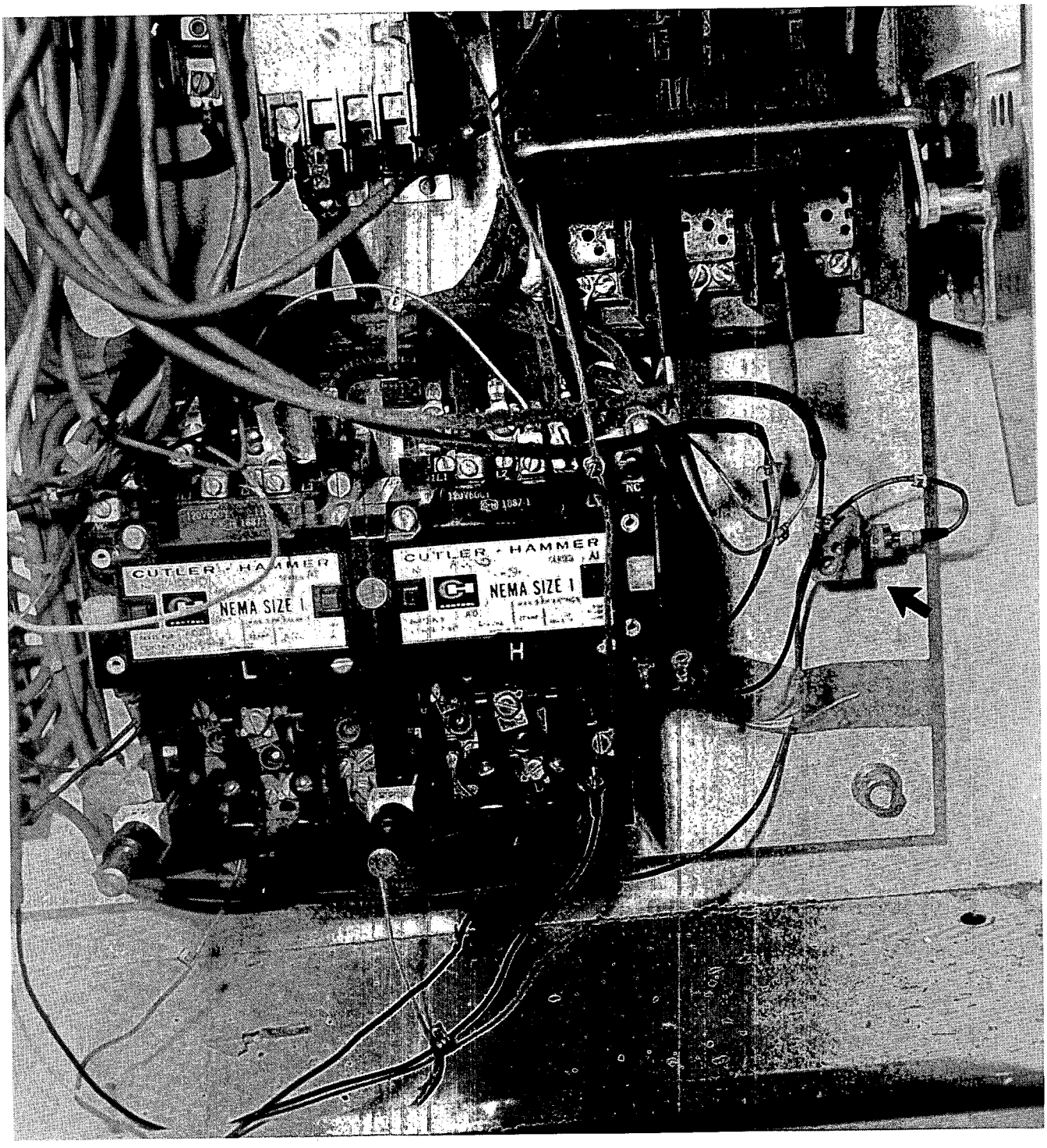

Fig. 4.7 Location of accelerometer on local starter LPF37 shown with cabinet door removed.

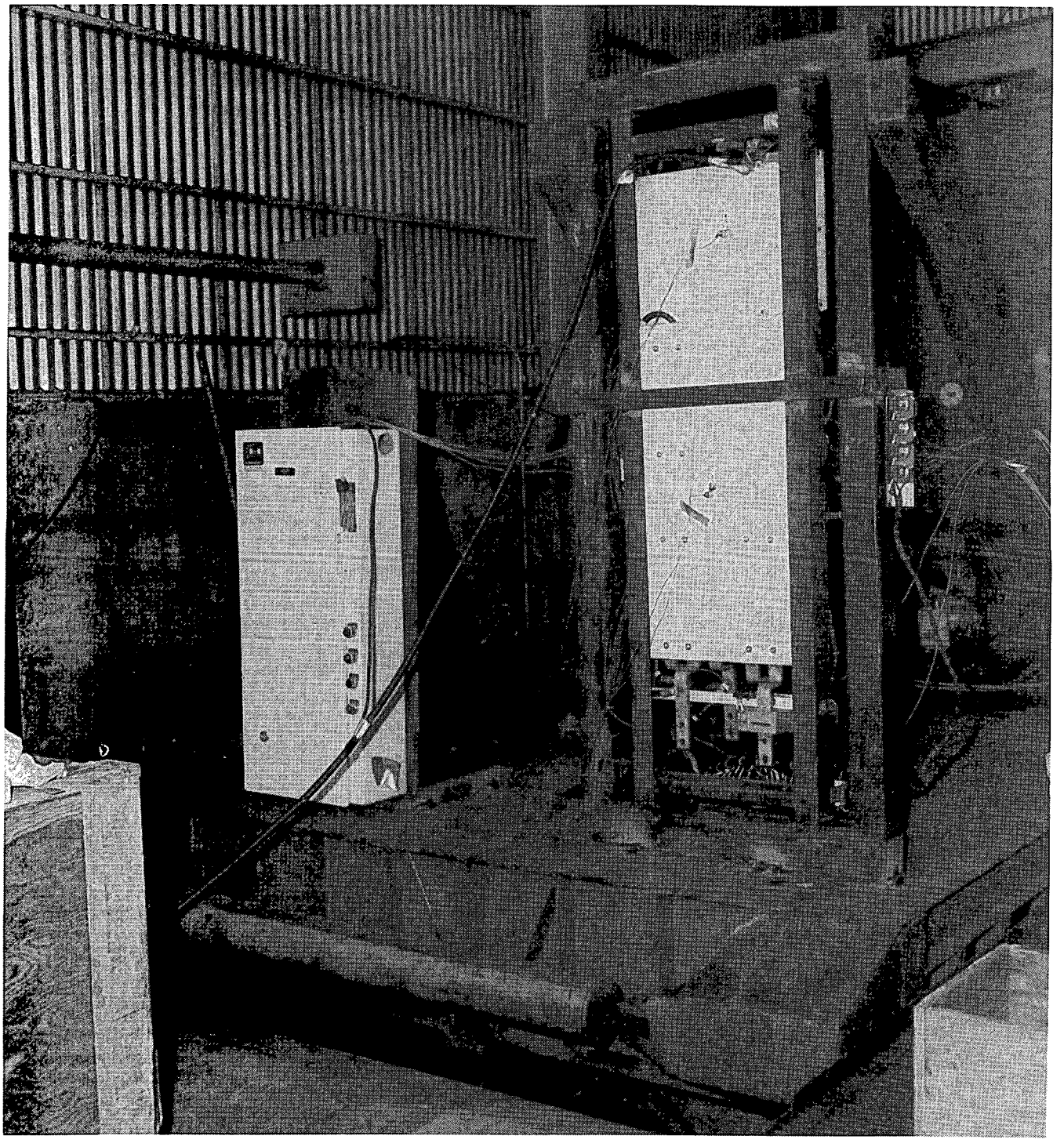

Fig. 4.8 Test setup for local starter LPG66 together with fan cooler controller and Fisher controller.

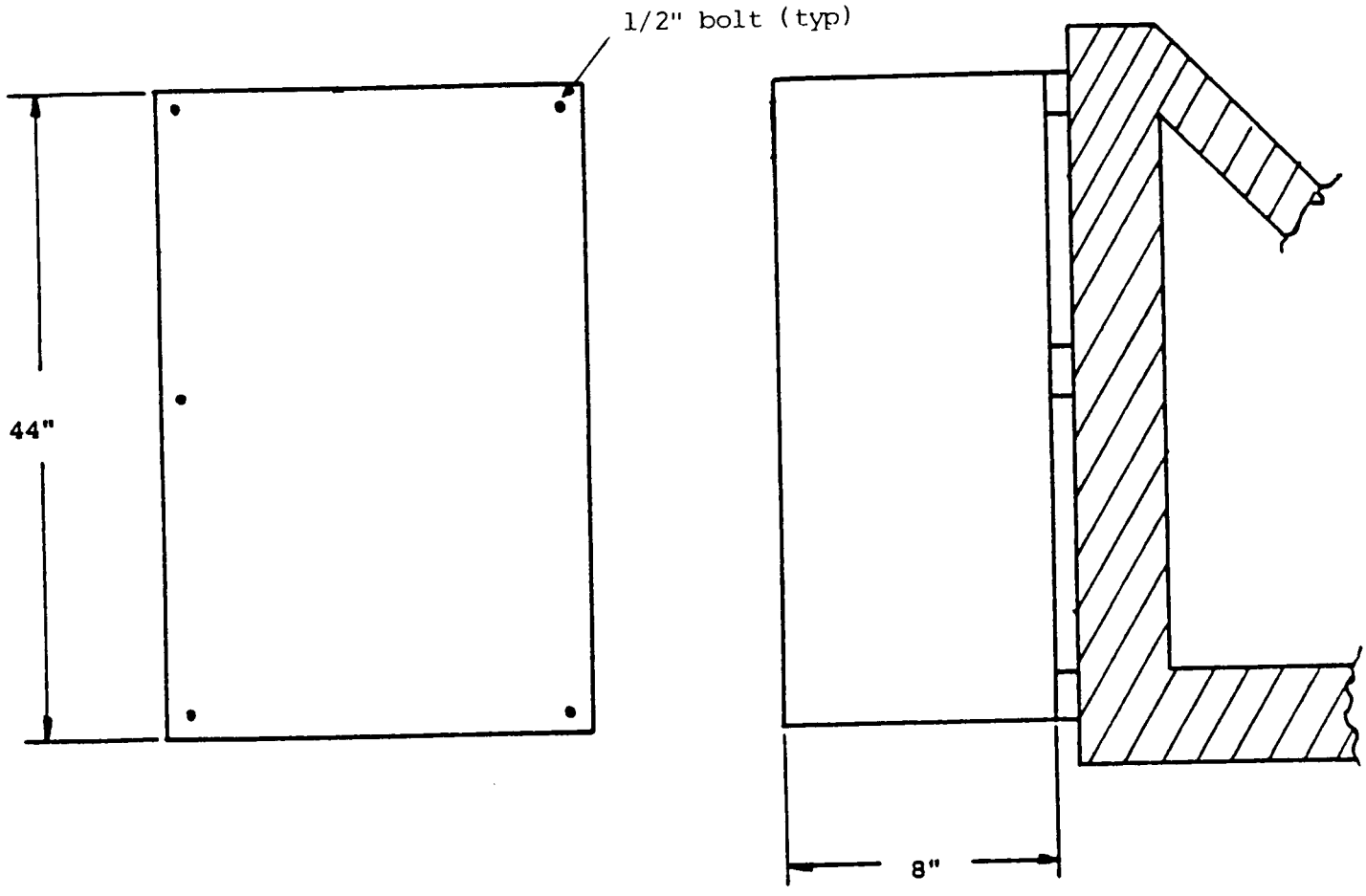

Five mounting bolts

Test specimen will be bolted to fixture.

Fig. 4.9 Mounting of local starter LPG66 to test fixture.

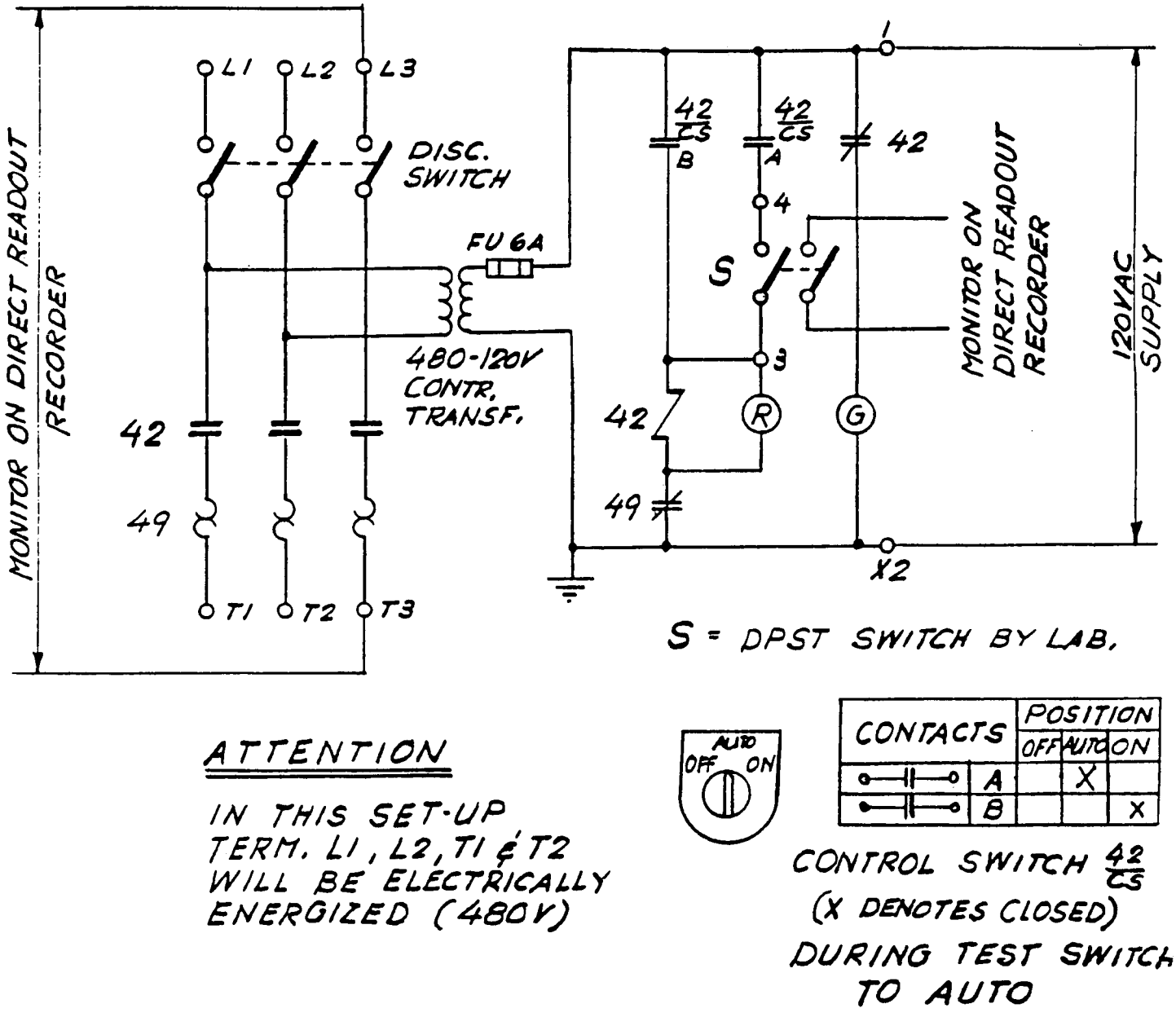

Fig. 4.10 Wiring diagram for local starter LPG66.

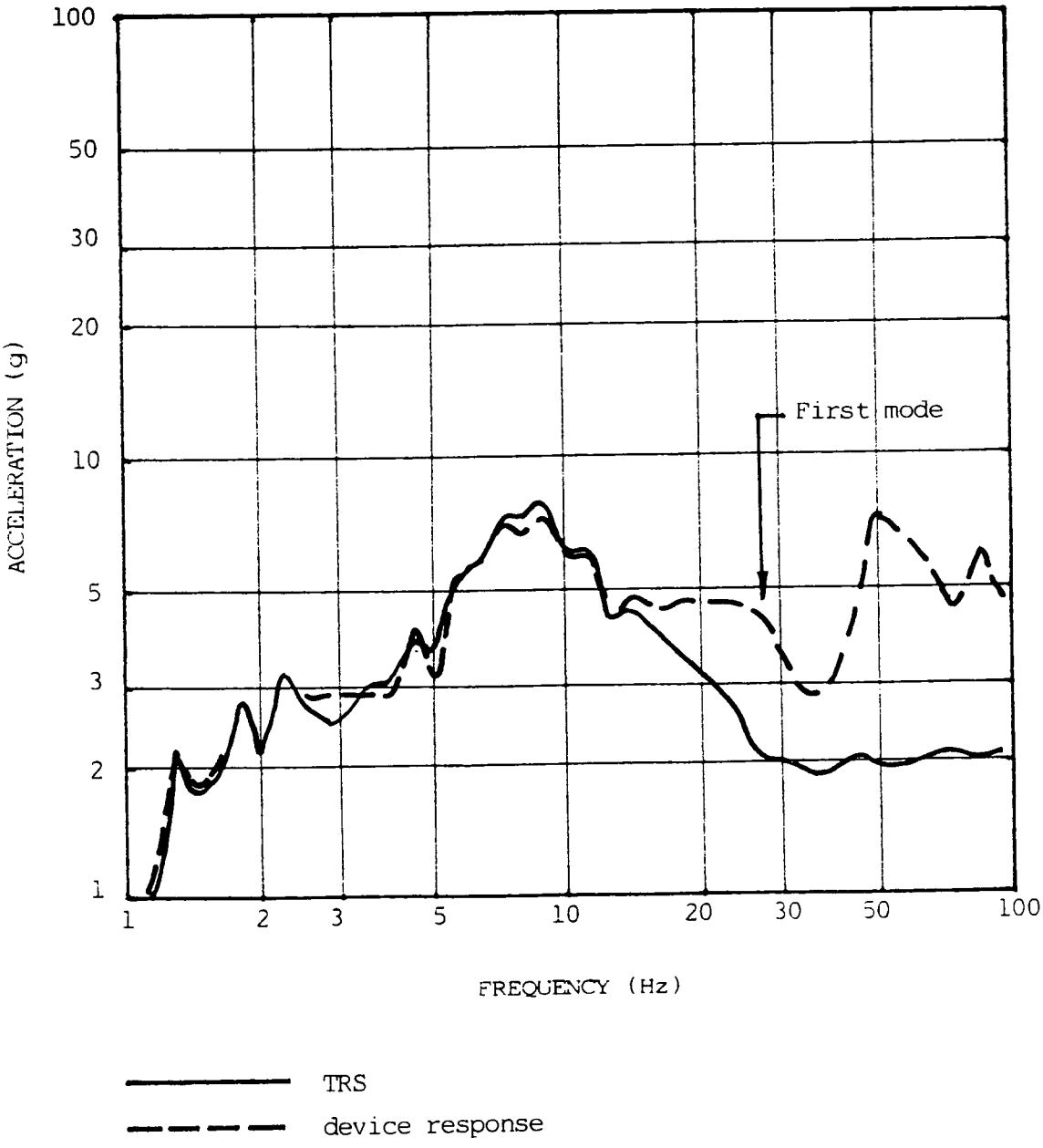

Fig. 4.11 Front-to-back TRS and device response spectrum for the first X-Y axis SSE test of local starter LPF36 (3% damping).

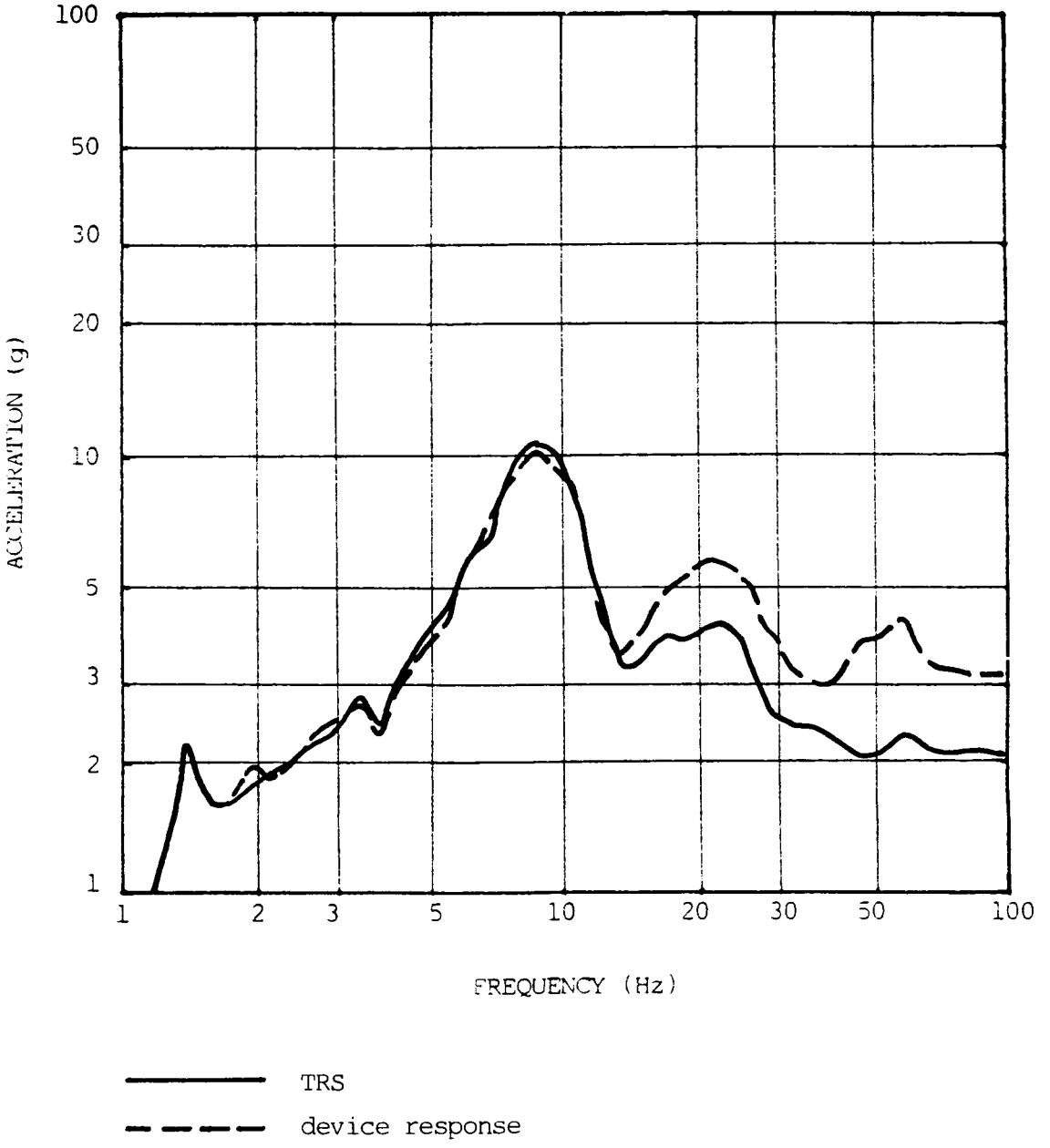

Fig. 4.12 Vertical TRS and device response spectrum for the first X-Y axis SSE test of local starter LPF36 (3% damping).

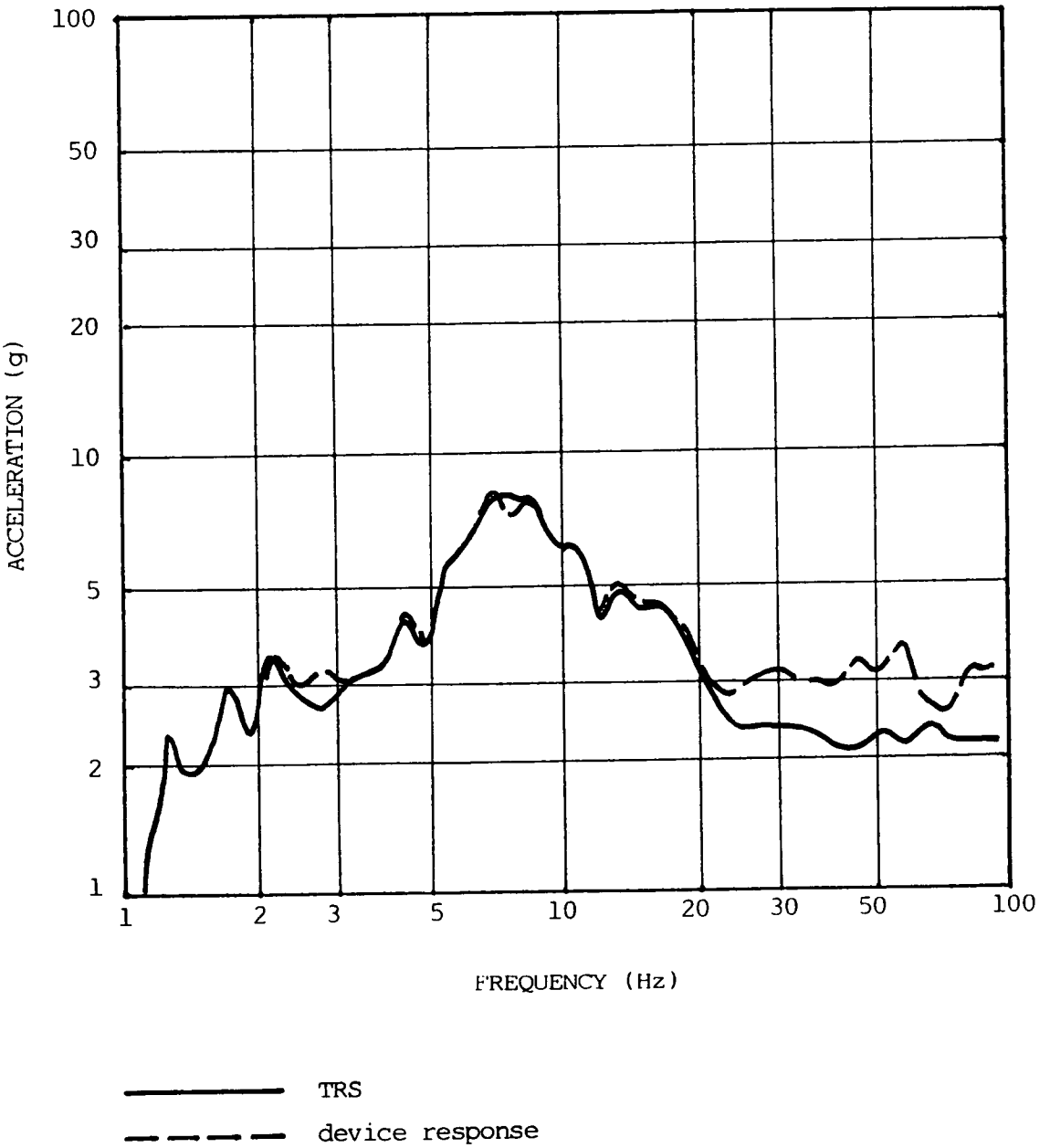

Fig. 4.13 Side-to-side TRS and device response spectrum for the first Z-Y axis SSE test of local starter LPF36 (3% damping).

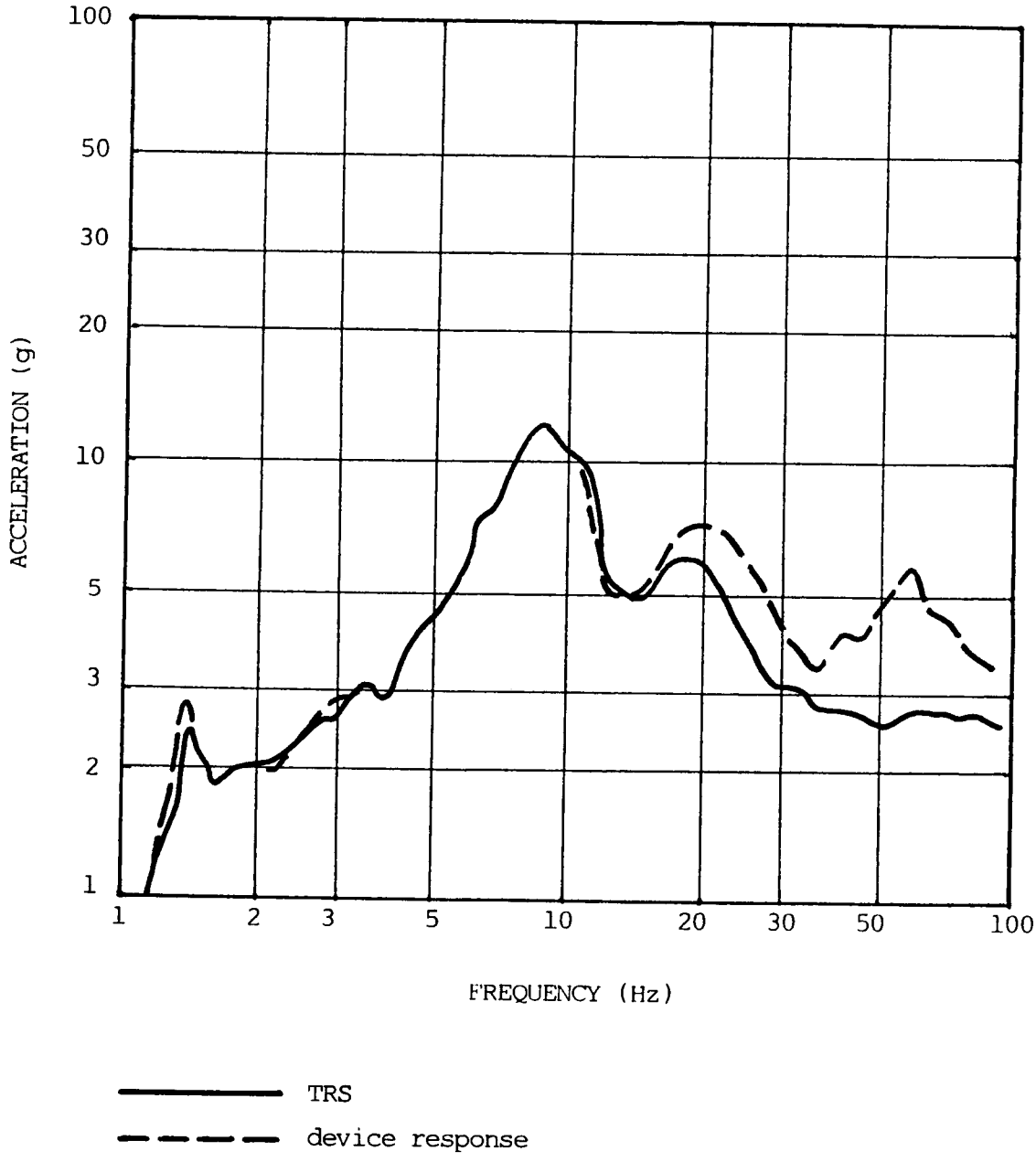

Fig. 4.14 Vertical TRS and device response spectrum for the fifth Z-Y axis SSE test of local starter LPF36 (3% damping).

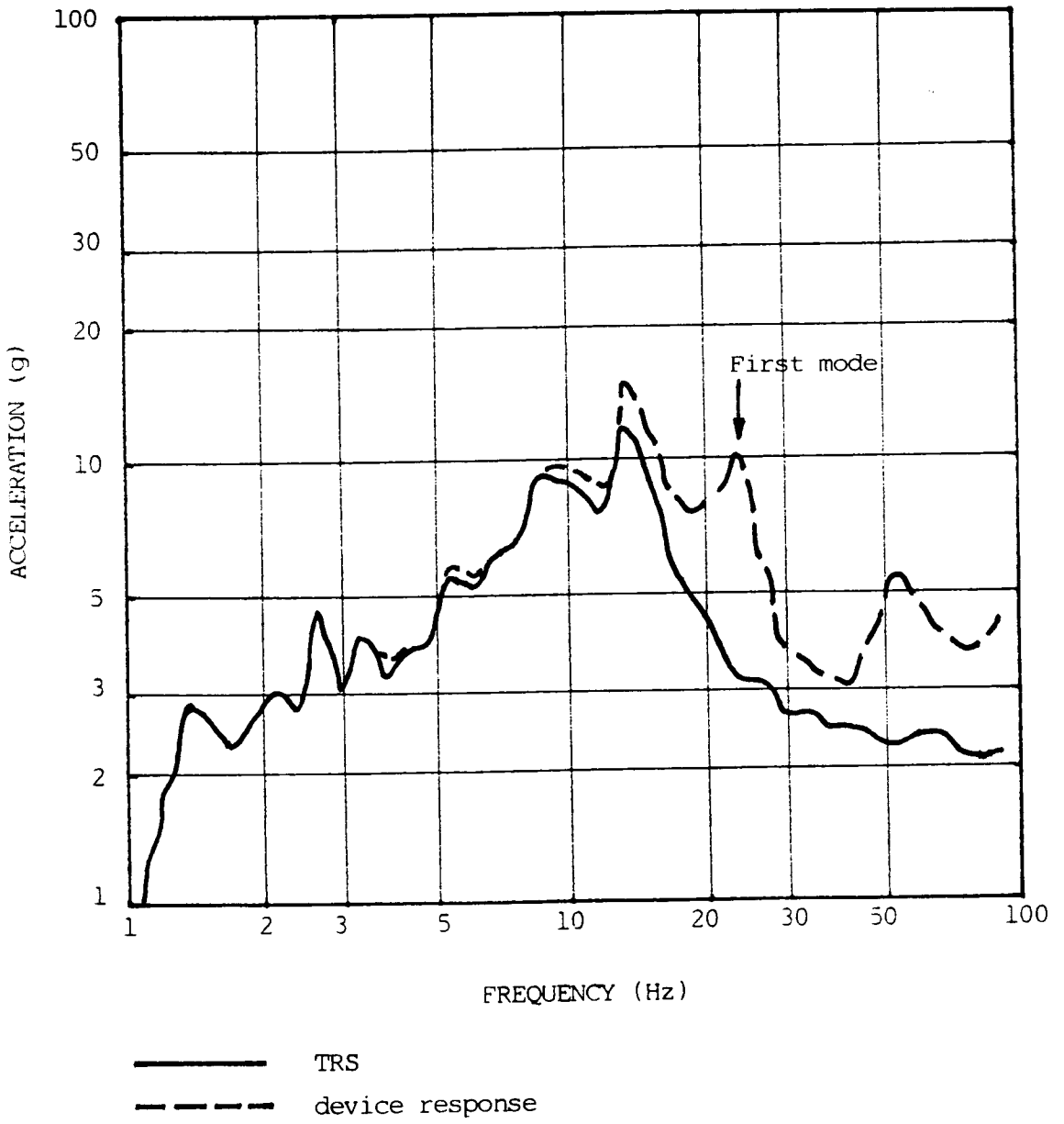

Fig. 4.15 Front-to-back TRS and device response spectrum for the third X-Y axis SSE test of local starter LPF37 (3% damping).

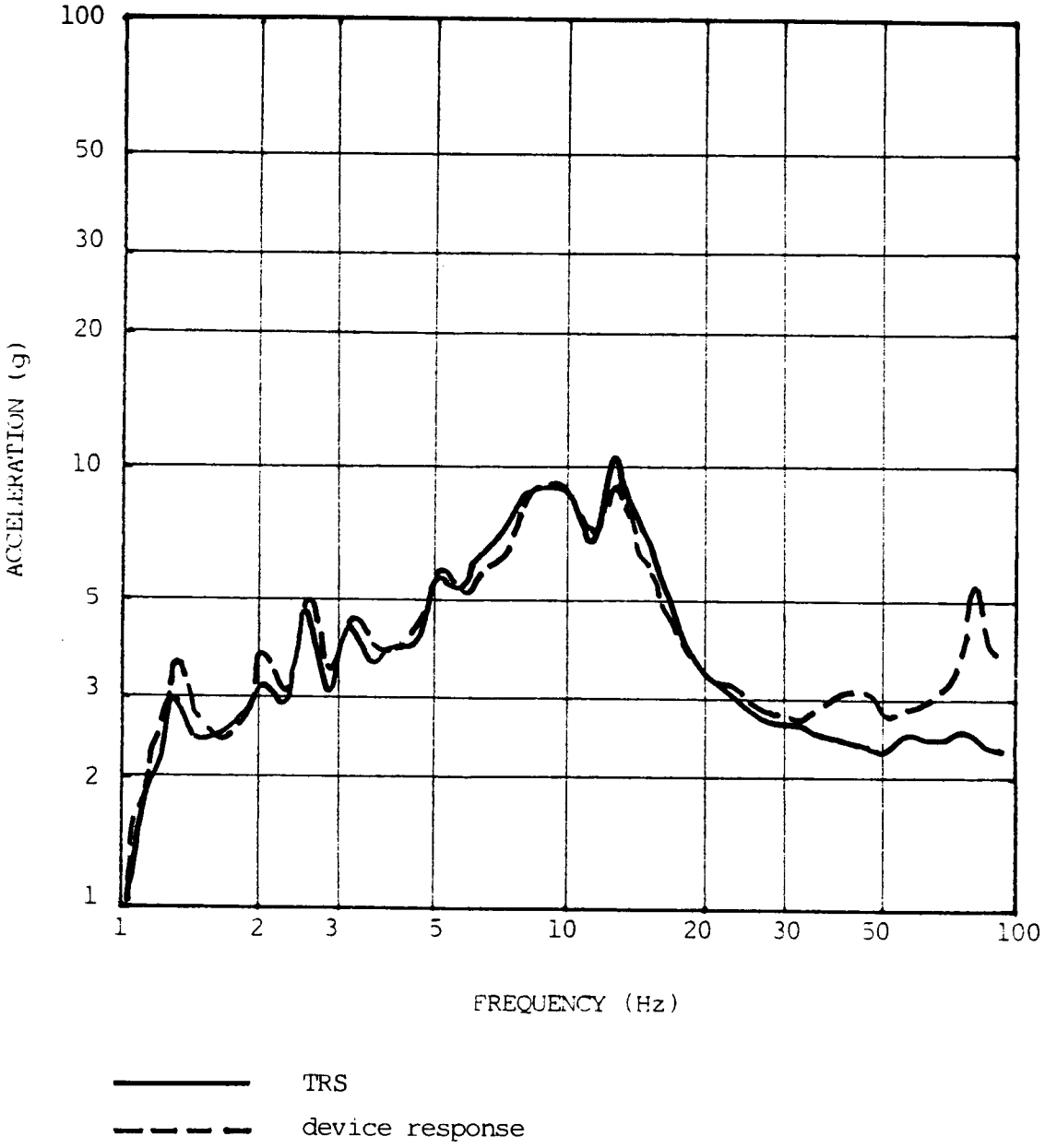

Fig. 4.16 Side-to-side TRS and device response spectrum for the third Z-Y axis SSE test of local starter LPF37 (3% damping).

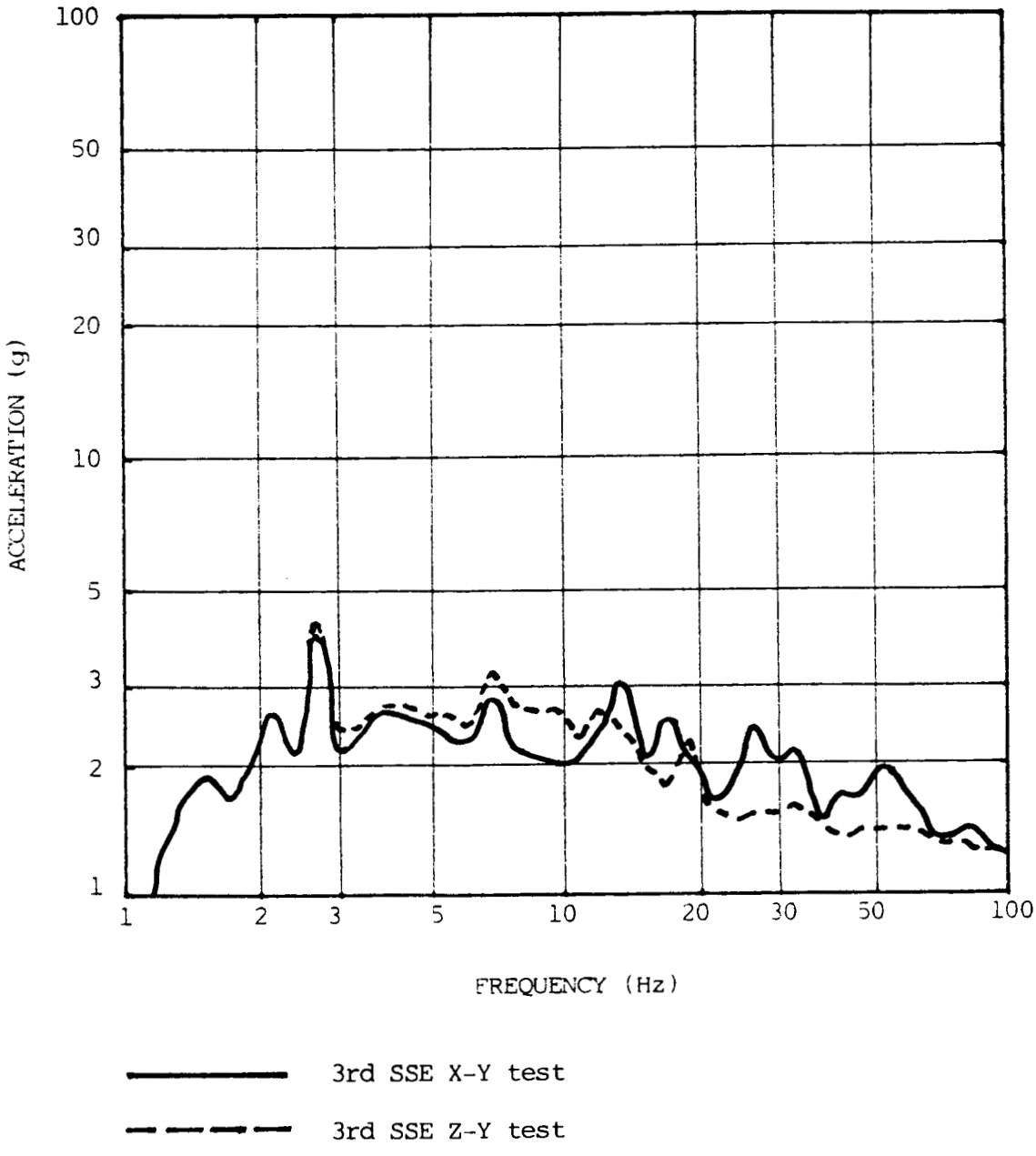

Fig. 4.17 Vertical TRS and device response spectrum for the third X-Y axis SSE test of local starter LPF37 (3% damping).

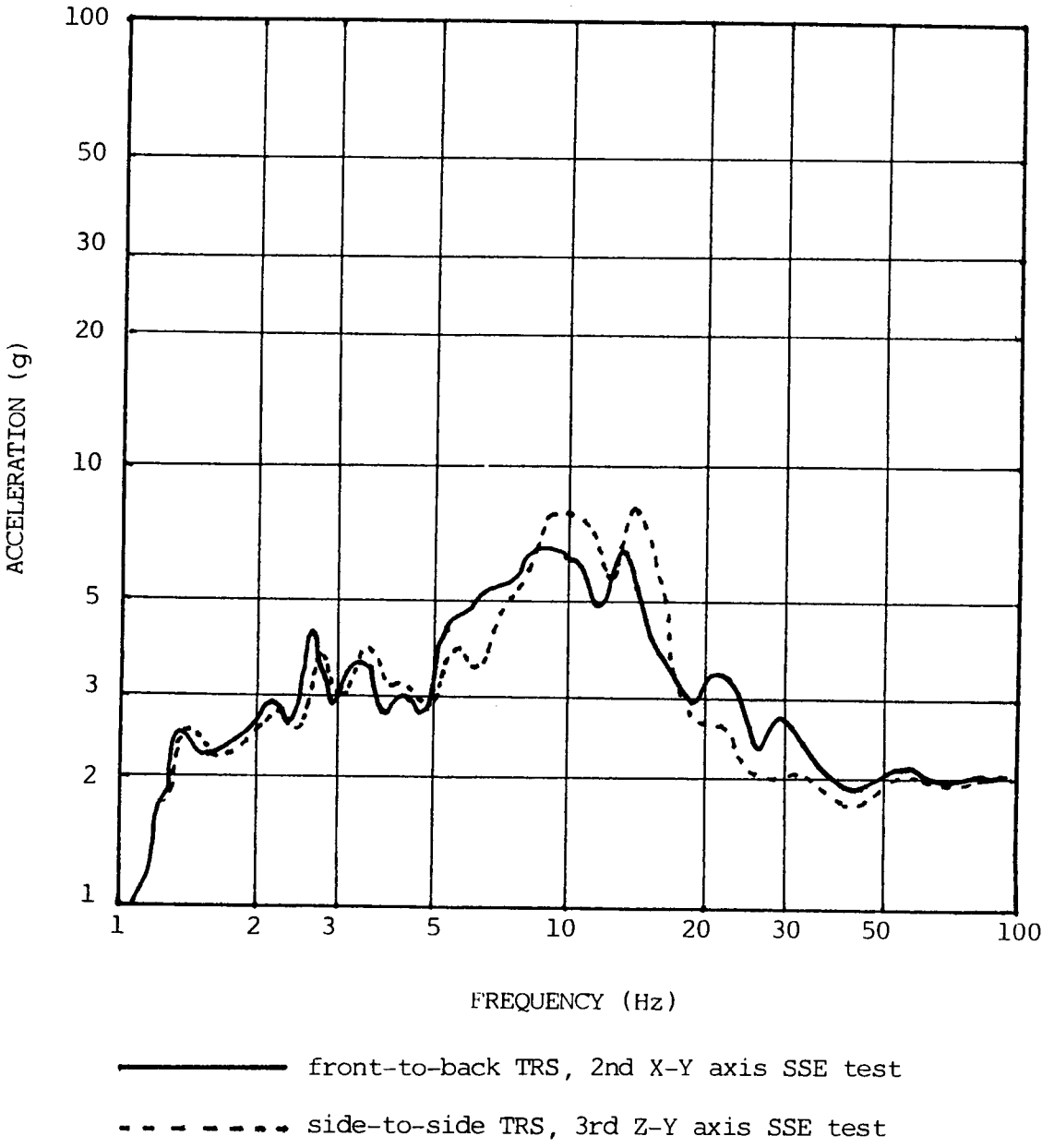

Fig. 4.18 Horizontal TRS and device response spectrum for the second X-Y and third Z-Y axis SSE qualification tests for local starter LPG66 (3% damping).

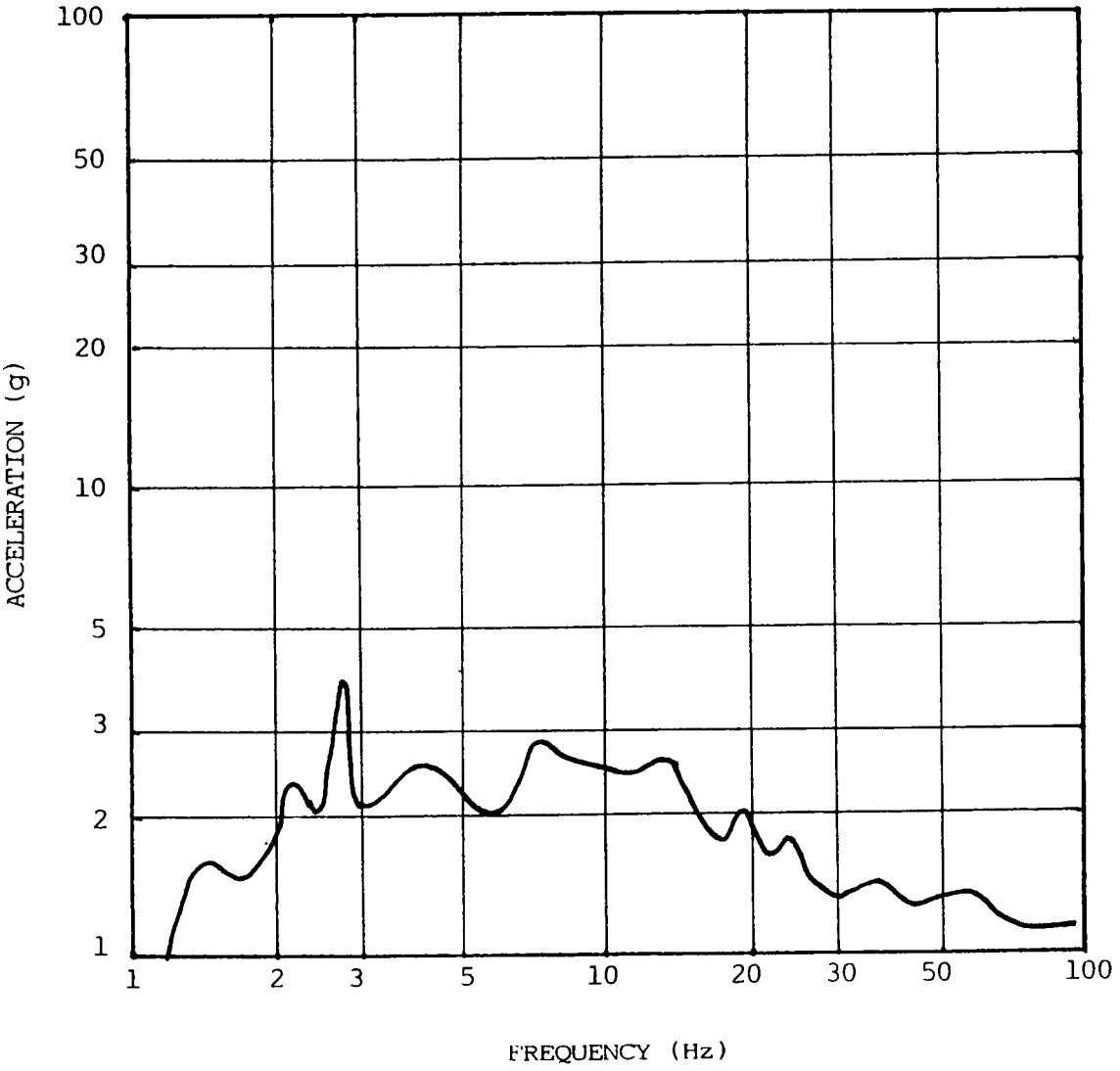

Fig. 4.19 Vertical TRS for the second X-Y axis SSE qualification test for local starter LPG66 (3% damping).

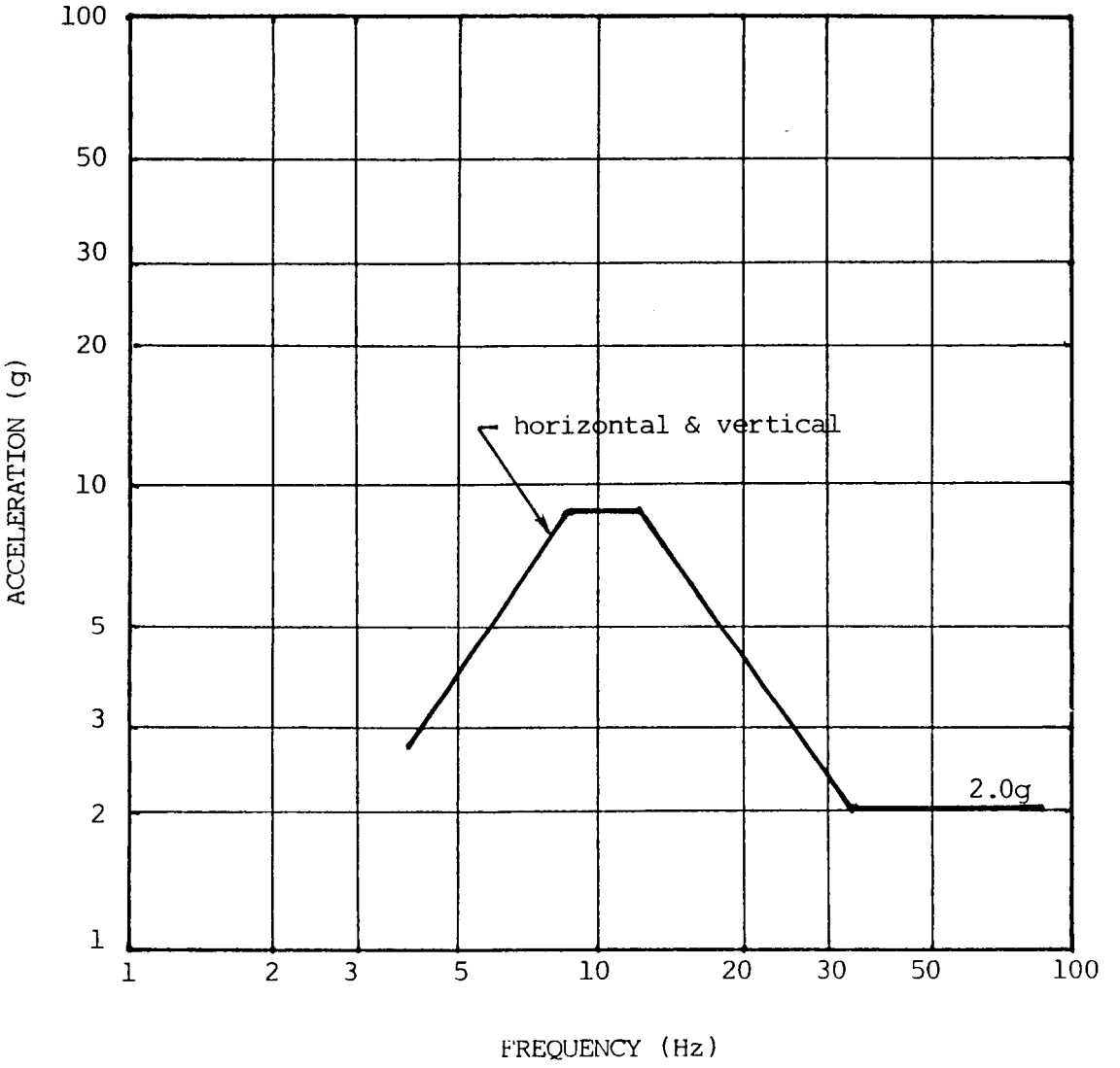

Fig. 4.20 Minimum seismic capacity of local starters LPF36 and LPF37 (with Size 1 starter) expressed as a 3% damping spectrum at equipment base.

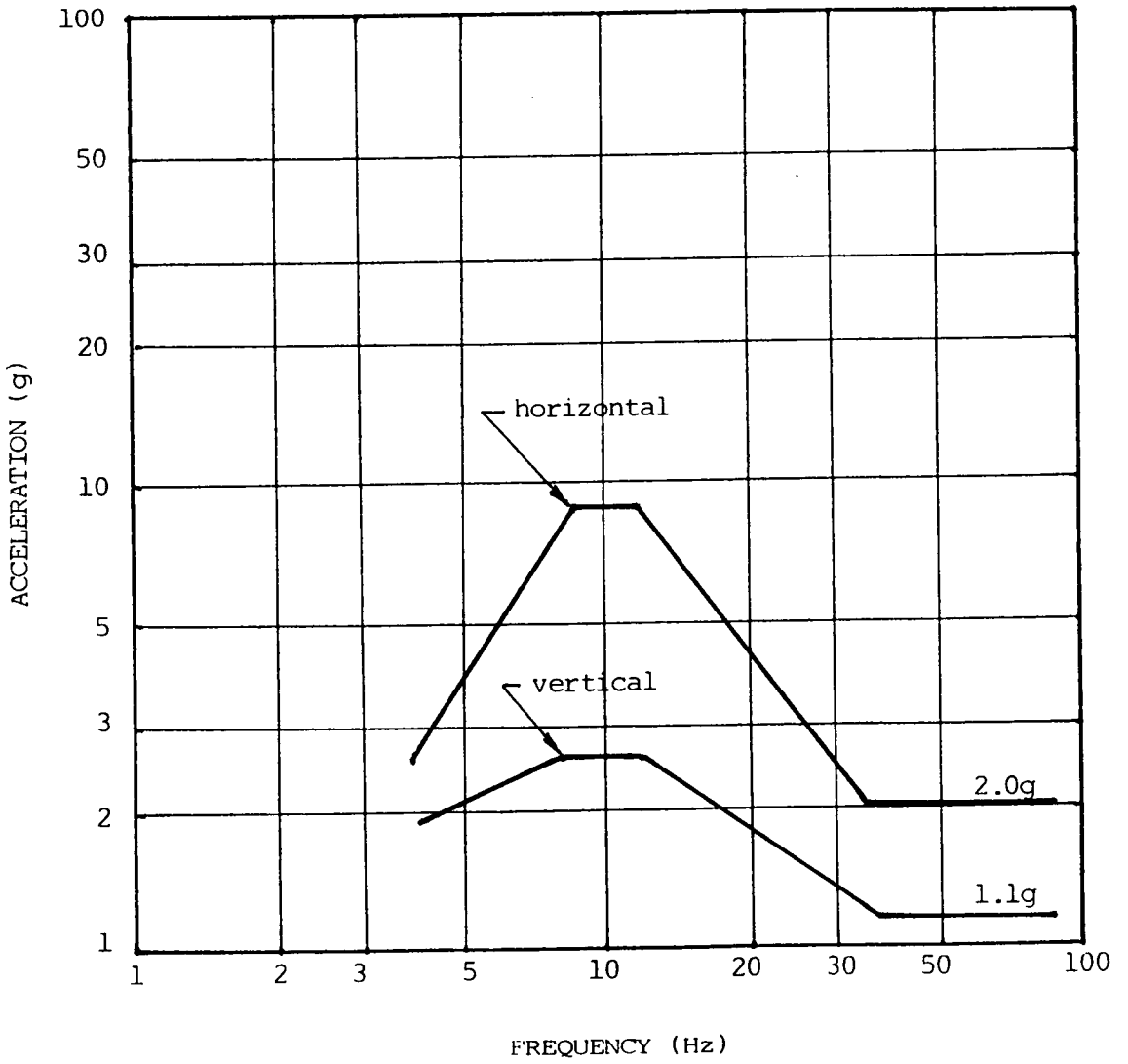

Fig. 4.21 Minimum seismic capacity of local starter LPG66 (with Size 4 starter) expressed as a 3% damping spectrum at equipment base.

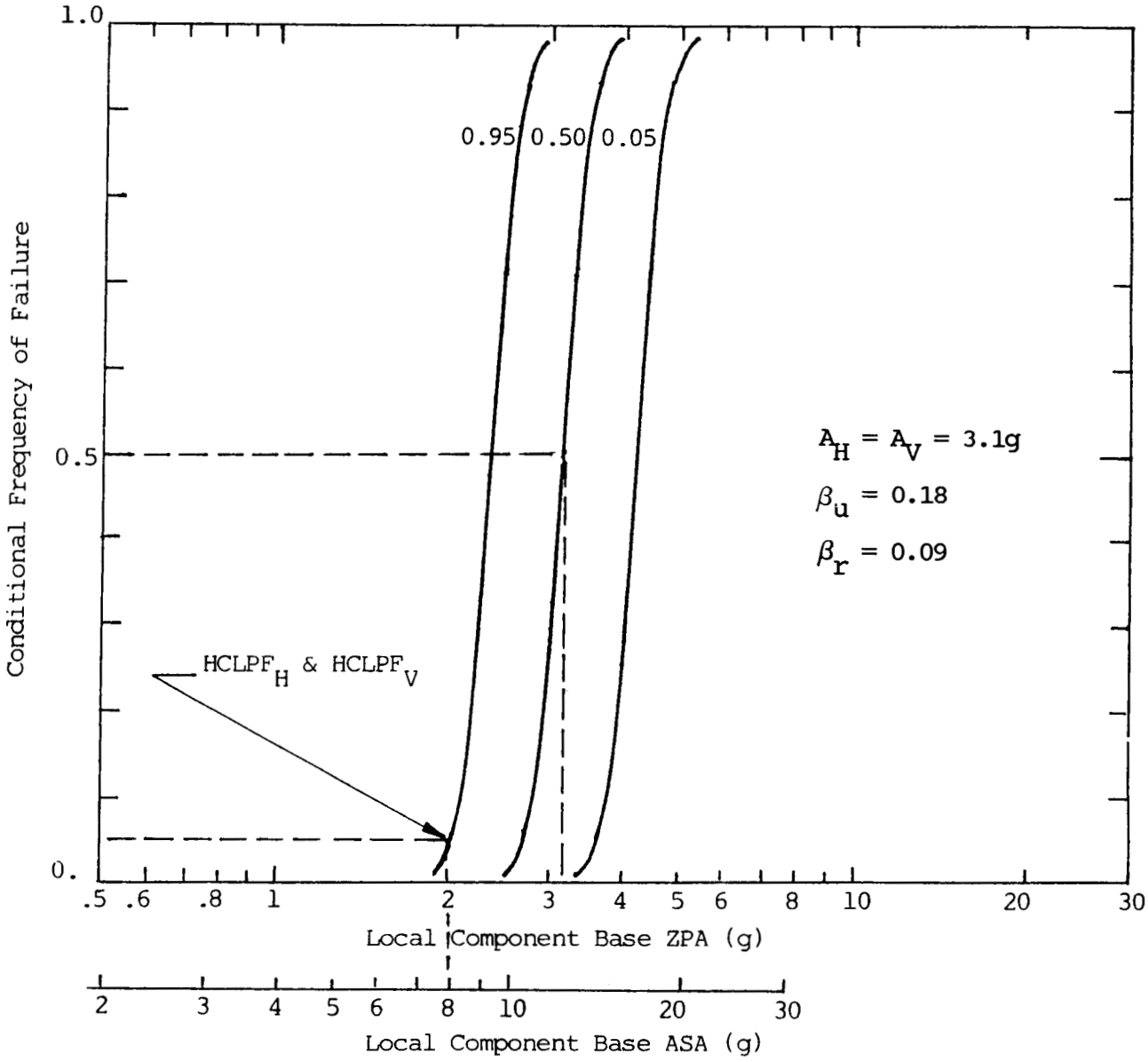

Fig. 4.22 Horizontal and vertical seismic fragility curves for commercial standard local starters LPF36 and LPF37 containing Size 1 starter.

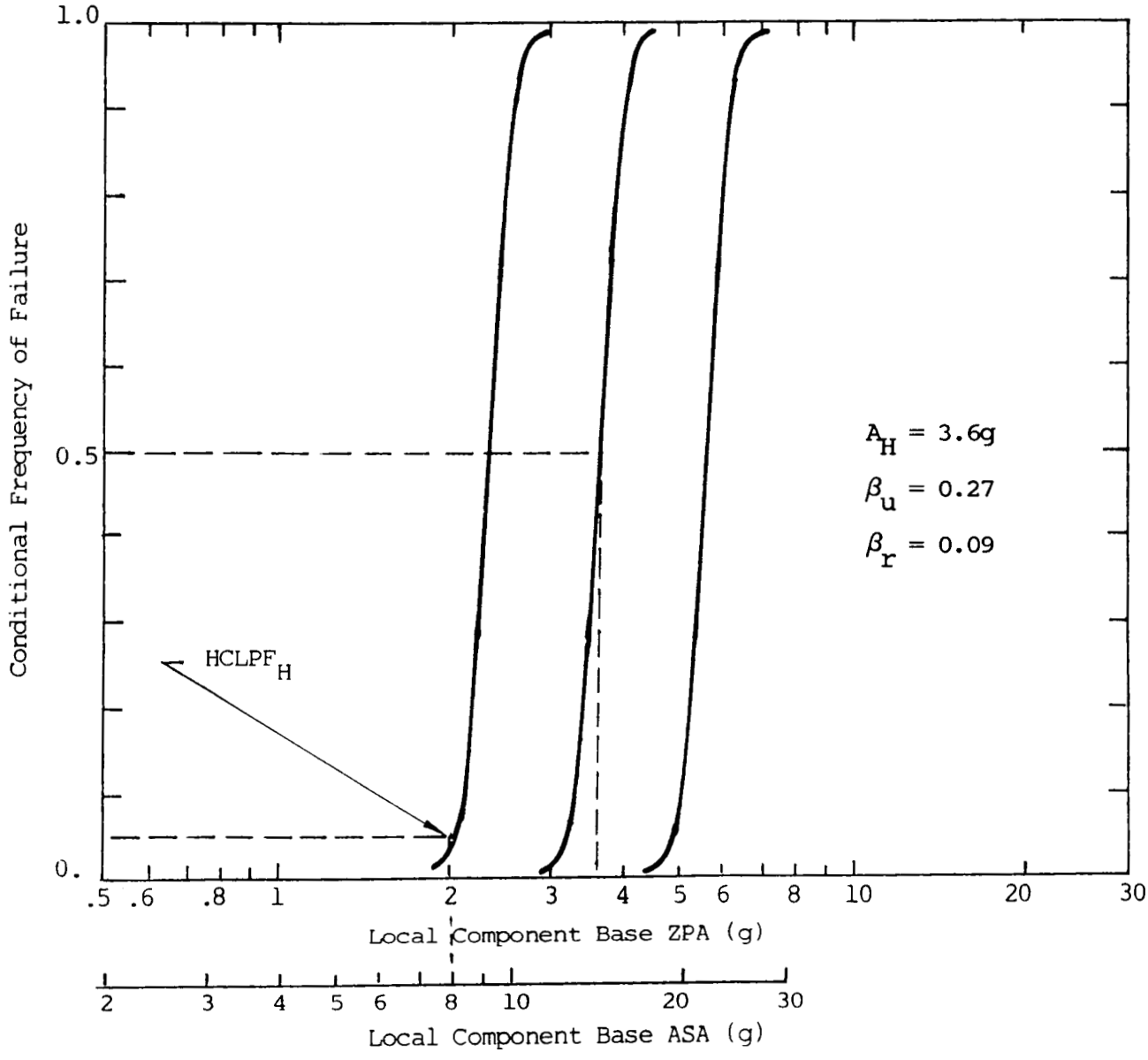

Fig. 4.23 Horizontal seismic fragility curves for commercial standard local starter LPG66 containing Size 4 starter.

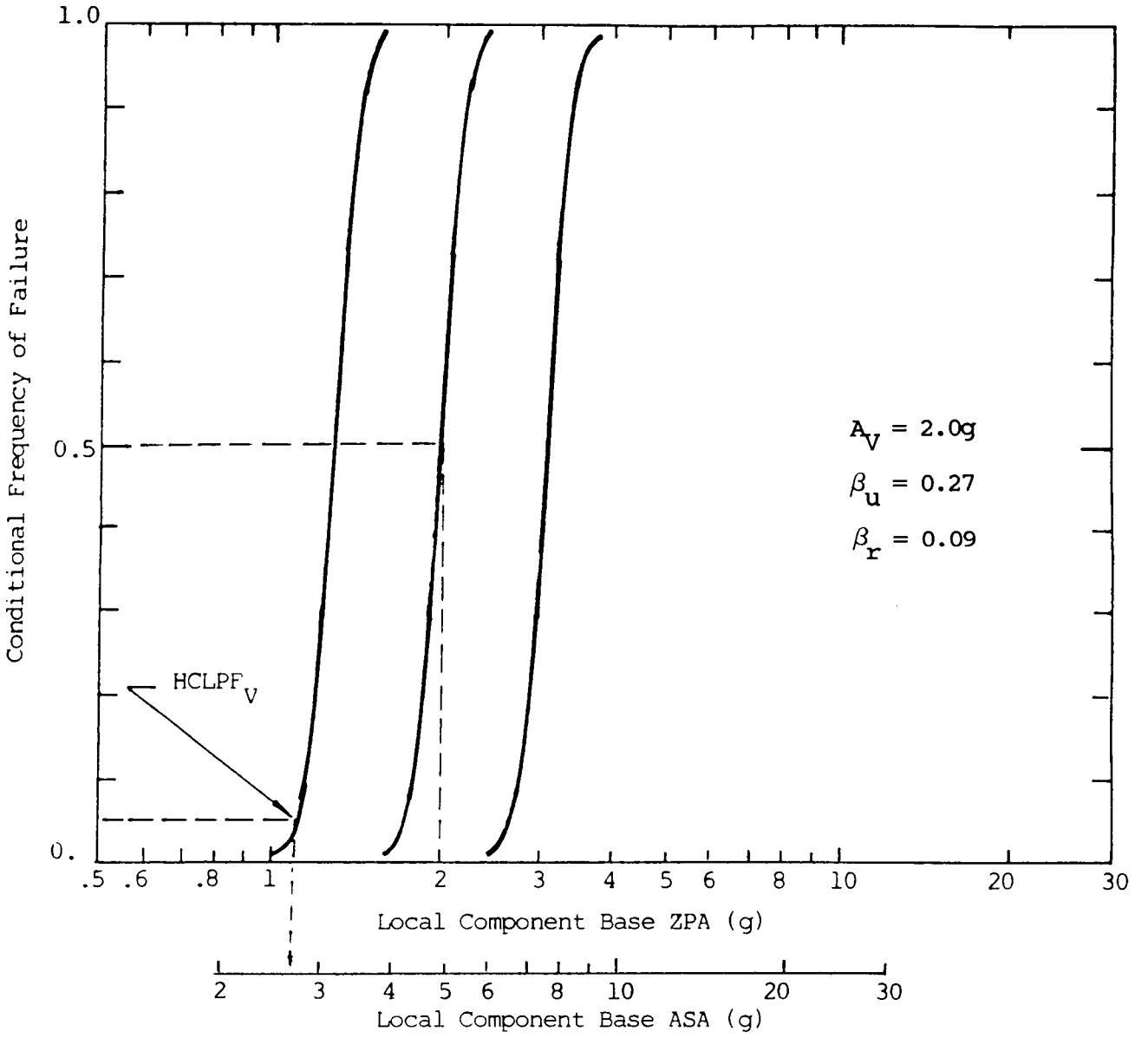

Fig. 4.24 Vertical seismic fragility curves for commercial standard local starter LPG66 containing Size 4 starter.

5. SUMMARY AND CONCLUSIONS

To demonstrate how qualification test data can be used to estimate the ultimate seismic capacity of nuclear power plant equipment, we have assessed in detail various components tested by the Pacific Gas & Electric Company (PG&E) for its Diablo Canyon nuclear power plant. As part of the Phase I Component Fragility Research Program, we evaluated the seismic fragility of five components: medium-voltage (4kV) switchgear; safeguard relay board; emergency light battery pack; potential transformer; and station battery and racks. The results of the Phase I evaluation (see Table 5.1) indicated that these components, even in their standard commercial configurations or with relatively minor structural modifications, would rate as "high capacity" according the guidelines established during our Phase I component prioritization effort [2], i.e. the median seismic capacity of each exceeds 2.0g based on local ZPA at the component base.

Our Phase II continues this evaluation by assessing seismic qualification test data for three additional types of components from the Diablo Canyon nuclear power plant. These included the following: (1) a single Westinghouse Type W motor control center column with top bracing added, (2) one fan cooler motor controller, and (3) two different sizes of local motor starters. As with the components considered in our Phase I evaluation, the qualification tests were conducted by PG&E as part of its Hosgri seismic requalification program for the Diablo Canyon plant. We selected these particular components not only for safety significance, but also because they represent different applications and mounting configurations of nominally similar electrical devices, i.e. contact-operated motor starters.

For each component, we presented a brief description of the component, its safety functions, mounting condition, potential seismic failure modes, modifications (if any) to enhance seismic capacity, and qualification test methods and results. Based on the test methods and results, we empirically estimated the minimum seismic capacity as being equal to the highest seismic level to which the component was subjected during the qualification tests. Contact chatter observed during the qualification tests was not considered a functional failure if a circuit analysis showed that the safety function of the controlled load was not compromised; this definition of "failure" we refer to as failure criterion (1) in our study. We represented the minimum seismic capability by an idealized version of the test response spectrum (TRS) at the component base, and then assumed that the ZPA of the minimum seismic capability represents the "high-confidence, low probability of failure" (or "HCLPF") seismic capacity; in statistical terms, we define the HCLPF capacity as that value of ZPA associated with a 5% probability of failure at a 95% confidence level. Assuming that fragility can be represented by a log-normal distribution having random and uncertain variabilities β_r and β_u, respectively, we extrapolated the HCLPF capacity to infer a median seismic capacity A similarly based on the

ZPA at the component base. This was the same procedure applied in our Phase I evaluation.

In our Phase II evaluation only, we also used another fragility descriptor, the average spectral acceleration (or "ASA"), developed by the Brookhaven National Laboratory as part of its study of generic seismic fragilities for nuclear power plant electrical components [6]. The ASA, defined as the average spectral acceleration of the applicable 2% damping response spectrum for the frequency range from 4 to 16Hz, is a single-parameter attempt to account for the fact that, at least for relatively "flexible" components, the spectral acceleration is a more appropriate parameter on which to base a fragility description. Consistent with the assumptions we applied to the estimate of the HCLPF ZPA based on failure criteria (1), the HCLPF ASA was established from the TRS representing the minimum seismic capability. Because the TRS in the qualification tests was associated with a 3% damping, the ASA derived from this TRS was increased by 1.2 (as suggested by BNL) to account for the adjustment between 3% and 2% damping spectra. The median ASA capacity S was then derived from the HCLPF ASA capacity by assuming the same variabilities as those for the ZPA capacity, usually $\beta_r = 0.09$ and $\beta_u = 0.18$.

Table 5.2 summarizes the seismic fragilities of the components considered in the Phase II evaluation. The corresponding seismic fragility curves are shown in Figs. 2.20 and 2.21 for the MCC, in Figs. 3.16 and 3.17 for the fan cooler motor controller, and in Figs. 4.22 and 4.23 for the local starters. We also compared the horizontal seismic fragilities of the Type W MCC with those for the Westinghouse Five-Star MCC (with top bracing) developed from the LLNL demonstration tests, and with generic fragilities established by BNL for free-standing motor control centers on the basis of qualification test and fragility test data. This comparison is shown in Table 2.2. The LLNL results were originally presented in terms of the local base ZPA of the Size 2 starters at the mounting locations. We estimated an average dynamic amplification factor of 2.1 from the base of MCC to the starter mounting locations, to convert the starter base ZPA capacity to the MCC base ZPA capacity. We then estimated the MCC base ASA capacity for the Five-Star MCC by first determining the ASA from the TRS and computing the ratio of the ASA to the ZPA of the TRS. The ASA capacity was then determined by multiplying the MCC base ZPA capacity by the ASA-to-ZPA ratio. Because the fragilities from both the LLNL and BNL study were originally based on a different failure criterion ("failure criterion (2)", i.e. <u>any</u> contact chatter, regardless of safety implication, represents functional failure) than that used in the PG&E tests, Table 2.2 also includes our estimate for the fragilities for the Type W MCC based on the same failure criteria so as to facilitate more direct comparisons. This estimate was facilitated by OBE-level qualification test data that presented in Refs. 3 and 7.

To study the effect of the larger variabilities from the BNL study on the median capacity, we computed the median capacities of the Type W MCC from the HCLPF capacities using the generic variabilities as shown in Table 2.2. The results are presented in Table 2.3 which shows that

the median ZPA capacities are about the same as those estimated based on $\beta_r = 0.09$ and $\beta_u = 0.18$, but the median ASA capacities based on the generic variabilities are somewhat higher.

From the assessments presented previously in the report, we make the following observations:

- in principle, a "HCLPF" approach can be used to infer ultimate capacity provided that sufficient information is available from which to estimate how various factors affect seismic performance. These factors include not only specific hardware modifications made to enhance seismic performance, but also how the component is mounted.

- based on the results of our evaluation, each of these components in its as-qualified configuration would rate as a "high capacity" component according to our prioritization guidelines, i.e. median capacity greater than 2g ZPA at the component base. Note that the "as-qualified" configuration includes the rigid mounting condition applied for all components in addition to modifications, if any, in the component itself.

- all of the components considered in this evaluation are standard commercial items (before modification, if any), suggesting a high degree of commonality with similar equipment installed in other plants. It is of interest to note further that the modifications to the MCC and and to the fan cooler motor controller were done not to strengthen the component structurally, but to improve the functionability so that the component would qualify for the Hosgri seismic criteria. In their standard commercial configurations, the estimated capacities for these components is only about 15% lower than with their respective modifications.

- when based on the same failure criterion, i.e. criterion (2), the horizontal capacities of the top-braced Type W and the top-braced Five-Star MCC are consistent with one other. When compared with the BNL results, the capacities of the Type W MCC are higher than the generic MCC capacities even though the variabilities assumed in our study are smaller. This is expected because our study considered only a plant-specific MCC and did not attempt to address a broad (and potentially diverse) range of motor control centers. The agreement among our Phase II evaluation, the LLNL tests, and the BNL generic study is encouraging because a high degree of consistency in the ZPA capacity and variabilities was observed.

  Similar consistency in ASA capacities, however, is not immediately apparent. This is likely a result of the large variability in the characteristics and shape of the test response spectra used in each individual study. It suggests that while spectral acceleration is arguably a more reasonable descriptor for the seismic fragility, the current definition of ASA (i.e. a simple average of

spectral response over a defined frequency range) might not be totally adequate.

- with one exception (the medium-voltage switchgear), all of the components considered in both our Phase I and Phase II evaluations were qualified in their standard commercial configurations or with only relatively minor modifications. This result suggests that the seismic capacity of like equipment in other plants could be markedly improved, if necessary, through similar modifications. Note for each component that particular emphasis was placed on rigid mounting conditions.

- a detailed evaluation of high-level qualification data can suggest component modifications that may significantly increase seismic capacity, or areas of emphasis in seismic margins reviews.

However, it is also important to keep in mind that a "bottom-up" assessment of seismic capacity (i.e. fragility level estimated from HCLPF capacity) as applied in this evaluation suggests that median capacity increases with uncertainty, which is clearly non-conservative. Consequently, extreme care must be exercised in selecting the uncertainty parameters used to infer the "actual" fragility level of a component. Unfortunately, the information necessary to select these parameters is often not available from existing data, in which case the HCLPF-derived fragility descriptions have a high degree of inherent uncertainty. For certain high-capacity components, this uncertainty may be tolerable if only a "lower bound" fragility (a HCLPF capacity, for example, or a 95% fragility curve) is needed for regulatory decision-making or is adequate for PRA applications. This may be true, for example, for the Diablo Canyon components considered in this evaluation. In general, however, this uncertainty implies a "top-down" approach -- estimating HCLPF capacities from measured fragility levels -- is still preferable to assessing seismic performance when a detailed fragility description is desired, particularly for a low-capacity component.

Table 5.1 Seismic fragilities of components considered in Phase I evaluation, expressed in terms of local ZPA at the component base.

Component	$\hat{A}_H^v$	$\hat{A}_V^v$	β_r	β_u	Modifications
Medium-voltage switchgear	3.9g	3.9g	0.09	0.18	• Stiffener plates added to frame structure • Potential transformer removed from top • Flexible joint inserted at entry of overhead bus duct • Top bracing added • Rigid base mounting
Potential Transformer	4.2g	5.3g	0.09	0.18	• Standard commercial item • Rigid base mounting
Safeguard Relay Board	4.2g	5.3g	0.09	0.18	• Standard commercial item • Rigid base mounting
Emergency Light Battery Pack	4.2	5.3	0.09	0.18	• Steel straps added across battery tops; straps bolted to mounting shelf
Balance-of-Plant Batteries and Racks	3.9	1.7	0.09	0.18	• Standard commercial batteries • Bracing and side rail shims added to rack

Notes: $\hat{A}_H^v$ = median seismic capacity, horizontal direction

$\hat{A}_V^v$ = median seismic capacity, vertical direction

Table 5.2 Seismic fragilities of components considered in Phase II evaluation, expressed in terms of local ZPA and ASA at the component base.

Component	$\hat{A}_H$	$\hat{A}_V$	$\hat{S}_H$	$\hat{S}_V$	β_r	β_u	Modifications
Type W MCC	2.3g	1.7g	8.0g	4.1g	0.09	0.18	• Top braces added in F-B direction
	2.6g	1.7g	9.1g	4.1g	0.09	0.18	• Top braces added in F-B direction • Seismic clips added to draw-out units.
Fan cooler motor controller	2.3g	2.2g	8.0g	4.2g	0.09	0.18	• Standard commercial item
	2.6g	2.2g	9.1g	4.2g	0.09	0.18	• Mechanical interlocks between high- and low-speed contacts
Local starters LPF36, LPF37	3.1g	3.1g	12.4g	12.4g	0.09	0.18	• Standard commercial item
Local starter LPG66	3.6g	2.0g	14.4g	4.8g	0.09	0.27	• Standard commercial item

Notes: $\hat{A}_H$ = median seismic capacity, horizontal direction (ZPA)

$\hat{A}_V$ = median seismic capacity, vertical direction (ZPA)

$\hat{S}_H$ = median seismic capacity, horizontal direction (ASA)

$\hat{S}_V$ = median seismic capacity, vertical direction (ASA)

REFERENCES

1. G.S. Holman, et al., **Component Fragility Research Program, Phase I Demonstration Testing**, Lawrence Livermore National Laboratory, Report UCID-21002, NUREG/CR-4900, Vols. 1 and 2 (August 1987).

2. G.S. Holman and C.K. Chou, **Component Fragility Research Program, Phase I Component Prioritization**, Lawrence Livermore National Laboratory, Report UCID-21003, NUREG/CR-4899 (June 1987).

3. Pacific Gas & Electric Company, "Seismic Evaluation for Postulated 7.5M Hosgri Earthquake, Units 1 & 2, Diablo Canyon Site," Vol. 3, NRC Docket Nos. 50-275 and 50-273 (1979).

4. R.D. Campbell and M.K. Ravindra, et al., **Compilation of Fragility Information from Available Probabilistic Risk Assessment**, Lawrence Livermore National Laboratory, Report UCID-20571 (September 1985).

5. L.E. Cover and M.P. Bohn, et al., **Handbook of Nuclear Power Plant Seismic Fragilities**, Lawrence Livermore National Laboratory, Report UCRL-53455, NUREG/CR-3558 (June 1985).

6. K.K. Bandyopadhyay and C.H. Hofmayer, et al., **Seismic Fragility of Nuclear Power Plant Components (Phase II): Motor Control Center, Switchboard, Panelboard and Power Supply**, Brookhaven National Laboratory, Report BNL-NUREG-52007, NUREG/CR-4659, Vol. 2 (December 1987).

7. Pacific Gas & Electric Company, "Diablo Canyon Power Plant Units 1 and 2 Seismic Qualification of Class 1E Electric Equipment," File No. ES 24 (August, 1984).

8. Wyle Laboratories, "Seismic Testing of Safety-Related Electrical Equipment for Diablo Canyon for Pacific Gas & Electric Company," Report No. 58255 (April 1978), with Addendum 2 (March 1979).